



UPPSALA
UNIVERSITET

*Digital Comprehensive Summaries of Uppsala Dissertations
from the Faculty of Medicine 1893*

Factors influencing transferrin receptor-mediated brain delivery

*Evaluating preclinical antibody-based proteins for
PET imaging in Alzheimer's disease*

REBECCA FARESJÖ MELANDER



ACTA
UNIVERSITATIS
UPSALIENSIS
UPPSALA
2023

ISSN 1651-6206
ISBN 978-91-513-1685-7
URN urn:nbn:se:uu:diva-494103

Dissertation presented at Uppsala University to be publicly examined in Rudbecksalen, Dag Hammarskjölds väg 20, Uppsala, Friday, 3 March 2023 at 09:15 for the degree of Doctor of Philosophy (Faculty of Medicine). The examination will be conducted in English. Faculty examiner: Associate Professor Robert Thorne (University of Minnesota - Department of Pharmaceutics/Denali Therapeutics, Biology Discovery, South San Francisco, USA).

Abstract

Faresjö Melander, R. 2023. Factors influencing transferrin receptor-mediated brain delivery. Evaluating preclinical antibody-based proteins for PET imaging in Alzheimer's disease. *Digital Comprehensive Summaries of Uppsala Dissertations from the Faculty of Medicine* 1893. 83 pp. Uppsala: Acta Universitatis Upsaliensis. ISBN 978-91-513-1685-7.

Antibody-based proteins targeting amyloid-beta ($A\beta$) could be used as radioligands in positron emission tomography (PET) to study Alzheimer's disease (AD) pathology in the living brain. The prospective advantages of antibody-based PET are to detect pathology earlier, with higher sensitivity, and to evaluate treatment effects of emerging immunotherapies against $A\beta$. However, antibodies and other proteins are too large to cross the blood-brain barrier (BBB). This can be circumvented by fusing antibodies with transferrin-receptor (TfR) binders that penetrate the BBB via receptor-mediated transcytosis.

In this thesis, I evaluated different bispecific antibody-based proteins that bind both TfR and $A\beta$. The overall aim was to determine which factors are important for TfR-mediated brain delivery of these proteins and their use as PET radioligands.

In paper I, we studied a large, high TfR-avidity antibody compared with a smaller antibody fragment fusion with lower TfR avidity. The small antibody had fast elimination from blood and was cleared from the brain earlier than the large antibody, thus providing better signal-to-noise ratio for brainPET. In paper II, antibody-like proteins (affibodies), even smaller than the previously studied antibody, had enhanced TfR-mediated brain delivery but had an imbalance in binding to TfR and $A\beta$. This resulted in poor pathology-related retention of ^{125}I -radiolabeled affibodies. In paper III, we observed that aged mice had poorer brain delivery of the bispecific antibody, mAb3D6-scFv8D3, compared with young mice. Age was also related to increased blood cell binding of the bispecific antibody, and a lower dose resulted in higher relative delivery to the brain parenchyma. In paper IV, we evaluated single domain llama-based antibodies, VHHs, which bound both mouse and human TfR, and were characterized by rapid elimination from blood and brain. The VHHs were fused to an $A\beta$ binding antibody fragment, scFv3D6, which enabled increased brain retention of the ^{125}I -radiolabeled antibodies in an AD mouse model, and, thus, provided high contrast to healthy controls.

In conclusion, antibody format, size, mouse age, dose, and TfR binding were important factors influencing brain delivery and retention.

Keywords: brain delivery, bispecific antibody, transferrin receptor, Alzheimer's Disease, amyloid-beta, aging, single domain antibody, PET

Rebecca Faresjö Melander, Department of Public Health and Caring Sciences, Geriatrics, Box 609, Uppsala University, SE-75125 Uppsala, Sweden.

© Rebecca Faresjö Melander 2023

ISSN 1651-6206

ISBN 978-91-513-1685-7

URN urn:nbn:se:uu:diva-494103 (<http://urn.kb.se/resolve?urn=urn:nbn:se:uu:diva-494103>)

“Little by little, one travels far”

J.R.R. Tolkien

*Till min familj: Tomas Faresjö, Åshild Olsen Faresjö
och Joel Faresjö Melander*

List of Papers

This thesis is based on the following papers, referred to in the text by their Roman numerals.

- I. **Faresjö, R.**, Bonvicini, G., Xiaotian, T. F., Aguilar, X., Sehlin, D., Syvänen, S. (2021) Brain pharmacokinetics of two BBB penetrating bispecific antibodies of different size. *Fluids Barriers CNS*, 18(1):26.
- II. **Faresjö, R.**, Lindberg, H., Ståhl, S., Löfblom, J., Syvänen, S., Sehlin, D. (2022) Transferrin receptor binding BBB-shuttle facilitates brain delivery of anti-A β -antibodies. *Pharm Res*, 39:1509-1521.
- III. **Faresjö, R.**, Sehlin, D., Syvänen, S. Age, dose, and binding to blood cells influence brain delivery of a TfR1-transported antibody. *Submitted*.
- IV. **Faresjö, R.**, Sjöström, E. O., Berglund, M. M., Eriksson, J., Sehlin, D., Syvänen, S. Single domain antibody conjugated to A β -binding scFv penetrates BBB via TfR to interact with A β . *Manuscript*.

Reprints were made with permission from the respective publishers.

Additional Publications

Publications not included as part of this thesis:

- V. Syvänen, S., Fang, X.T., **Faresjö, R.**, Rokka, J., Lannfelt, L., Olberg, D.E., Eriksson, J., Sehlin, D. (2020). Fluorine-18-Labeled Antibody Ligands for PET Imaging of Amyloid- β in Brain. *ACS Chem Neurosci* 11:4460-4468
- VI. Syvänen, S., Meier, S. R., Roshanbin, S., Xiong, M., **Faresjö, R.**, Gustavsson, T., Bonvicini, G., Schlein, E., Aquilar, X., Julku, U., Eriksson, J., Sehlin, D. (2022). PET imaging in preclinical anti-A β drug development. *Pharm Res* 39:1481-1496.
- VII. De la Rosa, A., Metzendorf, N., Morrison, J., **Faresjö, R.**, Rofo, F., Petrovic, A., O'Callaghan, P., Syvänen, S., Hultqvist, G. (2022) Introducing or removing heparan sulfate binding sites does not alter brain uptake of the blood-brain barrier shuttle scFv8D3. *Sci Rep* 12(1):1-17.

Cover image by Rebecca Faresjö Melander, 2023 ©.

“Mouse brain capillaries and schematic illustrations of antibody-based proteins used in this thesis.”

Contents

Introduction.....	11
Biological drugs	11
Antibodies	11
The structure of IgGs.....	12
Engineered antibodies and antibody fragments	13
Affibodies.....	15
Alzheimer's disease.....	16
Amyloid- β	16
Tau	17
The amyloid cascade hypothesis	17
Anti-A β antibodies	19
Fluid biomarkers in AD.....	20
Positron Emission Tomography in AD	21
Antibody-based A β -PET	22
Barriers of the brain.....	23
Transport routes at the BBB.....	26
Receptor-mediated transcytosis.....	27
The transferrin receptor (TfR).....	27
TfR-mediated brain delivery of antibodies	28
Translation of TfR-antibodies	30
Pharmacokinetics of therapeutic antibodies	31
Methodology.....	33
Recombinant expression of fusion antibodies.....	33
Animals	34
Radiochemistry.....	35
ELISA	35
LigandTracer®	36
Immunostaining.....	37
SDS-PAGE and immunoblotting	37
Autoradiography.....	38
<i>Ex vivo</i> autoradiography	38
Nuclear track emulsion (NTE) autoradiography	39
<i>In vitro</i> autoradiography	39
Capillary depletion	40
PET.....	41

Aims.....	43
Summary of papers I-IV	44
Paper I	44
Paper II.....	45
Paper III.....	46
Paper IV	47
Results and discussion	49
Factors influencing transferrin receptor-mediated brain delivery	49
Does size matter?.....	49
Binding - affinity and avidity	51
Periphery.....	53
Is age just a number?	54
A β pathology	56
Dose.....	56
Conclusions and future perspectives.....	58
Popular Science Summary	60
Populärvetenskaplig sammanfattning	63
Funding	65
Acknowledgments.....	66
References.....	69

Abbreviations

^{11}C	Carbon-11
^{125}I	Iodine-125
^{18}F	Fluorine-18
A β	Amyloid beta
A β PF	A β protofibril
AD	Alzheimer's disease
APP	Amyloid precursor protein
Arc	Arctic mutation
BBB	Blood-brain barrier
BCSFB	Blood-cerebrospinal fluid barrier
CNS	Central nervous system
CSF	Cerebrospinal fluid
ELISA	Enzyme-linked immunosorbent assay
FAD	Familial Alzheimer's Disease
Fab	Fragment antigen binding
Fc	Fragment crystallisable
FcRn	neonatal Fc-receptor
Fv	Fragment variable
HRP	Horseradish peroxidase
ID	injected dose
IgG	Immunoglobulin G
ISF	Interstitial fluid
kDa	kilo Dalton
mAb	monoclonal antibody
MCI	Mild cognitive impairment
mTfR1	murine Transferrin receptor 1
NFTs	Neurofibrillary tangles
NTE	Nuclear track emulsion
NVU	Neurovascular unit
PBS	Phosphate buffered saline
PD	Parkinson's disease
PET	Positron emission tomography
PiB	Pittsburgh compound B
p-tau	phosphorylated tau
PVS	Perivascular space

RMT	Receptor mediated transcytosis
sdAb	single domain antibody
SDS-PAGE	Sodium dodecyl sulfate polyacrylamide gel electrophoresis
SPR	Surface Plasmon Resonance
SUV	Standard uptake volume
Swe	Swedish mutation
TCO	Tetra-cyclooctene
tg	transgenic
scFv	single-chain variable fragment
TfR	Transferrin receptor
VHH	Variable heavy chain domain
WT	Wild type

Introduction

Biological drugs

Biological drugs have emerged in the latest 40 years with advances in biotechnology. In contrast to conventional drugs, which are chemically synthesized, biological drugs are pharmaceutical products that originate from biological material like cells or microorganisms. These products vary from nucleic acid material and cells to protein-based therapeutic peptides, antibodies, and antibody fragments¹. Compared with classical drugs (known as "small molecules"), biological drugs are generally larger and more complex. Since they have different properties from small molecule drugs, they can be an alternative to treat otherwise "undruggable" targets². There has been extensive growth in approved biological drugs in the last decade, and the market for biological drugs is expected to increase even more in the future³. Most biological drugs on the market are protein-based, with the main class being monoclonal antibodies (mAbs)⁴.

Antibodies

In nature, antibodies are part of the body's natural defense; plasma B-lymphocytes produce antibodies in response to exogenous proteins or pathogens, such as viruses and bacteria entering the body⁵. In humans, there are five different isotypes of antibodies; IgA, IgD, IgE, IgG, and IgM, where IgG is the most common antibody found in serum and the basis for most approved therapeutic antibodies^{3,6}. IgGs bind with high affinity and selectivity to their target (antigen) and help to identify and neutralize these pathogens by activating effector mechanisms of the immune system. These effector functions can be divided into four mechanisms; blocking, complement-dependent cytotoxicity (CDC), antibody-dependent cell-mediated cytotoxicity (ADCC), and opsonization resulting in antibody-dependent cellular phagocytosis (ADCP)⁷.

IgG has four classes (IgG1, IgG2, IgG3, IgG4) that differ in immunologic effector function profiles⁶. The most common subtype for mAbs is IgG1, but there are also drugs approved of the subtype IgG2 or IgG4³. IgG1 can efficiently trigger both complement and cellular effector functions⁸. Human IgG1 is similar to mouse IgG2a in its effector function⁹. Endogenous IgGs have a long blood half-life of up to three weeks to provide long-term immunity¹⁰.

Antibodies were first isolated from the serum of animals injected with a target protein. These antibodies are genetically diverse or “polyclonal”. To produce genetically identical antibodies (mAbs), for higher reproducibility, splenic B-cells from the immunized animal are isolated and fused with lymphoma cancer cells to create immortalized cells lines (hybridomas) that produce clones of the antibody (thereby “monoclonal”)¹¹. Today, many mAbs are generated *in vitro* by recombinant gene technology³. The genetic sequences for the antibodies are stored in large libraries; these proteins are displayed on the surface of phages, bacteria, mammalian cells, or yeast cells at a large scale. The best binders can be isolated through multistep binding assays toward the target protein⁷. Antibodies are widely used for bioanalytical, diagnostic, and therapeutic purposes¹². The advantages of antibodies are that they are very specific and bind with high affinity; they are easily engineered and in theory, can be raised against any suitable biological molecule⁷.

Therapeutical mAbs have been effective in treating autoimmune diseases. For example, TNF- α inhibitors are used in disorders like rheumatoid arthritis, inflammatory bowel disease, and psoriasis^{13–15}. They have also been groundbreaking in oncology as treatment and diagnostic imaging agents owing to their high specificity^{16,17}.

The structure of IgGs

Structurally, IgG antibodies are proteins made of four peptide chains; two heavy chains (50 kDa) and two light chains (25 kDa)⁶. The chains are connected with disulfide bonds to form a symmetric Y-shaped protein (Fig 1A). Each heavy chain has three constant domains and one variable domain. The light chains consist of one constant and one variable domain. One arm of the heavy and light chain is called a Fab (fragment, antigen binding) (Fig. 1B). The variable domains of the heavy and light chains constitute the Fv (fragment, variable) region, which contains the antigen binding sites. They bind to antigens through six variable amino acid loops called complementarity-determining regions (CDRs)⁷. The variable heavy and light chains from one arm of the antibody can be recombinantly linked to form an antigen-binding protein called a single variable chain fragment (scFv) (Fig. 1C). Lastly, the Fc (fragment, crystallizable) region consists of constant domain 2 and 3 of each heavy chain. The Fc region modulates immune responses by binding to Fc receptors to activate cellular effector functions¹⁰.

Heavy chain IgG antibodies (Fig. 1D) are unique to species of the family *camelids* (camels, dromedaries, llamas, and alpacas) and *cartilaginous fishes* (i.e., sharks)^{18,19}. The antigen-binding region consists of two single domains; as the name suggests, the antibodies lack light chains. From these antibodies, the smallest possible IgG-based antigen-binding unit has been isolated; single domain antibodies (sdAb)²⁰. The camelid sdAbs are often referred to as VHHs

to denote the “variable domain of a heavy-chain antibody”. The shark-derived sdAbs are called VNARs (from “immunoglobulin new antigen receptor: IgNAR”)^{18,19}. The sdAb can bind targets with high affinities to act as biological drugs despite lacking the light chain variable domain. In 2018, the first sdAb drug, Caplacizumab, was approved for clinical treatment of adult-acquired Thrombotic Thrombocytopenic Purpura (aTTP)²¹.

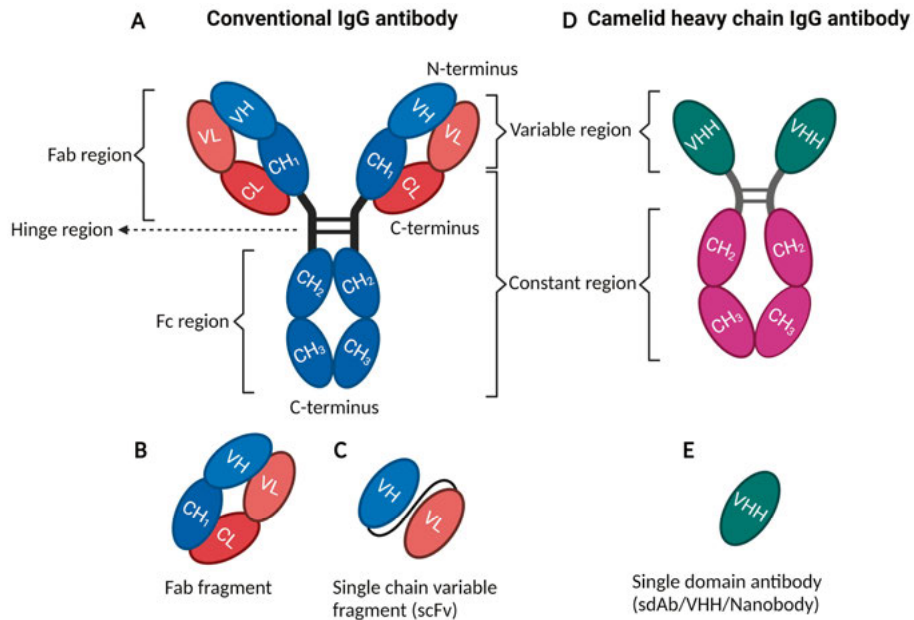


Figure 1: **A** Full-size IgG1 antibody; VL: variable light chain, VH: variable heavy chain, CL: constant light chain, CH: constant heavy chain, Fab: antigen-binding fragment, Fc region: constant Fc-receptor binding domain. **B** Fab fragment **C** Single chain variable domain (scFv) **D** Full-size heavy chain IgG antibody; VHH: single domain variable heavy chain **E** Single domain antibody (sdAb/VHH/Nanobody)²².

Engineered antibodies and antibody fragments

Recombinant gene technology enables the production of non-naturally existing antibody formats and fusion proteins in prokaryotic or eukaryotic cells. Engineered antibodies can be divided into two main groups; IgG-like and non-IgG-like²³. The IgG-like antibodies remain in the classical Y-shaped format, while non-IgG-like antibodies can be of various sizes and formats but are typically antigen-specific fragments or several fragments fused with linkers⁷.

The valency, i.e., the number of binding sites for the same antigen, can be one (monovalent) or two (bivalent), or multiple (multivalent). The specificity, i.e., the number of antigens that the antibody can recognize, can be one (mon-

ospecific) like for a conventional IgG or more than one (bispecific, multi-specific). A monovalent or bivalent antibody towards one antigen can be made bispecific by adding target binding domains towards a second antigen, such as additional scFv fragments, or by modifying the existing target-binding domains, for example, so that each arm binds a different target^{24,25}.

Like endogenous IgGs, engineered IgG-like antibodies can display a very long half-life in blood, up to a few weeks^{26,27}. One reason for the prolonged circulation time is the molecular size larger than the renal filtration cutoff (around 60 kDa)²⁸. Additionally, because of the intact Fc region, the IgGs can be rescued from cell degradation by interacting with the neonatal Fc receptor (FcRn), which recycles IgGs back into the blood after they have been internalized by cells¹⁰. The Fc-region also allows interaction with Fc-receptors (FcγR) on cells to trigger desired immune responses but can contribute to a higher risk of adverse effects through immunoreactivity¹⁰.

Non-IgG-like antibodies usually lack the Fc-region and typically display a faster half-life in the blood. Three main types of antigen-specific fragments provide the basis for non-IgG-like antibodies; Fabs (≈ 50 - 55 kDa), scFv (≈ 25 kDa), or sdAbs (≈ 12 - 15 kDa) (Fig. 1 B, C, E). In this thesis, scFvs were frequently used to create bispecific antibodies (Fig 2 B, C, D, F), and in **paper IV**, a scFv was combined with a VHH domain (Fig. 2 F).

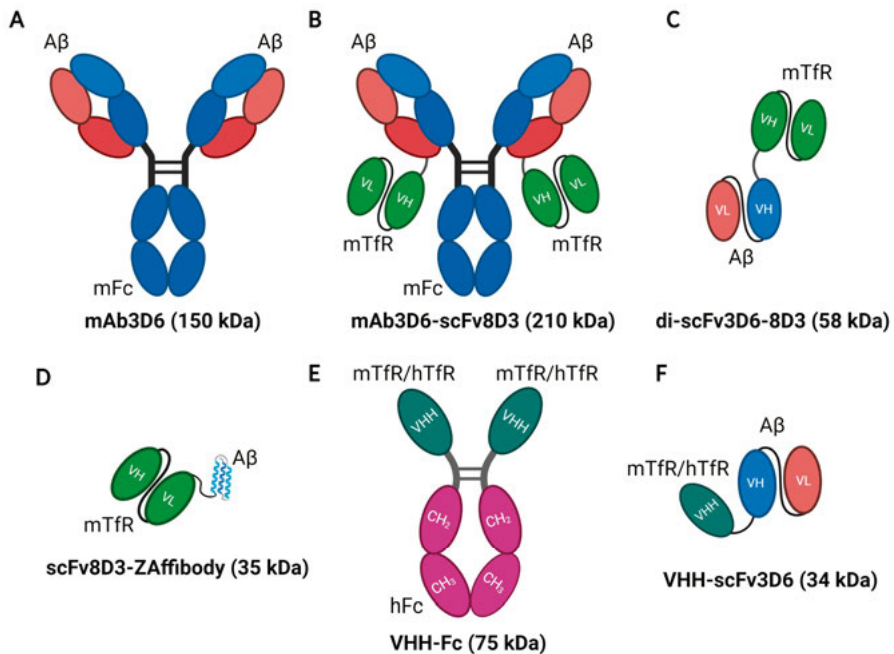


Figure 2: Examples of antibody-based proteins used in this thesis. A and E are monospecific (towards amyloid- β ($A\beta$) or mouse/human transferrin receptor (mTfR/hTfR)), while B, C, D, and F are bispecific proteins targeting $A\beta$ and TfR. mFc: mouse Fc region, hFc: human Fc region.

Affibodies

The affibody is a high-affinity protein that mimics antibodies but is not classified as such. Affibodies are the most widely used non-immunoglobulin antibody-mimetic proteins that have emerged²⁹. Affibodies are small protein scaffolds with the potential of antibody-like high affinity but with significantly smaller molecular size (around 6-7 kDa). Affibodies are based on the B-domain of protein A, naturally found in the bacteria *Staphylococcus aureus*. Protein A can bind to IgGs and is commonly used for affinity chromatography purification of antibodies³⁰. The B-domain of protein A was engineered for higher stability and solubility, providing the basis of the affibody scaffold domain used today, called the Z-domain³¹. The affibody scaffold protein consists of a bundle of three alpha-helix domains with a total length of 58 amino acids. The randomization of 13 amino acids in the target binding region of α -helix 1 and 2 in the affibody allows the creation of a wide variety of binders. These potential binders are collected in large genetic libraries, from which specific target binders can then be isolated, e.g., by phage display.

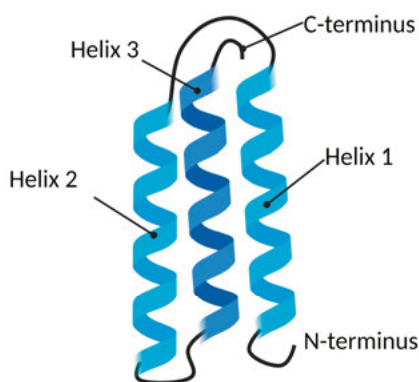


Figure 3: A schematic representation of the general structure of an affibody protein (6-7 kDa). Three linked α -helical domains (blue) form the affibody protein scaffold. The binding regions, 13 amino acid residues, are located on helix 1 and helix 2 of the affibody.

There are more than 800 publications and a wide range of applications for affibodies³². For example, affibodies have been able to substitute antibodies in analyses of human serum, affinity chromatography, and *in vitro* staining with fluorescent probes³³⁻³⁵. Their unique properties enable their use as theranostic (therapeutic and diagnostic) proteins. Affibodies combine molecular stability, solubility, a small size, relatively high tissue penetration, and fast blood clearance, with a potential for high affinity in the nanomolar to picomolar range. These properties have been of particular interest for affibody-based *in vivo* radioimaging applications in oncology. Rapid tumor penetration and high specific binding will retain the affibody at the target, while fast blood elimination will clear unbound affibody in the blood in a time frame suitable for short-lived clinical radionuclides such as fluorine-18 ^{18}F ($t_{1/2}$: 110 min) and gallium-68 ^{68}Ga ($t_{1/2}$: 68 min)³⁶. Tumor *in vivo* imaging has been

extensively evaluated with, e.g., EGFR-, HER2-, and HER3-specific affibodies using various labeling strategies^{37,38}. Affibodies for HER2 imaging have also advanced into clinical studies, with ⁶⁸Ga and ¹⁸F radiolabeling^{39,40}.

As therapeutic proteins, fast blood elimination can be problematic; therefore, affibody-based albumin-binding domains (ABD) are often conjugated to the affibody, increasing the circulation time⁴¹. The small size allows high doses to be administered in a smaller volume than antibodies, facilitating, e.g., subcutaneous injections.

Alzheimer's disease

Alzheimer's disease (AD) is the most common form of dementia, constituting around 60-80% of all cases; other forms of dementia include frontotemporal dementia (FTD), vascular dementia, and dementia with Lewy bodies⁴². AD is characterized by a progressive decline in two or more domains of cognition, such as memory, language, executive, or visuospatial function. As old age is the leading risk factor for developing the disease, AD is expected to increase from around 50 million to 150 million cases in 2050 due to the growing population of elderly worldwide⁴³.

AD is a progressive neurodegenerative disorder, mainly diagnosed by clinical symptoms, cerebrospinal fluid (CSF)-biomarkers, brain imaging techniques, and histopathological findings in the *post-mortem* brain. The AD brain is typically associated with neuroinflammation (activated microglia and astrocytes), synaptic loss, brain atrophy, and the aggregation of pathological forms of proteins forming senile plaques and neurofibrillary tangles (NFTs). The senile plaques are extracellular structures, mainly formed by aggregated amyloid-beta ($A\beta$) peptides, while NFTs are intraneuronal inclusions of aggregated hyperphosphorylated tau protein.

Amyloid- β

The $A\beta$ peptide is formed by cleavage of the transmembrane amyloid- β precursor protein (APP) expressed in the brain by neurons and astrocytes⁴⁴. Two enzymes are involved in producing $A\beta$; APP is first cleaved by β -secretase, followed by cleavage by γ -secretase. Since γ -secretase has different cleavage sites on APP, the resulting peptide fragment differs in length between 38-43 amino acids, but the most recognized forms are 40 or 42 ($A\beta_{40}$ and $A\beta_{42}$)⁴⁵. $A\beta_{40}$ is more abundant in the brain, $A\beta_{42}$ only differs from $A\beta_{40}$ by two amino acids at the C-terminus, but this contributes to $A\beta_{42}$'s hydrophobicity and a higher propensity to aggregate⁴⁶. Aggregated $A\beta_{42}$ is associated with early forms of pathology in AD^{47,48}.

In the brain, the A β peptides' physiological function is related to synaptic regulation and memory formation in the hippocampus⁴⁹ and has also been suggested to have protective antimicrobial effects⁵⁰. Aggregated A β could potentially be involved in repairing leaks in the brain's vasculature⁵¹, as plaques are typically found at or close to capillary vessels⁵², but is also known to disrupt it in AD⁵³.

Tau

The function of the tau protein is to stabilize axonal microtubules, a critical structure for maintaining neuronal signaling. Tau is phosphorylated to a certain degree in healthy conditions to regulate the binding to microtubules. However, in AD, tau phosphorylation is three to four-fold higher than in the healthy brain⁵⁴. Hyperphosphorylated tau (p-tau) results in self-assembly into aggregated tau, eventually forming insoluble NFTs inside neurons. It also leads to neurotoxicity, like disrupted neuronal signaling and, eventually, neuronal death⁵⁵. Pathologic tau deposition correlates better with cognitive decline than A β pathology in AD⁵⁶. The detailed interaction between A β and tau is still unknown, but they likely have a synergistic adverse effect that promotes the pathological process⁵⁷. Evidence point to aggregated A β as an early event or initiator of tau pathology. For example, it has been suggested that A β induces tau phosphorylation by activating the kinases involved in tau phosphorylation pathways⁵⁸. A β also seems to promote tau neurotoxicity and spreading^{59,60}.

The amyloid cascade hypothesis

The amyloid cascade hypothesis proposes that A β aggregation is the main cause of AD⁶¹. The aggregation of A β is believed to start with misfolded monomers that more easily dimerize and aggregate further into trimers, oligomers, and larger structures; these large elongated pre-stages of amyloid fibrils have also been referred to as "protofibrils"⁶². Protofibrils are soluble but eventually precipitate into insoluble β -sheet fibrils that form A β plaques⁶³ (Fig 4).

A β plaques can be divided into three forms; i) diffuse plaques of mainly unstructured A β fibrils, ii) compact fibrillary plaques without a dense core, and iii) plaques with a dense core of A β -fibrils; soluble A β -oligomers and protofibrils often surround the plaques^{64,65}. Plaques are also typically enclosed by activated microglia and astrocytes, indicating that the plaques are triggering neuroinflammation⁶⁶. The A β plaques were first considered the cause of AD, but A β plaque load fails to correlate with the severity of the disease or disease progression⁶⁷. Also, A β plaques are present in 10-30% of cognitively normal elderly, albeit with a higher risk of developing cognitive decline than individuals without A β -plaques⁶⁸. The focus has shifted from plaques towards the soluble oligomers and protofibrils as toxic agents initiating and driving pathology⁶⁹⁻⁷¹.

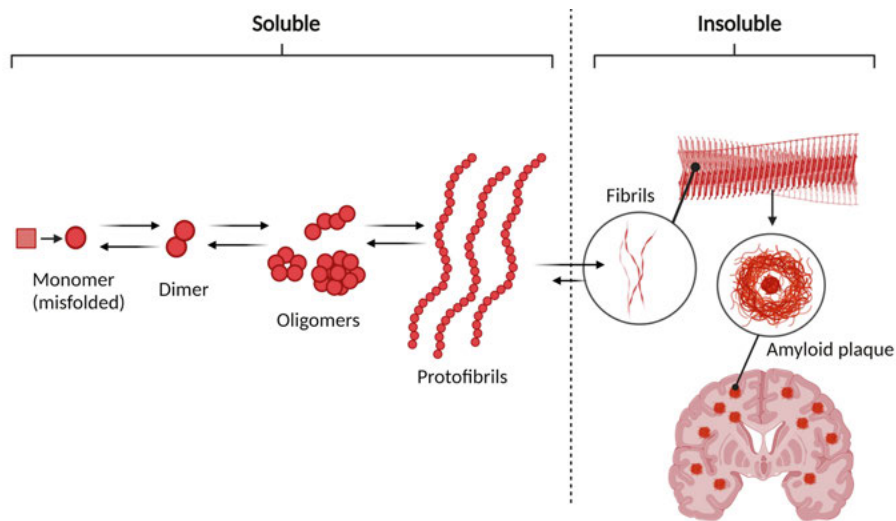


Figure 4: The aggregation pathway of Aβ.

There is much evidence of the harmful effects of aggregated Aβ related to pathological processes in AD. In rodents, soluble Aβ aggregates can inhibit long-term potentiation (LTP) and disturb signaling at the synapse⁷²⁻⁷⁵, impair memory^{69,76,77} contribute to neuroinflammation⁶⁶, and ameliorate tau pathology⁶⁰.

Genetic mutations cause 5% of AD cases, known as familial AD (FAD), while the majority of cases (95%) are called sporadic AD. The most common genetic mutations in FAD are related to Aβ. These mutations are mainly found in the genes encoding APP, or proteins of the γ-secretase complex, presenilin 1 (PSEN1) and presenilin 2 (PSEN2)⁷⁸. The mutations can result in increased total Aβ or Aβ₄₂ production, a shift in Aβ_{40/42} ratios, or alter Aβ's propensity to aggregate⁷⁹⁻⁸¹.

The risk of developing sporadic AD is increased for carriers of a particular polymorphism in the APOE gene, APOE-ε4⁸². APOE transcribes the lipid-transporter protein apolipoprotein E, the main transporter of cholesterol in the brain. Although it is not clear how APOE-ε4 interacts with Aβ, it has been shown that APOE-ε4 carriers have increased Aβ-plaque levels^{83,84}. APOE-ε4 has been suggested to be linked with impaired clearance of Aβ⁸³. The clearance rates of Aβ₄₀ and Aβ₄₂ are reduced in AD, presumably contributing to the pathological build-up of aggregated Aβ over several years⁸⁵. Therefore, both the production and clearance of Aβ are believed to play a central part in AD development.

The pathological changes, like Aβ aggregation, in the brain are likely to start 15-20 years before clinical symptoms of AD appear. Indeed, Aβ aggregation precedes tau aggregation, brain atrophy, and clinical decline and plateaus soon after clinical onset^{86,87}. Thus, there is a need to develop early Aβ-biomarkers

for pre-symptomatic and early diagnosis^{88,89}, as well as therapies that can intervene at an early stage to prevent the development of AD. Therefore, recent studies of anti-A β treatments have included patients with early AD or mild cognitive impairment (MCI)⁹⁰.

Anti-A β antibodies

Because of the increasingly heavy burden on patients, caregivers, and society, there is an urgent need for improved therapies for AD. To date, mainly symptomatic treatments are available that can mitigate symptoms short term. However, in 2021, the FDA conditionally approved the first disease-modifying therapy (a monoclonal antibody: *Aducanumab*, Aduhelm®)⁹¹, although the decision has been controversial²⁶. Cognitive decline was only slowed in one of two studies at the highest dose⁹².

A second therapeutic antibody, *lecanemab* (Leqembi®), was recently granted the same type of approval (January 2023) by the FDA⁹³. *Lecanemab* is the humanized version of murine mAb158 (developed in our group, with high selectivity for soluble protofibrils⁹⁴). The approval was based on phase 2 clinical data that *lecanemab* reduced A β -plaque load⁹⁵. However, results in the phase 3 study Clarity recently presented that *lecanemab* significantly slowed overall cognitive decline by 27% and had positive outcomes on biomarkers and secondary endpoints, further providing evidence of aggregated A β as a viable target for treatment in AD⁹⁶. Although these new therapies give hope to the field, there have been concerns about the safety and economic cost of these treatments^{97,98}.

The rationale for using administered exogenous antibodies (passive immunization) is that they can clear A β from the brain and thus halt the neurodegenerative progression. There are several hypotheses on how A β clearance is achieved, such as antibodies blocking the aggregation of A β or that the peripheral levels of A β are decreased, thus shifting the equilibrium to increased efflux of brain A β . However, the activation of microglial phagocytosis via Fc-effector functions has been the primary proposed mechanism, as suggested in the majority of studies⁹⁹⁻¹⁰².

Two other anti-A β -antibodies are evaluated in phase 3 clinical trials: *donanemab* and *gantenerumab*. All four A β -antibodies are more selective for aggregated A β than monomers. However, their binding profiles differ slightly within the spectrum from soluble to fibrillary A β ¹⁰³.

In the past, several antibody candidates have failed to meet clinical endpoints¹⁰⁴. *Bapineuzumab* (the humanized version of the murine 3D6) was the first anti-A β antibody that entered clinical trials. It binds to the N-terminal end (amino acid 1-5) and thus binds all forms of A β ¹⁰⁵. Despite showing reductions of A β plaques¹⁰⁶, *bapineuzumab* studies were terminated because it lacked

treatment effects in two phase 3 trials¹⁰⁷. Side effects related to vascular A β were also raised as a concern¹⁰⁸.

The failure of *bapineuzumab* and other first-generation anti-A β antibodies has been attributed to several reasons. Firstly, many patients were not A β -plaque positive in the *bapineuzumab* study owing to a lack of screening and could have suffered from a different type of dementia¹⁰⁷. Secondly, patients might have been too advanced in their pathology, and thus it was too late to slow cognitive decline. Later studies of *aducanumab* and *lecanemab* have included patients with generally higher cognition scores^{92,96,107}. Thirdly, early A β -antibodies targeted monomeric anti-A β antibodies; it is possible that targeting A β -aggregates is more beneficial. Lastly, antibodies might not have reached the target within the brain to a high enough extent because of too low either dose or overall low brain delivery. Indeed, *gantenerumab* doses have been increased in later studies¹⁰⁹, and the highest and most frequently dosed antibodies have so far proved to be the most efficient in halting cognitive decline, suggesting that high brain concentrations are needed to improve symptoms^{96,102}.

However, high doses also increase the risk of side effects. The main side effect of anti-A β antibodies is “amyloid-related imaging abnormalities” or ARIA, identified by MRI, classified into two subtypes, ARIA-E (edema) and ARIA-H (hemorrhage)¹⁰⁸. The condition can be asymptomatic; if symptoms occur, they are often mild and temporary. However, some patients that experienced more severe symptoms have been withdrawn from the clinical trials. There is a higher risk of developing this side effect for carriers of APOE- ϵ 4¹¹⁰.

Enhancing the brain delivery of therapeutic antibodies could potentially increase efficacy and lower the risk of side effects like ARIA for future immunotherapies.

Fluid biomarkers in AD

Proteins in the living brain are largely inaccessible for sampling. Therefore, finding suitable biomarkers has been a challenge in AD. The golden standard for fluid biomarkers in AD is sampling CSF by lumbar puncture. The CSF surrounds the entire brain as a protective fluid barrier in the subarachnoid space, the four ventricles, and the spinal canal. CSF is responsible for clearing waste products from the brain and thus can reflect the brain’s biochemical environment^{111,112}.

In AD patients, soluble A β ₄₂ is decreased by around 50% in the CSF as the accumulation of A β ₄₂ in the brain increases¹¹³. However, a ratio between A β ₄₂/A β ₄₀ is a better predictor of AD than A β ₄₂ alone¹¹⁴. Other common biomarkers measured in the CSF are total tau (t-tau) and p-tau levels. T-tau is an indicator of general neurodegeneration; it is elevated in AD but can also be increased in other dementias and traumatic brain injuries^{115,116}. Elevated p-tau

indicates neuronal damage and pathological tau phosphorylation in the brain¹¹⁷.

Novel biomarkers for neurodegeneration and synaptic function are also emerging. Increased CSF neurofilament (NFL) is associated with A β and tau deposition and cognitive decline¹¹⁸. Neurogranin (Ng) is a synaptic protein, and leakage to the periphery can indicate synaptic dysfunction¹¹⁹. Biomarkers for neuroinflammation have also gained interest, such as astrocytic YKL-40 and glial fibrillary acidic protein (GFAP)¹²⁰, and for microglia, soluble triggering receptor expressed on myeloid cells 2 (sTREM2)¹²¹.

CSF sampling is a relatively invasive procedure, not suitable for everyone, and sometimes declined by patients. Blood biomarkers would be more accessible, less expensive, and could be used for a broader population screening. Further, using blood biomarkers would enable faster and easier inclusion of patients in clinical trials and possibly a way to evaluate treatment outcomes. A promising blood biomarker is plasma p-tau217. It has shown high accuracy in discriminating between AD and other neurodegenerative disorders¹²² and correlates with disease progression in A β positive individuals¹²³. Another example is a novel sensitive assay for soluble A β oligomers in plasma, which predicts AD with very high accuracy¹²⁴. These methods need further clinical validation, but blood biomarkers could be a valuable tool in clinical trials and could potentially replace CSF sampling in the future.

Positron Emission Tomography in AD

Positron emission tomography (PET) remains the second most used biomarker-based diagnostic tool in AD. PET is a non-invasive molecular imaging method based on injecting a radiolabeled molecule (radioligand, or sometimes “tracer”) that binds to a target. A PET scanner detects the location of the radioligand in the body. PET is a valuable tool for gaining specific information on targets of interest, such as A β . In addition, PET can reveal the spatial distribution and quantity of pathology inside a living brain, in contrast to CSF or blood biomarkers.

PET has been vital in clinical trials for AD therapies and diagnosis, advancing research and understanding of AD pathology. The first ever A β -radioligand, Pittsburgh Compound B (PiB), was developed as a collaboration between the University of Pittsburgh (USA) and Uppsala University (Sweden), which conducted the first-in-human studies in 2004¹²⁵. PiB is derived from thioflavin T, which binds to the β -sheet structure in dense core plaques. PiB binds selectively to fibrillary A β and thus corresponds well with A β -plaque load in confirmed AD cases, while it does not bind to soluble A β or diffuse A β plaques^{126,127}. PiB is radiolabeled using carbon-11 (¹¹C), a short-lived radionuclide with a half-life of 20 min. Thus, for ¹¹C, a cyclotron facility that pro-

duces the radionuclide needs to be on-site. A second generation of A β -radioligands developed after [^{11}C]PiB are radiolabelled with fluorine-18 (^{18}F) (Florbetapir, Flutemetamol, and Florbetaben). The longer half-life of 110 minutes for ^{18}F facilitates transport from the production site to scanner sites¹²⁸. In addition, ^{18}F generally provides high-resolution images and allows for high specific activity¹²⁹.

Another widely used PET radioligand is [^{18}F]FDG (fluorodeoxyglucose, a fluorine-labeled glucose analog). [^{18}F]FDG uptake indicates glucose metabolism and is decreased in specific brain regions in different dementias; therefore, [^{18}F]FDG can aid in differential diagnosis and predict progression¹³⁰. However, [^{18}F]FDG-PET does not reveal the underlying pathological processes in AD.

A β -PET has been an essential tool in understanding the pathological trajectories in AD. A β aggregation, as measured by decreased A β_{42} levels in CSF, precedes A β -PET positivity¹³¹. Neurodegeneration and neuroinflammation biomarkers (tau, NfL, Ng, and YKL-40) rise around A β -PET positivity, suggesting A β as an initiator or early event in pathology⁸⁷. A β -PET is now standardly used in clinical trials for A β -therapies, both to make sure patients included are A β -positive, and to evaluate the treatment effects of A β -plaque clearance, for example, *aducanumab*, *bapineuzumab*, *gantenerumab*, and *lecanemab* were all assessed with A β -PET^{96,102,107,109}.

A drawback with current PET radioligands for A β is that they bind the dense core of plaques, while the evidence points towards soluble A β as more toxic. A β -plaque load plateaus early in AD, and thus A β -PET may be of limited value in assessing the later stages of the disease since it does not correlate well with symptom severity¹²⁸. In clinical trials, A β -PET-positive patients have plaque pathology, but it might be more beneficial to target A β at an even earlier stage⁸⁷. Novel therapies are more likely to affect the soluble portion of A β ; thus, there is a discrepancy between therapeutic targets and imaging targets with current PET radioligands. In addition, some patient groups with genetic mutations that do not produce dense core plaques are [^{11}C]PiB negative or show a weak signal^{127,132}. Emerging tau-PET-radioligands correspond better with disease progression compared with A β -PET in AD^{56,133}.

Antibody-based A β -PET

Antibodies and antibody-fragments, which have high affinity and selectivity, have been successfully used for oncology imaging¹³⁴. Antibody-based PET radioligands, which can bind all forms of A β , in contrast to current A β -PET radioligands that rather visualize insoluble amyloid, could improve understanding of AD progression and provide a way to follow the dynamic changes in early A β -pathology. They could also be of value for including patients in

clinical studies and a tool to evaluate the clinical effects of the emerging immunotherapies that target soluble and fibrillar A β .

Our group has been able to image A β -pathology in AD mouse models^{24,135-137} and recently rat¹³⁸ using antibody-based PET⁸⁹. Antibody-based detection of A β -pathology showed an increased signal with the age of the AD mice, while pathology was only detected in the oldest mice with [¹¹C]PiB¹³⁵. Similarly, an A β -oligomer specific peptide, radiolabeled with copper-64 (⁶⁴Cu), was able to monitor the progression of early A β pathology and had different distribution and improved contrast compared with [¹¹C]PiB¹³⁹. Antibody-based PET corresponds well with *ex vivo* examination of brain pathology in AD mice¹⁴⁰. It has also been used to evaluate A β -reduction after drug treatment and outperforms [¹¹C]PiB in detecting treatment effects^{140,141}.

Although these studies demonstrate proof-of-concept, challenges remain for antibody-based PET to be used clinically. For PET radioligands, it is important with a short blood half-life for several reasons:

1. Fast clearance of radiolabeled molecule from blood will decrease the background radioactivity originating from blood in the tissue (e.g., the brain consist of 5% blood), thus increasing the signal-to-noise ratio.
2. The biological half-life and the radionuclide's decay half-life need to be matched. In clinical PET, short-lived radionuclides, such as ¹⁸F, are used to minimize the duration of radiation exposure for the patient.
3. It is more practical and safer to do PET scanning shortly after injection to minimize the patient's hospitalization time and to avoid that the patient must be sent home between the radioligand injection and the scan, as this is associated with a risk of exposing others or contaminating the home environment with radioactivity.

However, antibodies typically have long biological half-lives, of hours to weeks, especially if they have a functioning Fc-domain and a large size. This thesis has focused on evaluating smaller formats of antibodies, with faster blood clearance, for brain PET imaging. Another hurdle with the use of antibodies for PET is that they are large molecules with limited brain delivery, and this has also been an obstacle to their use as brain PET radioligands.

Barriers of the brain

The brain is a highly protected organ; as a result, large molecules (like antibodies) are restricted from crossing the blood-brain barrier (BBB). Antibody bioavailability in the brain is low, often cited to be around 0.1% of circulating serum concentrations¹⁴². Measuring brain concentrations can be difficult; therefore, CSF is often used as a proxy for brain interstitial fluid (ISF). CSF-to-serum ratios are reported between 0.1%-0.2% for antibody-based drugs¹⁴³.

However, using CSF levels could result in overestimation of the brain parenchymal antibody concentrations¹⁴⁴⁻¹⁴⁶. Our studies using radiolabeled antibodies find that around 0.01% of the initial dose resides in the mouse brain 2 h after i.v. injection. Similar values of 0.009% of injected dose in the parenchymal cortex have also been reported elsewhere¹⁴⁷. When normalizing for the brain weight, we have observed values in the range of 0.03-0.14%ID/g mouse brain^{24,148-151}. Nevertheless, any of these estimates provide evidence that brain antibody concentrations after peripheral administration is generally low.

The BBB, also referred to as the neurovascular unit (NVU), is the largest and most highly regulated surface between the blood and the brain parenchyma and the main obstacle for antibodies to enter the brain¹⁵². The classical NVU consists of the endothelial cells of the capillary network in the brain, pericytes, and basement membrane, all enclosed by astrocytic endfeet (Fig 5 and Fig 6 A). The mesh of proteins and sugars coating the luminal side of the endothelial cells, the glycocalyx, can also be considered part of the NVU¹⁵³. In contrast to peripheral capillaries, the brain capillary endothelial cells completely lack fenestrations; instead, they are sealed with tight junctions¹⁵⁴. The tight junctions restrict the paracellular transport of molecules between blood and the brain, allowing the transport of small hydrophilic molecules or the regulated transport of immune cells¹⁵⁵.

CSF is secreted at the epithelial cells of the choroid plexus in the four ventricles and also partly mixed with interstitial fluid (ISF) from the brain parenchyma¹⁵². The CSF is turned over regularly 2-4 times a day in humans and more often in rats¹⁵⁶. The CSF is drained by a flow from the ventricles, via the cisterna magna, to the subarachnoid space; and exits the CNS via arachnoid granulations to venous sinuses and along cranial and spinal nerves to the lymphatic system¹¹¹. Blood-CSF transport is hindered by the blood-cerebrospinal fluid barrier (BCSFB) at the epithelial cells of the choroid plexus (Fig 6 B). The epithelium cells of the choroid plexus are connected by tight junctions similar to the BBB. However, the capillary endothelial cells are fenestrated, in contrast to BBB endothelial cells¹⁵⁷. Substances that can cross the BCSFB can diffuse across the ventricles' ependymal cells (Fig 6 C). Substances in the subarachnoid (SAS) CSF (Fig 6 D) can distribute into the brain via perivascular spaces (PVS) of leptomeningeal arteries¹⁵⁸. A potential transport at the capillary level allows exchange across the brain parenchyma from peri-arterial to peri-venous capillaries and clearance from the brain. It potentially involves the aquaporin-4 (AQP-4) water channel and has been referred to as the "glymphatic" system¹¹². However, the detailed mechanism of this brain clearance system is debated¹⁴⁴.

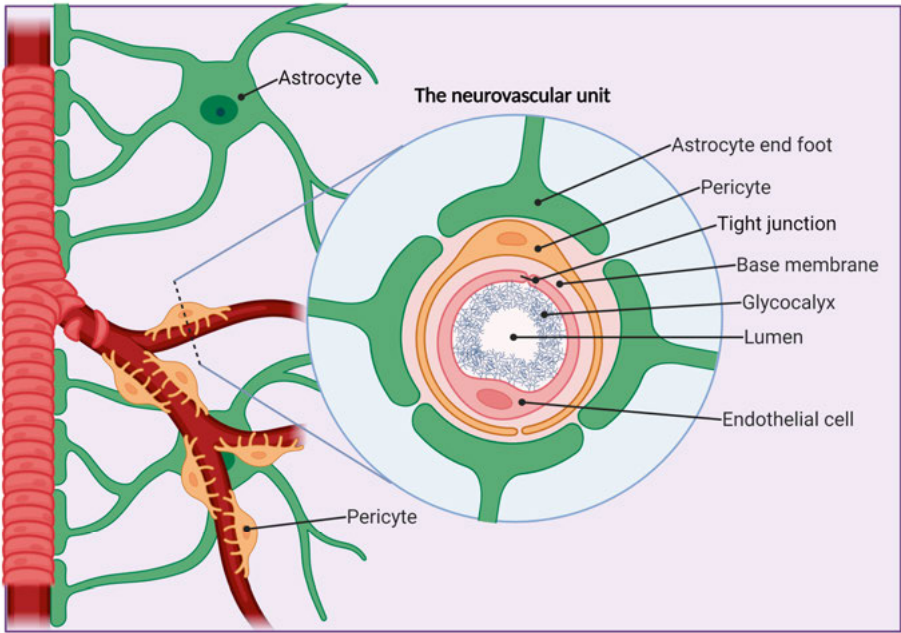


Figure 5: The neurovascular unit/the BBB at brain capillaries.

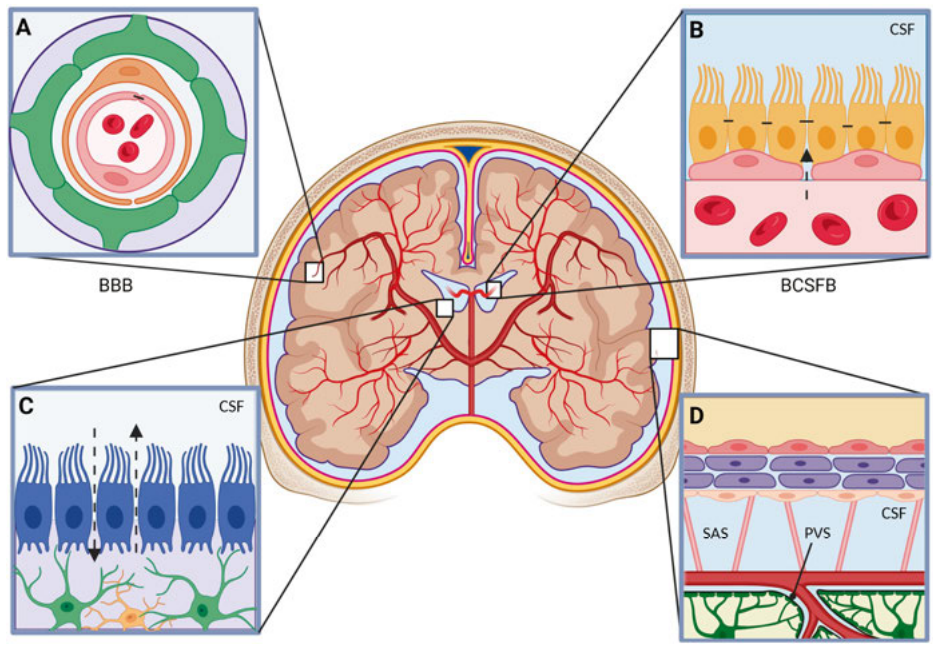


Figure 6: Illustration of the barriers of the brain **A** the BBB **B** the BCSFB **C** Ependymal layer at the ventricles **D** Arachnoid barrier and penetrating vessel in the subarachnoid space (SAS) with perivascular spaces (PVS).

Transport routes at the BBB

The NVU controls brain homeostasis allowing the passage of molecules necessary for brain cell function. Some essential molecules transported across the BBB are glucose, hormones, vitamins, insulin, leptin, and iron¹⁵⁹. The transport mechanism across the BBB depends on the properties of the molecule. Small lipophilic molecules can diffuse via the transcellular pathway across the cell membranes of the BCECs, whereas small hydrophilic molecules can be transported through the tight junctions in the paracellular pathway¹⁶⁰. Glucose and small amino acid-based molecules have specific transporter proteins, facilitating brain uptake by carrier-mediated transport¹⁵⁴. Larger molecules, like cationized albumin, can cross via charge-dependent adsorptive transcytosis (AMT)¹⁶¹, and others like insulin, low-density lipoprotein (LDL), and transferrin are transported via receptor-mediated transcytosis (RMT)¹⁶². For immunological surveillance, leucocytes can cross the BBB either through the BCECs or by the regulated opening of the tight junctions¹⁵⁵. Some small molecules are actively removed from the BCECs by efflux pumps, e.g., p-glycoprotein (P-gp). Antibodies may be effluxed from the brain via the FcRn receptor^{163,164}, but this is debated, e.g., FcRn-deficient mice do not have significantly higher brain levels of IgG¹⁶⁵.

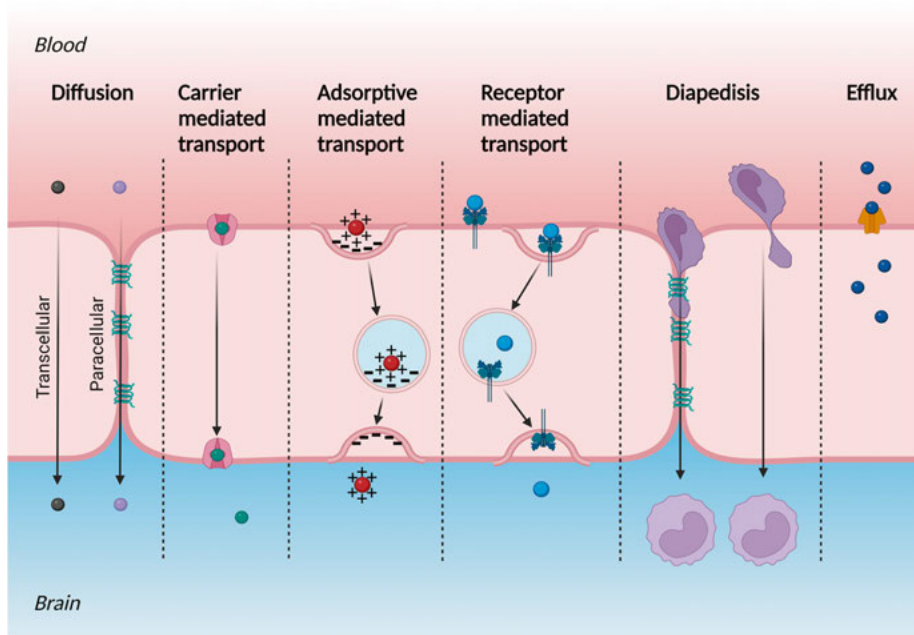


Figure 7: Transport routes at the BBB.

Receptor-mediated transcytosis

Various mechanisms to enhance the brain delivery of biological drugs have been explored. There are some techniques to disrupt the BBB, for example, based on osmotic shock or focused ultrasound^{166,167}. However, these methods are often costly and invasive and would require patient hospitalization for the procedure¹⁶⁸. A more convenient route of administration for patients could be intranasal, which has been shown to increase the brain distribution of IgG, although it is likely less efficient for larger molecules than small molecules¹⁶⁹.

The most well studied option to increase brain distribution of large molecules is to utilize specialized receptors highly expressed at the BBB via RMT. The approach is often referred to as the “Trojan horse” strategy since it uses an endogenous receptor system to transport the cargo across the endothelial cell and release it on the abluminal side. Several receptors have been explored, such as insulin¹⁷⁰, insulin-like growth factor 1 (IGF-1)¹⁷¹, low-density lipoprotein receptors¹⁷², CD98hc¹⁷³, and TMEM30a^{174,175}. However, the most well studied receptor for RMT is the transferrin receptor (TfR).

The transferrin receptor (TfR)

Iron is essential for metabolic functions, such as oxygen transport, neurotransmitter synthesis, respiration, DNA replication, and heme synthesis¹⁷⁶. However, iron can be toxic at high concentrations, and therefore there is a highly regulated system for the transportation of iron in the body and to the brain^{162,177}.

Transferrin (Tf) is a serum protein that carries iron in the form of ferric ions (Fe^{3+}). Tf has two binding sites for Fe^{3+} ; a non-bound Tf is called apo-Tf, while Tf bound to one Fe^{3+} is called mono-ferric, and two Fe^{3+} molecules di-ferric or holo-Tf¹⁶². Tf- Fe^{3+} complexes are delivered to cells via transferrin receptor 1 (TfR1), expressed on the cell surface of most cells in the body¹⁷⁸. A second TfR has also been identified, TfR2, which has a lower affinity for Tf and is not as widely expressed, mainly in liver^{179,180}. Hereafter, if the subtype is not specified, “TfR” will refer to the TfR1 protein. TfR1 is a transmembrane glycoprotein composed of two identical subunits of 90 kDa each, linked with disulfide bonds. Each subunit has three extracellular domains; the apical (A), the protease-like (P), and the helical domain (H) (Fig 8)⁹. The helical domain has the main sites for holo-Tf¹⁸¹. Holo-Tf binds with high affinity to TfR1 at physiological pH 7.4. After binding, the holo-Tf-TfR1 complex is internalized via clathrin-coated endosomes. The endosomes are acidified to pH 5.5, which results in dissociation from TfR1 and delivery of iron to the cell¹⁶².

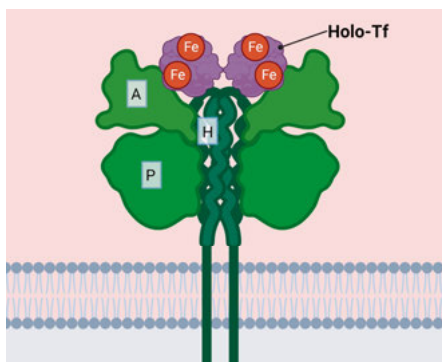


Figure 8: Transferrin receptor 1, a homodimer protein with three subdomains; apical (A), protease-like (P), and helical (H). Two holo-Tf proteins can bind the helical domain of TfR1.

Some cells have a higher demand for iron and express TfR1 to a greater extent. For example, early erythroid cells (e.g., erythroblasts, reticulocytes) require high amounts of iron for heme synthesis¹⁸². Iron is also required for cell division, and proliferating cells, such as tumor cells, express high amounts of TfR1⁹. Lastly, endothelial capillaries of the BBB have high TfR1 expression to deliver iron to the CNS, as the Tf protein cannot enter the brain without active transport¹⁸³. In 1987, it was discovered that Tf could transcytose and enter the brain parenchyma via TfR-mediated transcytosis¹⁸⁴.

TfR-mediated brain delivery of antibodies

TfR was the first and still widely used receptor for brain delivery of antibodies and other cargo in preclinical studies^{24,25,41,145,149,185–190}. A common feature for most of these antibodies is that they are bispecific; they have two targets, one for the transport across the BBB, e.g., TfR, and one for the target of interest within the brain, e.g., A β or β -secretase. Bispecific antibodies that bind TfR enter the brain via transcytosis, although the exact mechanism for parenchymal entry is still unknown. In short, the bispecific antibody circulates the blood and binds TfR on the BBB endothelial cells. After binding, the antibody and receptor are internalized via clathrin-coated vesicles^{191,192}. Proton pumps will decrease the pH of the endosome, and the antibody dissociates from TfR and can enter the brain parenchyma, where it binds the intrabrain target¹⁶². If the antibody is not dissociated, it will be sorted into lysosomes for enzymatic degradation (Fig 9)^{192,193}. Another possibility is that the antibody and receptor are recycled back to the luminal surface¹⁹⁴.

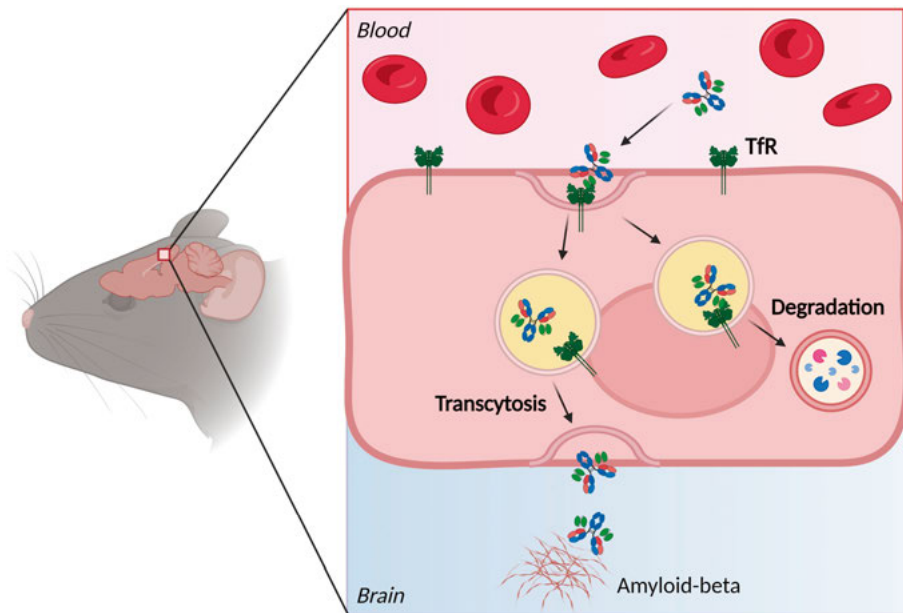


Figure 9: Schematic illustration of the transferrin receptor-mediated transcytosis or degradation of a bispecific antibody.

For Tfr-transported antibodies, several key features for optimal delivery to the brain have been established:

1. The antibody should be functional in a bispecific format, as it must bind Tfr and its main intra-brain target.
2. The antibody should preferably bind to a different epitope than Tf on the Tfr to avoid interference with the endogenous process of iron delivery to the brain. Many Tfr-antibodies bind the apical domain of Tfr^{145,188,195,196}.
3. Moderate affinity for Tfr in the nanomolar range (differing between mouse studies and doses, from 6-600 nM^{25,145,193,197}) has been suggested as optimal for brain delivery. High affinity might result in a lower ability of the antibody to dissociate from Tfr, which leads to sorting into lysosomes for degradation^{191,193,195}. In fact, the dissociation constant might be a more critical parameter than the association constant¹⁹⁷. Too low affinity might lead to poor ability of the antibody to bind Tfr at the BBB and, consequently, poor brain delivery^{195,198}.
4. Affinity can be pH dependent so that the antibody binds Tfr well at physiological pH but can dissociate at lowered pH in the early endosome^{25,199}.
5. The dose of the antibody is also an important factor. Higher affinity can increase brain uptake at low doses, e.g., tracer doses used in

PET imaging⁸⁹. While for high doses, as used in therapy, a lower affinity for TfR increases brain uptake²⁵. At non-saturable low doses, binding and brain uptake depends on affinity, while at saturable doses, lower affinity could be critical for the dissociation from TfR and entry to the parenchyma.

6. The valency of the antibody to TfR is crucial. A monovalent interaction with TfR is preferable for high parenchymal delivery^{188,192,200}. A bivalent binding to TfR is stronger due to high avidity and could cause clustering of TfR on the capillary cells and lead to intracellular sorting to the lysosomes rather than transcytosis^{188,192,196,201}. A bivalent antibody can also decrease TfR levels on cells^{193,196}.

The TfR antibody used most frequently by our research group is 8D3, a rat antibody that binds mouse TfR1 (mTfR1)²⁰². The 8D3 antibody efficiently increases the brain delivery of a protein cargo in mice, e.g., a second antibody or an antibody fragment¹⁸⁵. We have made several bispecific antibodies based on fusion to the scFv fragment from 8D3 (scFv8D3), which has a K_D of 15 nM for TfR²⁴. These bispecific antibodies are able to reach the brain parenchyma to visualize intra-brain targets by *in vivo* imaging^{24,135,137,203,204}. At low doses, an 80-fold difference in brain uptake was shown for the IgG antibody, mAb158, modified with two scFv8D3 domains, compared with the unmodified antibody²⁴. At therapeutic dosing, bispecific RmAb158-scFv8D3 reduced soluble A β aggregates in the mouse brain at similar levels to mAb158 but at a 10-fold lower dose¹⁵⁰.

Translation of TfR-antibodies

Despite many promising results in preclinical settings over the years, there has been relatively limited translation into human studies and the development of human TfR (hTfR) or cross-species reactive binders. One reason could be that binders for both mouse and human TfR have been challenging to produce. The amino acid sequence between mTfR and hTfR differs by 30% on the apical part of TfR, where most TfR-antibodies bind¹⁹⁶. There are two main strategies to study the same TfR-binder in mice and humans. The first one is to use genetically modified animals that carry the human TfR (hTfR) or apical domains^{145,195,201,205}. Recently, another approach has emerged: to develop cross-reactive TfR-binders, i.e., a protein that can bind both mTfR and hTfR. This has proved challenging for IgG-like antibodies; however, sdAbs from heavy chain-only antibodies have been developed that are cross-reactive^{149,206-208}. Potentially, the smaller size allows for binding at epitopes that are not reachable for larger antibodies²².

Even though there are challenges in translating TfR binders, there are currently a number of TfR-based BBB-shuttles in clinical studies and one approved drug, providing indications on clinical safety and efficacy. The hTfR-mAb conjugated to a lysosomal enzyme (Iduronate 2-sulfatase enzyme – IDS) for the treatment of Hunter syndrome was evaluated in phase 3 trials and approved for clinical use in Japan in 2021 (under the name Izcargo®)^{209,210}. A new format for BBB delivery, the transport vehicle (TV), with a TfR binding site on the Fc-region of human IgG, was shown to increase brain uptake in mice and cynomolgus monkeys^{145,211}. Several clinical studies for treatments based on the TV-transporter have been initiated, for example, immunotherapy activating TREM2 in AD (NCT05450549)^{190,212}. Moreover, a monovalent anti-TfR conjugate based on Roche’s *gantenerumab* (*Trontinemab*) was evaluated in a phase 1 trial (NCT04023994) in 36 healthy young participants. Preliminary reports indicated that RG6102 had an 8-fold higher CSF-to-serum ratio than *gantenerumab*, which allows a lower dose to be administered, potentially reducing the risk of side effects. There was no observed anemia or hematology-related toxicity²¹³. *Trontinemab* is currently in phase 1b/2a clinical trials in prodromal, mild, or moderate AD, expected to finish in January 2025 (NCT04639050).

Pharmacokinetics of therapeutic antibodies

Biological drugs have different and more complex physiochemical properties than small molecule drugs, which determines how the body affects the drug, i.e., pharmacokinetics (PK), and how the drug affects the body, i.e., pharmacodynamics (PD).

Like any protein, antibodies are sensitive to factors in the environment like pH, temperature, or enzymatic degradation. Therefore, they are not administered orally, as they cannot withstand the acidic environment and the proteases of the gastrointestinal tract and have limited ability to diffuse across cell membranes⁶. Antibodies are, therefore, typically administered by parenteral routes, like intravenous (i.v.), subcutaneous (s.c.), or intramuscular (i.m.) injection²¹⁴.

Antibodies are mainly constricted to the aqueous compartments of the body, such as blood, lymph, and interstitial fluid, as they are polar molecules with low tissue penetration⁶. This means that they typically have a small volume of distribution, even though they have high target affinity²¹⁴. Antibodies are mainly distributed from the blood into tissue by convection flow of fluid and sieving effects by fenestrations in the peripheral vascular epithelium²¹⁴. Antibodies are often distributed more highly to organs with sinusoidal (open pore) capillaries, such as the liver, spleen, and bone marrow²¹⁵. As described previously, the half-life of IgGs in the blood is prolonged because of FcRn-mediated recycling¹⁰.

Cells can internalize antibodies by receptor-mediated endocytosis, transcytosis, phagocytosis, and unspecific fluid phase pinocytosis^{216,217}. The elimination of IgGs can be affected by target-mediated drug disposition (TMDD). TMDD means that the binding of the drug to the target influences the target and leads to non-linear saturable elimination of the drug at low doses, while at high doses that saturate the target, linear elimination can occur^{217,218}. For TfR-antibodies, this is often referred to as TfR-mediated clearance²¹⁹. The main elimination pathway of antibodies is via lysosomal degradation into amino acids by proteases and peptidases. The body recycles the amino acids; some are secreted into the bile and feces or, if small enough, filtered in the urine²¹⁴. Full-size IgGs are too large for renal filtration; smaller antibody fragments <60 kDa can be filtered in the kidney, excreted, or reabsorbed in the proximal tubuli, and degraded²⁸.

Methodology

Recombinant expression of fusion antibodies

The antibodies studied in **paper I** and **paper III** were produced in-house by recombinant expression in human Expi-293 cells²²⁰. The DNA-sequences encoding the antibodies were cloned into a pcDN3.4 vector. Plasmid DNA was transformed and amplified in *E. coli* (Top10) cells, and the purified plasmid was transfected to Expi293 cells. The cells were incubated for 7-10 days before harvesting and purification by affinity chromatography in an ÄKTA protein purification system. Protein G columns that bind to the Fc-domain were used for IgG-like antibodies. The non-IgG-like antibody di-scFv3D6-8D3 had a histidine tag (6xHisTag) for purification with nickel ion columns¹³⁷. Polishing steps were done for di-scFv3D6-8D3 using ion exchange chromatography, which separates molecules based on their isoelectric point and the pH of the elution buffer. Finally, the antibody buffer was changed to phosphor-buffered saline (PBS) and concentrated to a suitable concentration for further experiments.

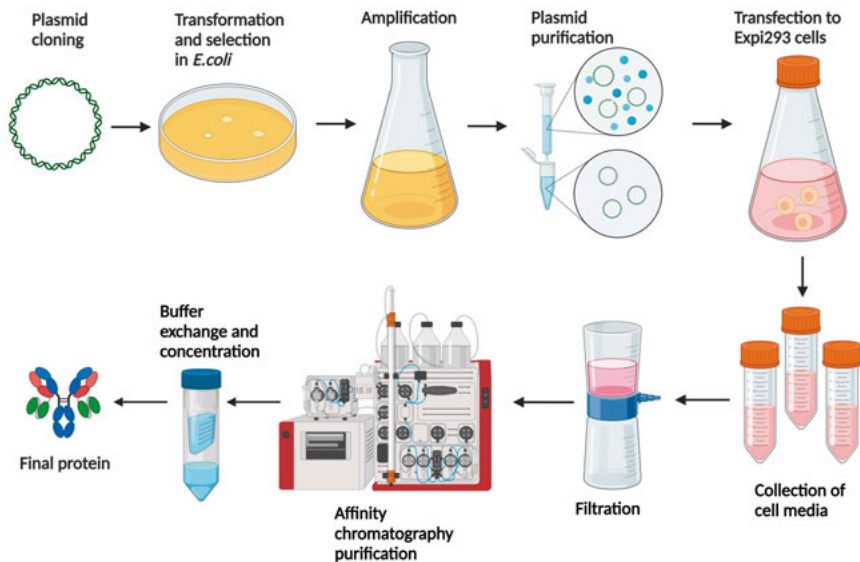


Figure 10: Schematic illustration of the protein production process.

For **paper II** and **paper IV**, the proteins were produced following similar steps as above, but not in-house. **Paper II** affibodies were produced by co-authors at the Royal Institute of Technology (KTH, Stockholm). Affibodies were expressed in an *E.coli* system, while scFv8D3-fused affibodies were expressed in Chinese Hamster Ovary (CHO) cells. Both affibodies were purified based on HisTag binding. For **paper IV**, VHH FP_{FC}-constructs were produced (by Thermo Fisher Scientific) in Expi293 cells and purified by affinity chromatography using a protein A column. The FP_{scFv} proteins were expressed in CHO cells and purified using HisTag-binding columns (by Genscript Corp.).

Animals

All procedures were approved by the Uppsala Country Animal Ethics board (5.8.18-13350/17 and 5.8.18-13350/20) following the legislation and regulations of the Swedish Animal Welfare Agency and European Communities Council Directive of 22 September 2010 (2010/63/EU).

Wild-type (WT) C57Bl/6 mice were used for all of the studies in this thesis. In **paper I**, we studied the brain pharmacokinetics of bispecific antibodies in C57Bl/6 WT mice. However, in **papers II, III, and IV**, A β expressing mice maintained on the C57Bl/6 strain were included to study the impact of A β pathology.

Three different mouse models with A β pathology were used in this thesis. Two A β PP transgenic mouse models, harboring the Swedish (A β PP KM670/671NL) APP mutation (tg-Swe) or a combination of the Arctic (A β PP E693G) and the Swedish APP mutations (tg-ArcSwe). The mutation in tg-Swe mice leads to increased production of A β and a later onset (at 12 months) of A β plaque pathology, but with rapid progression from the time of plaque deposition²²¹. In tg-ArcSwe mice, increased A β production in combination with an aggregation-prone A β mutant produces an earlier onset of plaque pathology (around 6 months) with dense core A β -plaques⁸⁰. These two models are suitable for studying the variation in A β pathology, from plaques to soluble oligomers. However, the dense core plaques in the tg-ArcSwe model more closely resemble the pathology found in humans, while tg-Swe pathology is unstructured and less dense^{221,222}.

In **paper IV**, a knock-in mouse model *App*^{N-L-GF} carrying three APP mutations, Swedish, Arctic, and the Iberian (I716F) mutation, was used to study the VHH-fusion proteins for A β imaging. In addition to the Swe and Arc mutations, the Iberian mutation causes an elevated A β ₄₂/A β ₄₀ ratio. *App*^{N-L-GF} mice display cortical A β deposits already at 2-4 months²²³. They have a dominating diffuse A β -plaque pathology, with smaller and less abundant dense cored plaques²²⁴.

Radiochemistry

Radiolabeling is a commonly used method, as it has a low limit of detection, enabling measurement of minute amounts of radiolabelled compounds. Radiolabeled proteins can be used for pharmacokinetic studies or radioimaging with techniques like PET. The half-lives and type of radioactive emission of the radioisotope determine how it can be used. Iodine-125 (^{125}I) has a half-life of 59.5 days, making it suitable for *ex vivo* tissue studies for a few weeks - to months after administration.

Paper I-IV utilized ^{125}I -iodinated fusion proteins to study distribution in tissues *ex vivo* by different radiosensitive methods. There are three chemical steps for the radioiodination of proteins. First, the radioiodide is oxidized by an oxidizing agent, and the oxidized radioiodide will substitute a hydrogen atom with an electrophilic attack on the protein's phenolic rings of tyrosine groups. Lastly, a reducing agent removes the excess oxidized iodine and stops the reaction. Radioiodination by the Chloramine T method (**paper I-IV**) was developed in the 1960s and is still widely used²²⁵. Here, chloramine T is used as an oxidizing agent and sodium metabisulphite as a reducing agent.

One of the aims of this thesis was to investigate proteins compatible with short-lived radionuclides that are relevant for clinical use. One such radionuclide is fluorine-18 (^{18}F), with a half-life of 109.7 minutes. Click chemistry was awarded the Nobel Prize in 2022²²⁶. It allows stable ligation of two molecules. We have used this strategy to achieve ^{18}F -radiolabeling of proteins, using trans-cyclooctene (TCO)-modified antibodies that click with a [^{18}F]tetrazine¹³⁶. The reaction is irreversible, biocompatible, and provides high selectivity and fast reactivity.

ELISA

Enzyme-linked immunosorbent assay (ELISA) is a widely used and sensitive method to detect proteins in biological samples. Different setups can be used; direct ELISA, indirect ELISA, sandwich ELISA and competition ELISA (Fig 11). Indirect ELISAs were used regularly as quality control to determine antibody and affibody binding to A β and TfR before and after radiolabeling. In an indirect ELISA, the target protein adheres to the bottom of the plate wells. Sample protein is added in serial dilution and detected by horseradish peroxidase enzyme (HRP) conjugated secondary antibodies. Adding K blue aqueous TMB substrate as a developing agent enables spectrophotometric measurement. Sandwich ELISA was used to determine the concentration of antibody or affibody in **paper I-III**. Here, the plates are coated with a capture antibody, creating a “sandwich” of the sample between the capture and detection antibody. However, this method requires two antibodies to detect and capture the protein of interest sufficiently. Competition ELISA was used in **paper I** to

evaluate mTfR binding before and after radiolabeling of di-scFv3D6-8D3. Serially diluted sample protein is incubated in competition with a constant concentration of biotinylated sample protein. The biotinylated sample protein is detected with HRP-conjugated streptavidin. The higher concentration of the competing functional sample, the lower concentration of biotinylated protein will be detected.

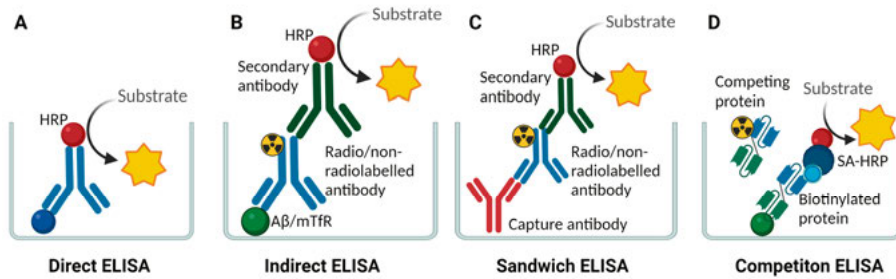


Figure 11: Different ELISA setups. In this thesis, the setups in **B**, **C**, and **D** were used.

LigandTracer®

LigandTracer® provides real-time measurements of protein-to-protein interactions on immobilized proteins or proteins expressed on cells²²⁷. A Ligand-Tracer-Grey instrument was used in **paper I**, as it can detect low-energy γ -radiation from iodine-125 labeled proteins. The target protein is coated in a defined area on a petri-dish, while a non-coated area is defined as the background. The petri-dish is placed in a tilting position, and the radiolabeled sample protein is added to the dish (Fig 12). Signal (target minus background) will be recorded once per rotation of the tilting petri-dish to measure binding interaction in real-time. From the resulting target binding curve, kinetic parameters can be calculated, such as on- (K_a) and off-rates (K_d) and affinity (K_D).

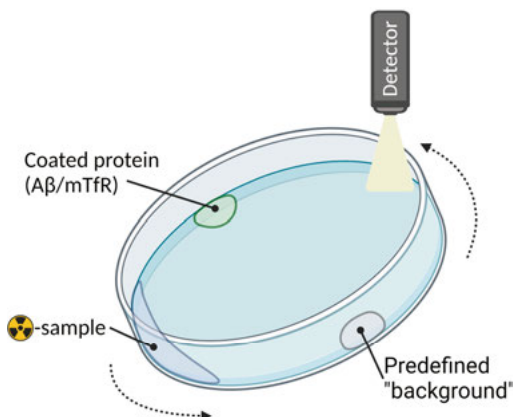


Figure 12: Schematic illustration of Ligand Tracer setup. The target protein and background area are on opposite sides of a petri dish. The sample is rotated, and a detector measures the bound protein at the target and background areas.

Immunostaining

Immunostaining is used to visualize proteins present in *post-mortem* tissue using antibodies. This method was used throughout **paper I-IV**. The tissue is sectioned into thin micron-sized slices. The sections were prepared from frozen brains in a cryostat that maintains the sample at -20°C . Before the staining, the sections were mounted onto microscope glass slides and fixated using 4% paraformaldehyde (PFA) or ice-cold methanol. The protocol includes a blocking step, usually with serum that contains antibodies that bind to non-specific sites and “block” them. Thereafter, primary antibodies that recognize the specific protein of interest are incubated with the tissue. Fluorescently labeled secondary antibodies were used to detect the primary antibodies' species, thereby visualizing the target protein under the microscope.

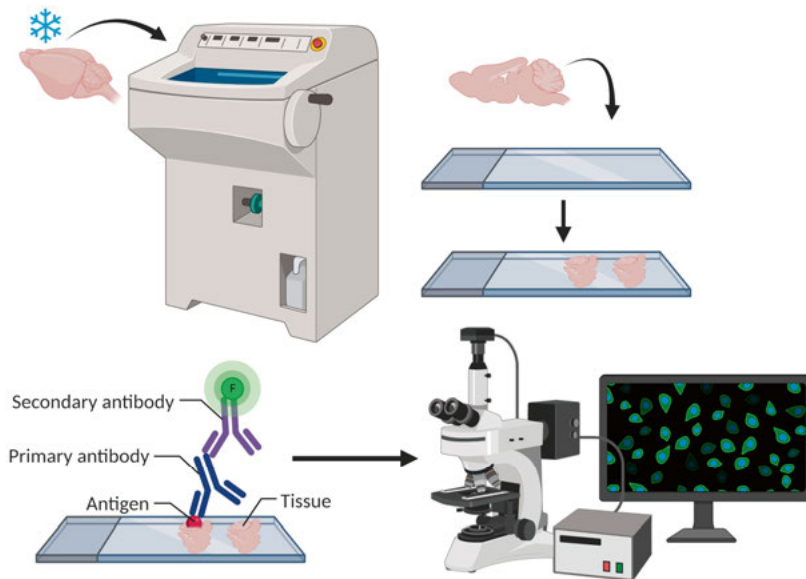


Figure 13: Cryosectioning and immunostaining of mouse brain tissue. Brains are sectioned in a cryostat at -20°C . The sections are placed on microscope glass slides. The sections are stained using primary antibodies against the desired target and secondary antibodies (fluorescently labeled) against the primary antibody. Stained sections can be imaged in a fluorescence microscope.

SDS-PAGE and immunoblotting

It is possible to separate proteins by molecular size in sodium dodecyl sulfate-polyacrylamide gel electrophoresis (SDS-PAGE). SDS is an anionic surfactant that masks the proteins' intrinsic charge by covering the protein with a

negative charge. Thus, separation is based solely on molecular size as the protein travels toward the anode at different speeds through the porous polyacrylamide gel. Gels are often designed so that smaller molecules travel faster as they encounter less resistance in the gel. SDS can be replaced with lithium-dodecylsulfat (LDS), which is more soluble and can tolerate high salt concentrations. A reducing agent can be added to break disulfide bonds; however, non-reducing conditions are often used to detect intact IgG antibodies²²⁸.

After SDS-PAGE, the proteins can be transferred to a membrane by an electric current. The gel and membrane are "sandwiched" between blotting filters and sponges to keep the system saturated with transfer buffer. An electrical current causes the proteins to migrate from the gel into the membrane. A blocking step is required to minimize nonspecific binding to the membrane, usually with a solution high in protein, like non-fat milk. Primary antibodies are incubated with the membrane to detect a protein of interest, usually overnight at 4°C. The following day, secondary antibodies are added, enabling either HRP-based chemiluminescence or fluorescence detection.

Autoradiography

Autoradiography refers to techniques based on visualizing the radioactivity in a sample. Different types of autoradiography were used in this thesis;

Ex vivo autoradiography

Ex vivo autoradiography reveals radioactivity distribution in a tissue *post-mortem*, for example, to measure the radioactivity from radiolabeled antibodies in the brain after systemic administration. Traditionally, radioactivity was visualized using photographic or X-ray films and developing solutions. Today, the image can be scanned by a laser beam and directly digitalized. The radioactive cryo-sectioned tissue of interest is exposed to a phosphor imaging screen, which captures the energy from the radiation. The exposure time is relative to the radioactive sample's expected amount of radioactivity and half-life. When the plate is developed in a phosphor imaging system, scanning with a red laser will release the energy as blue light, producing a digital visual representation proportional to the amount of radioactivity. These images were converted from grayscale with a lookup table (LUT) to represent the radioactivity intensity (Fig. 14 a).

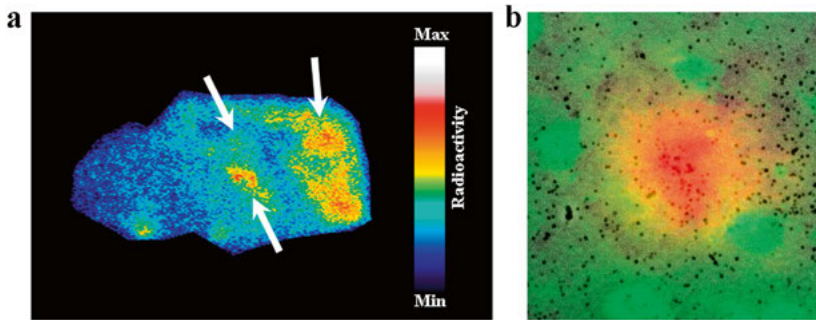


Figure 14: **a** Example of *ex vivo* autoradiography in tg-Swe sagittal brain section, radioactivity derived from the bispecific antibody [^{125}I]mAb3D6-scFv8D3 24 h after injection, mainly accumulated around areas with $\text{A}\beta$ pathology (white arrows; cortex, hippocampus, thalamus). **b** Example of nuclear track emulsion image, showing immunofluorescent staining of $\text{A}\beta$ plaque in red and neuronal marker (NeuN) in green. Black puncta are developed metallic silver grains activated by the ^{125}I -radiolabelled antibody.

Nuclear track emulsion (NTE) autoradiography

Nuclear track emulsion (NTE) is a high-resolution autoradiography technique, often referred to as “microautoradiography” (MARG)²²⁹. The advantage of this method is that it is possible to visualize interactions on a microscopic level and capture very low concentrations of radiolabeled compound. The method was used throughout **paper I-IV**, qualitatively and semi-quantitatively. Tissue sections containing radiolabeled compounds are submerged in a photographic emulsion, so a thin layer covers the slide. The emulsion consists of silver halide crystals of uniform size in a gelatin matrix. The silver halide crystals absorb ionizing radiation (radioactivity) that activates them. However, light can also activate the crystals, meaning the procedure must be done in a dark room. The crystals activated by radioactivity will form so-called “latent image centers” consisting of free electrons, halide ions, and clusters of silver atoms. These activated latent image centers will be reduced to metallic silver grains (0.2 μm) by the photographic development process performed after a few weeks of exposure. The reduced silver grains appear as black puncta, representing areas where the radiolabeled antibody is situated. The NTE can be imaged in a light microscope, and the tissue can be stained by immunohistochemistry, or immunofluorescent markers before or after nuclear track emulsion, to visualize structures and cell types (Fig 14 b).

In vitro autoradiography

In vitro autoradiography uses the same principle as *ex vivo* autoradiography, only instead of injecting a radiolabeled compound, it is done by applying the

radioactive sample directly on a blank tissue section. This approach was used in **paper II** with radiolabeled affibodies. It follows blocking and washing steps similar to immunohistochemistry, but the detection is direct through the radiolabeled primary antibodies. This allows visualizing the binding of the radiolabeled compound on tissue *in vitro*. This means that there is likely higher access to intracellular and extracellular structures, such as A β plaques, due to the sectioning of the tissue. In addition, the amount of injected radiolabeled antibody is restricted *in vivo* by the BBB, but the availability of targets is not affected by the BBB *in vitro*.

Capillary depletion

When studying brain delivery of a compound, it may be difficult to distinguish between parenchymal compound and compound within the blood of the brain, adsorbed to or within the endothelial cells of the brain vasculature¹⁵⁶. Many studies measure total brain concentrations, which contain the vasculature compartment of the brain, and thus could overestimate the amount of antibody that reaches brain parenchyma. The capillary depletion technique separates the brain capillaries from the brain parenchyma and allows quantitative estimation of the partitioning between these two compartments for molecules that transcytose at the BBB.

Capillary depletion was first developed by Triguero *et al.*, published in 1990²³⁰. The original method was developed for rats but was soon adapted to mouse brain²³¹. Capillary depletion has been applied frequently in various studies of BBB transcytosis^{186,200,201,232–236}. The technique can be used with *in situ* brain perfusion or after peripheral administration of the compound of interest.

The separation of brain capillaries and brain parenchyma is based on density gradient centrifugation of a brain homogenate dissolved in a polysaccharide solution. In short, the mouse brain cortex is dissected and minced on a petri dish in ice-cold buffer. The minced brain is homogenized in a glass dounce homogenizer, and polysaccharide solution is added before centrifugation at 4°C. Three fractions form after centrifugation; a fatty fraction of, e.g., myelin, a fraction of parenchymal cells depleted from the microvasculature, and a pellet enriched with microvasculature. The supernatant and pellet are separated, and the compound is measured, e.g., by radioactivity in a gamma counter. The relative distribution in these fractions can be useful for understanding the parenchyma-to-capillary ratios of different compounds and estimating the efficiency of brain delivery.

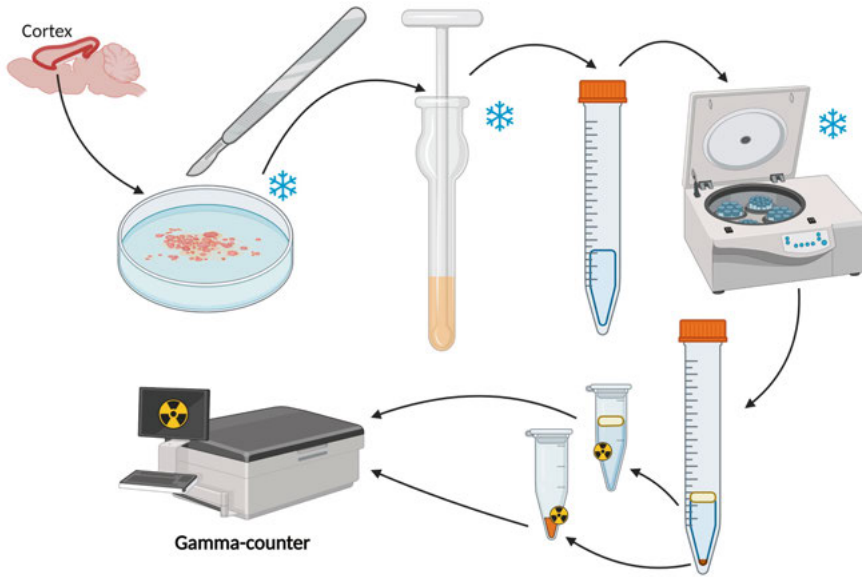


Figure 15: Schematic representation of the steps in capillary depletion.

PET

PET is a non-invasive functional imaging technique that can be performed *in vivo* in animals or humans. The method is frequently used in oncology (medical imaging of tumors and searching for metastases), for diagnosing dementias, and in preclinical studies.

PET is based on injecting a radiolabeled compound (radioligand) that binds to a target of interest. Radioligands are often pharmacologically active compounds that bind specifically to a target in the body, but they are usually administered at a low non-pharmacologically relevant dose (tracer dose).

When the radionuclide used for radiolabeling decays, a proton in the nucleus is converted to a neutron, releasing a positron (β^+) in the process. When the positron collides with a negative electron in the surrounding tissue, they annihilate and emits two gamma-ray photons at a 180° angle from each other. Two photos hitting a detector ring at opposite sides simultaneously (within nanoseconds) are recorded as an annihilation event and used to calculate the original position of the radioligand in the body.

PET data is often displayed as standardized uptake value (SUV). SUV is calculated by equation 1:

$$SUV = \frac{C(t)}{ID/BW} \quad \text{Eq.1}$$

Where $C(t)$ is the decay-corrected radioactivity concentration in a region of interest at time t , ID is the decay-corrected injected radiodose of the radioligand, and BW is the body weight of the patient. SUV thus represents the radioactivity concentration in a tissue of interest in relation to injected dose per gram body weight. If the SUV is $= 1$, the average tissue radioactivity is the same as the average whole-body radioactivity, while if it is >1 , the tissue has a higher radioligand concentration, and if it is < 1 , the tissue has a lower radioligand concentration. SUV relative to a reference region that lacks pathology, SUV_R, can also be used to estimate uptake associated with pathology.

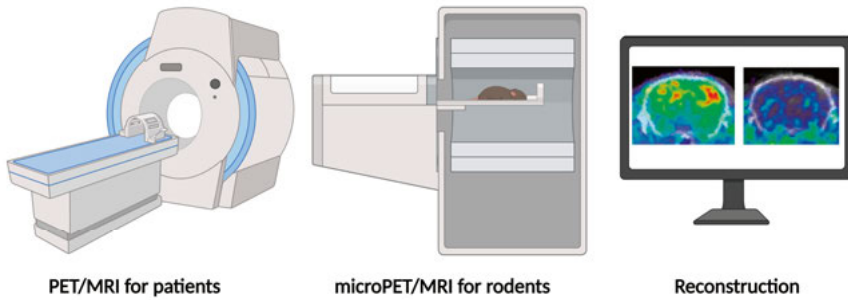


Figure 16: Positron emission tomography scanners for patients and rodents.

In *ex vivo* studies in **paper I-IV**, we use similar outputs as the SUV, i.e., the *% dose corrected* (Eq.2) or *% dose and body weight corrected* (Eq.3) radioactivity concentrations:

$$\% \frac{ID}{g} = \frac{\text{measured radioactivity per gram tissue}}{\text{total injected radioactivity}} \times 100 \quad \text{Eq.2}$$

$$\% \frac{ID}{g} (bw) = \frac{\text{measured radioactivity per gram tissue}}{\text{total injected radioactivity per gram animal}} \times 100 \quad \text{Eq.3}$$

Aims

The overall aim of this thesis was to evaluate factors important for the brain delivery of TfR-transported antibody-based proteins for use as PET radioligands for imaging of A β .

More specifically, the aim of **paper I** was to study the brain pharmacokinetics of two BBB-penetrating antibody-based proteins differing in size and avidity within the first 24 h after administration. We wanted to know if the faster systemic clearance of the smaller non-IgG antibody (a property beneficial for PET imaging) was also reflected in the brain compared with the IgG-based bispecific antibody.

In **paper II**, we explored brain delivery and retention to A β of even smaller proteins associated with faster blood kinetics than the previously studied proteins. The specific aim was to study A β -protofibril targeted antibody-mimicking proteins (affibodies), with or without conjugation to a TfR-transporter, in WT and two transgenic AD mouse models, to evaluate their potential as PET imaging agents.

In **paper III**, observations regarding plasma distribution and age differences in the brain delivery of the bispecific antibodies from previous studies led to the aim of investigating how age, blood cell binding, but also dose and pathology influenced the brain delivery of a TfR-transported A β -antibody.

In **paper IV**, we aimed to evaluate new TfR-transporter proteins, including human-mouse cross-reactive TfR binders for translatability, that were of smaller size and lower TfR affinity, with faster clearance from the blood. The studied TfR-binders were based on single domains from heavy chain antibodies (VHH) and were combined with an A β -binder (scFv3D6) for evaluation as an A β -PET imaging radioligand.

Summary of papers I-IV

Paper I

In **paper I**, we studied the brain pharmacokinetics within the first 24 h after administration of two BBB-penetrating antibody-based proteins that differed in size and avidity.

The IgG-like antibody mAb3D6-scFv8D3 (210 kDa) was compared with the smaller non-IgG-like tandem protein di-scFv3D6-8D3 (58 kDa). The larger mAb3D6-scFv8D3 is a full-sized IgG, with an intact Fc domain, based on 3D6, which binds the N-terminus of A β . It also has two scFv fragments, based on 8D3 (scFv8D3), which bind mouse TfR, attached by linkers on the light chains of the 3D6 antibody. The smaller antibody di-scFv3D6-8D3 consists of two scFvs, one from 3D6 and one from 8D3, joined by a linker, thus binding A β and mTfR monovalently. Di-scFv3D6-8D3 does not have an Fc-domain, and the smaller size results in a shorter half-life in the blood. Di-scFv3D6-8D3 was developed as an antibody-based PET radioligand¹³⁷.

The lack of Fc-region likely influenced di-scFv3D6-8D3's blood half-life, together with its smaller size, as it displayed 2-fold faster blood clearance compared with mAb3D6-scFv8D3. The faster systemic clearance was also reflected in the brain, as the exposure was 2-fold lower for [¹²⁵I]di-scFv3D6-8D3 compared to [¹²⁵I]mAb3D6-scFv8D3. Furthermore, peak antibody concentration in brain (C_{\max}) was observed earlier for [¹²⁵I]di-scFv3D6-8D3 compared with [¹²⁵I]mAb3D6-scFv8D3. After net elimination started for respective antibody, the rate of elimination from brain was similar for both antibodies, despite their difference in size. [¹²⁵I]mAb3D6-scFv8D3 showed a higher degree and prolonged association with brain capillaries throughout the study period, as shown by both capillary depletion and nuclear track emulsion. When correction was made for the capillary/parenchymal partitioning, brain concentrations 2 h post-injection did not differ in the parenchyma between [¹²⁵I]mAb3D6-scFv8D3 and [¹²⁵I]di-scFv3D6-8D3. We also observed that the *in vitro* binding to mTfR1 was 5-fold higher for [¹²⁵I]mAb3D6-scFv8D3 compared to [¹²⁵I]di-scFv3D6-8D3. This was somewhat surprising since we previously had shown that [¹²⁵I]mAb3D6-scFv8D3 was sterically hindered from bivalent binding in ELISA²⁴. However, we speculate that [¹²⁵I]mAb3D6-scFv8D3 was able to bind bivalently at a high concentration of mTfR1, both *in vitro* and potentially *in vivo* at the BBB, causing a higher degree of capillary association.

In conclusion, the small [125 I]di-scFv3D6-8D3 showed faster elimination from blood, a lower maximum brain concentration, a faster peak concentration, a larger relative distribution to parenchyma, and a net elimination from brain at an earlier time point after injection compared with the larger [125 I]mAb3D6-scFv8D3. However, the elimination rate from brain did not differ between the two bispecific antibody-based proteins, consistent with elimination from the brain via perivascular bulk flow. The study also indicated that [125 I]di-scFv3D6-8D3 displayed lower avidity than [125 I]mAb3D6-scFv8D3 towards mTfR1 *in vitro* and potentially *in vivo*. Thus, small size and likely lower mTfR1 avidity are important for fast parenchymal delivery, while the elimination of brain-associated bispecific antibody may not be dependent on these characteristics.

Paper II

In **paper II**, we studied affibodies, i.e., antibody-mimicking proteins, around 20 times smaller than IgGs. Affibodies have desirable properties regarding size, chemical stability, and blood half-life, suitable for imaging applications. Affibodies targeting the aggregated forms of A β could potentially be developed into therapeutics or positron-emission tomography (PET) imaging agents for pre-symptomatic detection of A β .

Two A β -protofibril targeted affibodies were fused to the mTfR1-binder scFv8D3, yielding the four affibody constructs evaluated in **paper II**: Z5, Z1, scFv8D3-Z5, and scFv8D3-Z1.

The affinity estimation from ELISA indicated that the affibodies had a 12-35 nM affinity for A β protofibrils and largely retained binding after the fusion to scFv8D3. However, the affinity to A β -protofibrils was around 100-fold lower than the 58 kDa antibody-based construct di-scFv3D6-8D3. Also, the binding to mTfR differed from di-scFv3D6-8D3, with more than 20-fold higher binding of the scFv8D3-fused affibodies.

The total brain concentrations 2 h after administration of the unmodified affibodies Z5 and Z1 showed more than 10-fold higher brain concentrations than regular IgG antibodies²⁴. However, nuclear track emulsion indicated that the radiolabeled affibodies without scFv8D3 were clustered in larger brain vessels and were not detected in the parenchyma, possibly indicating that the affibodies could not cross directly at the BBB. This was also supported by the very low retention of Z5 and Z1 in the brain 24 h after injection, both in WT and AD mice.

In **paper II**, we observed that scFv8D3 enhanced the brain and parenchymal delivery of affibodies. However, scFv8D3-Z5 suffered from an additional protein that could not be removed in the purification, potentially causing an underestimation of the brain uptake of scFv8D3-Z5. Parenchymal distribution for the scFv8D3 affibodies was higher than Z5 and Z1 and similar to di-

scFv3D6-8D3, with scattered signal in both capillaries and parenchymal regions 2 h after injection. This indicates that scFv8D3-fusion of affibodies can enhance brain delivery. Moreover, fusion with scFv8D3 also increased the half-life of the affibodies, likely because of peripheral binding to TfR, potentially giving the affibodies more time to penetrate the BBB and bind to their target.

In vitro autoradiography of the affibodies Z5 and scFv8D3-Z5 indicated pathology-related binding to AD-mouse brain sections. The brain retention was greater for the scFv8D3-fused affibodies 24 h after injection than the non-fused affibodies. A trend towards higher retention in the AD mice was also observed for scFv8D3-Z5, potentially related to A β interaction; however, the difference did not reach statistical significance ($p = 0.06$). In addition, the nuclear track emulsion experiments could not support a specific accumulation around A β -plaques.

In conclusion, the affibodies had enhanced brain delivery after scFv8D3-fusion. Non-fused affibodies accumulated in brain vasculature, resulting in high total brain concentrations but low parenchymal interaction with A β . For the fused affibodies, a suboptimal balance between a high TfR1 affinity and a low A β affinity resulted in a low ability of the affibodies to differentiate between WT and AD mice 24 h after injection. Future studies should focus on improving small protein affinity to A β .

Paper III

In **paper III**, we studied how different factors influenced brain delivery of the monospecific mAb3D6 and the bispecific mAb3D6-scFv8D3; age, dose, binding to blood cells, and A β -pathology.

Young (3-5 months) and aged (17-20 months) WT and tg-ArcSwe mice were injected with ^{125}I -labeled mAb3D6-scFv8D3 or mAb3D6. Three different doses were used in the study, 0.05 mg/kg (low dose), 1 mg/kg (high dose), and 10 mg/kg (therapeutic dose), with equimolar doses for mAb3D6. The antibodies' whole blood, blood cell, plasma, spleen, and brain concentrations were evaluated 2 h post-administration. Isolated brains were studied by autoradiography, capillary depletion, and nuclear track emulsion to investigate the intrabrain distribution further. An *in vitro* binding study was also done in blood isolated from young and aged WT mice.

Age-dependent differences in blood and brain concentrations were observed for the bispecific antibody, mAb3D6-scFv8D3. The aged mice showed lower brain bispecific antibody concentrations compared to young mice. These differences were not observed for a regular A β antibody, mAb3D6, indicating that differences were TfR-related. This was further supported by increased TfR levels in brain capillary enriched samples from the young mouse brains compared with the aged, as measured by Western blot, and that

[¹²⁵I]mAb3D6-scFv8D3-derived signal at the capillaries were more concentrated in young mice compared with the aged. Our results also indicated that there was no widespread antibody leakage to the brain at old age for the mAb3D6-injected animals but that there were local leakages and retention of [¹²⁵I]mAb3D6 at vascular A β -pathology. Blood cell concentrations were increased in the aged mice. The increased blood cell concentrations could indicate that aged mice had lower availability of the bispecific antibody in plasma, as suggested by *in vitro* study of [¹²⁵I]mAb3D6-scFv8D3 plasma-blood-cell distribution. Increased blood cell distribution was more pronounced for the low-dosed mice. Low-dosed mice also had an increased relative parenchymal delivery of the bispecific antibody, as indicated by both capillary depletion and nuclear track emulsion. Tg-ArcSwe mice did not differ significantly in brain antibody uptake from WT at this early time point, indicating that A β -pathology did not influence the early brain distribution of the bispecific antibody. Thus, age, dose, and potentially blood cell binding of bispecific antibody were important factors determining brain delivery, while genotype was not.

The study showed that young mice had increased brain concentrations of a TfR-targeting antibody compared with aged mice. This is relevant, as new immunotherapies are often first tested in young individuals, which could lead to an overestimation of brain delivery. Additionally, a lower dose was associated with higher relative BBB penetration; thus, the study demonstrated dose as a significant factor for parenchymal delivery. The study is also the first to our knowledge that describes an increase in antibody binding to blood cells in aged mice.

Paper IV

In **paper IV**, we describe novel llama antibody-based VHH constructs for transcytosis across the BBB. Both mouse (m), human (h), and cross-reactive mouse and human TfR1-binders were evaluated *ex vivo* after ¹²⁵I labeling.

Two cross-reactive VHHs towards both mTfR and hTfR were used, together with exclusive binders of mTfR or hTfR; thus, four different fusion proteins (FPs) were compared initially. The VHHs were designed in a bivalent format, coupled with a human Fc-fragment, for increased protein stability to prolong the circulation time in the blood (FP_{Fc}). In the next set of experiments, single VHHs were fused with the A β binder, scFv3D6, either at the C-terminus or the N-terminus of scFv3D6 (FP_{scFvA} or FP_{scFvB}, respectively). *In vitro* binding was assessed by ELISA and surface plasmon resonance (SPR). All FPs were radiolabeled with iodine-125 (¹²⁵I) and studied *ex vivo* 2 h, 6 h, or 24 h after injection in WT and AD mouse model *App*^{NL-G-F}. Brain, blood, plasma, and organ concentrations of the ¹²⁵I-radiolabeled FPs were measured

in a γ -counter. Autoradiography, nuclear track emulsion, and immunofluorescent stainings were used to study the distribution of the proteins.

The FP_{Fc} proteins displayed significantly higher brain uptake (around 1-3%ID/g_{brain}) compared to non-TfR-targeting IgGs (0.03%ID/g_{brain})²⁴, indicating that they had *in vivo* binding to mTfR. The hTfR binder did not show binding to TfR on mouse capillaries and had a low brain concentration (0.17%ID/g_{brain}), in line with what is expected for a VHH without active transport. The monovalent fusion antibodies with scFv3D6 had lower brain concentrations, and FP_{scFv}B-constructs (fusion of the VHH to the N-terminus of scFv3D6) showed higher potential at delivering the protein to the brain. There were clear differences in brain concentrations of FP_{scFv} between WT and *App*^{NL-G-F} mice 24 h after administration. For one of the FPs, FP_{scFv}1B, this difference could be seen already after 6 h in *ex vivo* studies. This protein also showed consistently higher relative parenchymal delivery compared to the other FPs before and after fusion to scFv3D6. This could be explained by its higher dissociation rate, as measured in SPR.

We showed that cross-reactive VHH-based BBB-shuttles are promising for brain delivery and that they can successfully be fused with an A β -binding scFv-fragment, maintaining high brain and parenchymal delivery. The cross-reactive nature allows for a more straightforward translation from a preclinical to a clinical therapeutic protein. The FP_{scFv}-constructs were able to differentiate between WT and AD-model mice *ex vivo*, and for FP_{scFv}1B, already after 6 h. PET imaging that can distinguish AD from WT has not been achieved at 6 h (within the time frame feasible for short-lived radionuclides such as ¹⁸F) with radiolabeled antibodies that are transported via TfR previously. Thus, these novel VHH-based constructs are promising for future PET imaging using short-lived clinically compatible PET radionuclides.

Results and discussion

Factors influencing transferrin receptor-mediated brain delivery

The papers within this thesis contribute to knowledge about TfR-transported antibodies in the brain and to increased understanding of which factors are important for their use as PET radioligands or therapeutics. The studies started by exploring the difference in the pharmacokinetics of a “small” and a “large” antibody, but we became increasingly aware of the complexity of the interactions that exist for this class of proteins. Therefore, here I summarize and discuss the main factors studied in this thesis.

Does size matter?

The first successful antibody-based brainPET performed by our group was with an F(ab')₂ fragment of protofibril-specific h158 antibody (humanized mAb158), conjugated to the TfR1 antibody 8D3; 8D3-F(ab')₂-h158¹³⁵. The molecular size of 8D3-F(ab')₂-h158 was 270 kDa, its half-life in blood was 15 h, and it could discriminate AD from WT mice three days after injection when circulating radiolabeled antibody had cleared from the blood.

Next, a slightly smaller (210 kDa) recombinant mAb158-based antibody with two scFv of 8D3 attached at the light chains was developed²⁴. The antibody had an intact mouse Fc-domain, which prolonged its blood half-life to around 19 h, but a PET image displaying A β pathology was still achieved three days after injection. The third bispecific protein was the Tribody, based on two scFvs of mAb158 and a Fab-8D3, with a size of 110 kDa and a blood half-life of 9 h. With this antibody, PET scanning performed two-three days after injection could reveal differences between AD and WT mouse brains²⁰⁴. The strive to reduce the time between injection and scan even further led to the development of di-scFv3D6-8D3 of 58 kDa, which also lacked an Fc-domain, and had a half-life of 3 h and could image A β within one day of injection (14 h)¹³⁷.

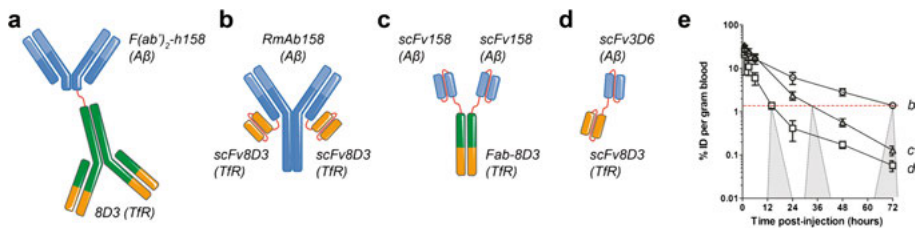


Figure 17: Antibody constructs for antibody-based PET produced by our group **a** 8D3-F(ab')₂-h158 **b** RmAb158-scFv8D3 **c** Tribody **d** di-scFv3D6-8D3 **e** blood concentration curves (%ID/g blood) for b, c, and d showing decreasing half-lives with size. From Sehlin *et al.*, 2019⁸⁹.

In this present work, the focus has been partly on finding even smaller proteins that can bind TfR and A β to be used for imaging. **Paper I** established that di-scFv3D6-8D3 had an earlier elimination from WT mice brains than mAb3D6-scFv8D3 and that mAb3D6-scFv8D3 had a prolonged association with the vasculature. Thus, **Paper I** concluded that a smaller size is optimal for reducing background radioactivity from unbound antibodies in the blood and brain. It further strengthened the notion that smaller proteins are favorable for brainPET, such as affibodies and VHHs, later used in **Paper II** and **Paper IV**.

Overall, antibody size is a factor that has not been investigated much regarding brain distribution or pharmacokinetics. Peripherally administered non-targeting antibodies of different sizes were studied by microdialysis in an experiment by Chang *et al.* They found a bell-shaped correlation between size and brain exposure, where the 50 kDa antibody fragment had the highest whole-brain exposure, while the unbound concentration in ISF was highest for 100 kDa Fab fragments²³⁷. This work indicates that a size between 50-100 kDa could be optimal for high brain delivery. However, this study applies to antibodies that are not actively transported across the BBB, while the antibodies in this thesis rely on brain-wide TfR-mediated delivery.

A study by Pizzo *et al.* demonstrated that intrathecally administered sdAb had a wider brain distribution than an IgG antibody¹⁵⁸. Diffusion in the brain parenchyma is inefficient over long distances since the extracellular space is tortuous and narrow²³⁸. Instead, the perivascular spaces (PVS) provide a more spacious “highway” driven by convective flow, allowing for faster transportation and clearance of larger molecules¹⁴⁴.

In **paper I**, di-scFv3D6-8D3 and mAb3D6-scFv8D3 had similar brain half-lives, which indicates convective bulk clearance via the PVS. However, when corrected for capillary-parenchymal partitioning, mAb3D6-scFv8D3 had slightly slower elimination from parenchyma, which could potentially be due to its larger size (slower diffusion), or its higher retention to, e.g., TfR on neurons, due to its higher avidity²⁰¹.

In **paper II**, affibodies were 7 kDa, i.e., 30 times smaller than mAb3D6-scFv8D3 in **paper I**. Despite this, the BBB penetration appeared low, showing

that a smaller size does not necessarily equate to better BBB penetration. Indeed, a low CSF-to-serum ratio of 0.12%, similar to a larger IgG antibody, has been previously reported²³⁹. On the other hand, the affibodies used in **paper II** were able to enter the brain when conjugated to a TfR-binding scFv8D3. We also found that a 6xHis-Tag (often used for purification) likely increased the affibodies' association to the BBB vasculature²⁴⁰, resulting in slightly higher total brain concentrations of around 0.4%ID/g brain 2 h after injection; however, this does not necessarily indicate penetration of the BBB. In **paper IV**, the VHH domains were around twice the size of an affibody, 12 kDa, and fused to bivalently to an Fc or monovalently to an scFv fragment, i.e., in total around 75 kDa and 34 kDa, respectively. In **paper IV**, we found that the non-TfR targeting FP_{Fc} had a brain uptake in mice of 0.17%ID/g brain, and as a monovalent FP_{scFv}, 0.07%ID/g brain, which is slightly higher than for IgGs²⁴.

Size is, however, important in the periphery, as it can determine how the antibody is eliminated. This is demonstrated by the large difference in blood half-life (9 h vs 3 h) between the Tribody (100 kDa) and di-scFv3D6-8D3 (58 kDa), which both lack an Fc-domain. The renal filtration cutoff for proteins is around 60 kDa, and this criterion was fulfilled for di-scFv3D6-8D3 (**paper I**), affibodies and affibody-scFv8D3 conjugates (**paper II**), and FP_{scFv} conjugates (**paper IV**). Likely because of renal elimination, they all displayed fast systemic elimination compared to IgG-like antibodies. However, a very short half-life could contribute to a decreased chance for the protein to interact with the BBB and enter the brain. This may have been the case for the non-fused affibodies in **paper II**.

The size of the binding domains can also be important regarding reaching certain epitopes. In line with this, it appears easier to develop cross-species reactive (mTfR/hTfR) binders using sdAbs, such as VHHs, and VNARs, compared to IgGs. This is one of the reasons, together with size-related fast blood clearance, that we used VHHs in **paper IV**.

Binding - affinity and avidity

Affinity is the binding strength between the binding site and the epitope, while avidity is the combined binding strength from all binding sites of a construct.

In **paper I**, we primarily compared bispecific antibodies of different sizes, but in addition to size, also the binding strength differed between the two studied antibodies. The “large” antibody was an IgG-like construct with two potential binding sites for TfR and bivalent binding to A β . Di-scFv3D6-8D3, on the other hand, had monovalent binding towards TfR and A β . The rationale for the comparison was that they were, at the time, our “top candidates” for antibody-based PET imaging, and we wanted to chart the radioactivity originating from brain antibody that was not retained by A β to get an understanding of their respective background signal for PET imaging within the first 24 h after injection.

A bell-shaped relationship between affinity and brain uptake has been suggested¹⁹⁵. Low TfR-affinity leads to higher systemic exposures but impedes BBB binding. High-affinity TfR-binders are more rapidly cleared from the blood due to TfR-mediated degradation and are more likely to be “trapped” or saturate TfR in the brain endothelial cells, which inhibit brain delivery^{219,241}.

Di-scFv3D6-8D3 has high and equivalent affinity to mAb3D6 for A β monomers and protofibrils¹³⁷. However, the avidity for TfR was higher for mAb3D6-scFv8D3 than di-scFv3D6-8D3. In **Paper I**, we used WT mice; hence, the TfR-binding influenced the antibodies' pharmacokinetics, while A β -binding did not. A previous study using the same large antibody format but another A β -binder, mAb158-scFv8D3, indicated that this format had 2-fold higher avidity to TfR *in vitro* compared with scFv8D3, i.e., monovalent binding, despite the two scFv8D3 domains²⁴. In **paper I**, we discovered that mAb3D6-scFv8D3 had a 5-fold higher affinity for mTfR than the ‘true’ monovalent binder di-scFv3D6-8D3 using an *in vitro* real-time binding assay and that it had a prolonged association to the brain capillaries *in vivo*. This led us to conclude that mAb3D6-scFv8D3 was not strictly monovalent but likely could bind TfR with both scFv8D3, at least at higher concentrations of TfR. Thus, **paper I** indicated that mAb3D6-scFv8D3 had high avidity towards TfR, and in **paper III**, we also observed that its relative distribution to parenchyma was higher at a low dose compared with a high dose, which is in line with previous studies of high-affinity/avidity TfR antibodies^{25,188}.

Later, in **paper IV**, VHH-Fc fusions were investigated (FP_{Fc}), which had two TfR-binding domains, compared to monovalent scFv3D6-VHH/VHH-scFv3D6 fusions (FP_{scFvA/B}). The binding strength towards TfR measured by ELISA and surface plasmon resonance (SPR) decreased for the monovalent constructs, compared with the bivalent constructs. In addition, *in vivo*, the monovalent constructs had lower brain uptake, although this could also be attributed to their faster blood clearance. Monovalent TfR binding has been associated with better brain penetration, especially at high doses or for high-affinity binders^{188,193}. In **paper IV**, fusion protein 2 (FP_{Fc2}/FP_{scFv2})-constructs displayed the highest mTfR affinity, FP_{Fc4}/FP_{scFv4} second highest, followed by FP_{Fc1}/FP_{scFv1}. Despite this, FP_{Fc1}/FP_{scFv1B} had higher relative parenchymal distribution, both as a bivalent and monovalent construct. This could indicate that the affinities of FP_{Fc2}/FP_{scFv2B} and FP_{Fc4}/FP_{scFv4B} were in the higher range, even as monovalent binders, resulting in more endothelial cell trapping compared with FP_{Fc1}/FP_{scFv1B}. This indicates that the dissociation rate may be another important factor influencing the extent of parenchymal delivery¹⁹⁷. For example, FP_{Fc1} showed a 40-fold higher dissociation rate constant but similar association rate constants to mTfR compared with FP_{Fc4}. However, even though there is an increased relative parenchymal delivery, we do not know whether it is more critical for imaging with higher *absolute concentrations* in the parenchyma, like for FP_{Fc2}/FP_{scFv2B} or FP_{Fc4}/FP_{scFv4B}, or

if relative delivery is more important. Low affinity could contribute to decreased off-target binding to brain vasculature or TfR on parenchymal cells, which in turn could lead to faster clearance from WT mouse brain and improved contrast, but could also impede the absolute brain delivery of the antibody, leading to low detection of the primary target, A β . Conversely, FP_{scFv1B} did display significant and the greatest difference, in *ex vivo* perfused brains between WT and *App*^{N-L-GF} mice after 6 h and 24 h, indicating A β -related binding; however, FP_{scFv1B} remains to be tested *in vivo* in brainPET.

The relative affinities between the primary brain target, e.g., A β oligomers and TfR, turned out to be important in **paper II** and possibly **paper IV**. ELISA demonstrated that the studied affibodies displayed an affinity for A β that was 100-fold lower than di-scFv3D6-8D3. Consequently, the combination of fast elimination from blood and low ability to bind A β *in vivo* resulted in low overall brain retention of the affibodies. Better optimization of the binding through affinity maturation and/or using more than one affibody (dimerization) could be a future option. Overall, we learned that the protein domain designed to bind A β likely requires a low nanomolar or picomolar affinity to be retained at the target to enable its use as an *in vivo* imaging agent. Moreover, the affinity for TfR was higher than that observed for the di-scFv3D6-8D3 reference, which could have contributed to the imbalanced retention, potentially leading to a preference for endothelial or neuronal TfR binding over A β . In **paper IV**, the balance between A β affinity and mTfR affinity was more favorable, and the cross-reactive mTfR/hTfR constructs had increased brain uptake and could distinguish WT from *App*^{N-L-GF} mice.

Furthermore, the orientation of the fusion in **paper II** and **paper IV** had an impact on affinity and distribution. In **paper IV**, the anti-TfR VHHs were fused either to the C-terminus of scFv3D6 (A) or the N-terminus of scFv3D6 (B). In **paper II**, the affibodies were fused to the C-terminus of scFv8D3. Interestingly, it appeared as fusion to the C-terminus of a scFv for FP_{scFv1A} and scFv3D6-Z1 impacted their ability to bind to mTfR and A β , respectively. Similarly, transcytosis of the VHH-based brain-shuttle FC5, was impaired when fused to the C-terminus of its cargo^{174,242}. This indicates that the N-terminal of these constructs may have important properties for target binding.

Overall, affinity and avidity are well-established factors that influence TfR-mediated transport. The work in this thesis further highlights the importance of optimizing affinity and avidity for successful TfR-transport and A β -retention.

Periphery

Peripheral concentrations drive the brain concentrations; this is why brain-to-serum ratios can be more representative than total brain concentrations when comparing brain uptake of different antibodies. For TfR-antibodies, binding to TfR in the periphery affects the antibody distribution. TfR-antibodies are

subjected to TfR-mediated clearance, typically resulting in faster blood clearance for TfR-antibodies than conventional antibodies^{195,196,243}. This was observed in **paper III**, where mAb3D6-scFv8D3 had lower blood concentrations than mAb3D6 already at 2 h post-injection.

In the blood, TfR is expressed to a high degree on reticulocytes, while TfR is almost completely absent in mature red blood cells. Mice have a 10-fold higher level of circulating reticulocytes compared with humans and non-primate monkeys, and bispecific TfR-antibodies seem to affect the reticulocyte count to a lesser degree in monkeys, and potentially in humans, compared with mice^{195,198}. In **paper I**, we observed that a large portion of mAb3D6-scFv8D3 present in blood was associated with blood cells. The dose administered in **paper I**, was a non-saturable tracer dose, which probably resulted in fast sequestering of antibody by blood cells, likely largely by reticulocytes. In **paper III**, we further studied the plasma vs. blood cell partitioning of mAb3D6-scFv8D3 at high and low doses and in young and aged mice. As observed in **paper I**, low doses were associated with high blood cell concentrations of mAb3D6-scFv8D3. Interestingly, we also found a higher blood cell distribution of mAb3D6-scFv8D3 in aged mice compared to young mice at low and high doses. This could potentially be explained by higher reticulocyte counts in aged mice²⁴⁴.

It should be noted that the soluble portion of TfR, sTfR, in plasma was not investigated in these studies. The level of sTfR could potentially also affect the availability of [¹²⁵I]mAb3D6-scFv8D3 for interaction with TfR at the BBB. Since [¹²⁵I]mAb3D6-scFv8D3 has two binding sites for TfR, it is possible that even if one scFv8D3 domain is bound to blood TfR, the other arm is still available for binding to TfR at the BBB. It would be interesting to study further the effect of blood binding with a strictly TfR-monovalent antibody.

Is age just a number?

In **paper III**, we observed that the age of the mice influenced the brain concentrations of mAb3D6-scFv8D3. Aged mice had significantly lower brain concentrations of the bispecific antibody than young mice, both at low and high doses.

As previously discussed, antibody availability in the blood could be important for brain delivery. As described above, aged mice had a higher distribution of the bispecific antibody to the blood cells than young mice. *In vitro* experiments, carried out during 2 h after spiking whole blood with radio-labeled mAb3D6-scFv8D3, showed that aged mice had a lower exposure of bispecific antibody in plasma compared with young mice. *In vivo*, the lower availability in plasma of bispecific antibody could have contributed to a lower brain concentration at 2 h in aged mice. On the other hand, the process of

elimination or tissue binding cannot be measured *in vitro*, and therefore exposure measured *in vitro* cannot be directly compared with *in vivo* blood pharmacokinetics.

Moreover, aged WT mice displayed significant positive correlations between plasma and brain concentrations of [¹²⁵I]mAb3D6-scFv8D3 at non-saturable and saturable doses, indicating that the brain delivery was directly influenced by the amount of antibody in the plasma. In contrast, brain concentrations in young mice were less affected by plasma concentrations and possibly more affected by TfR-binding at the BBB (Fig. 18).

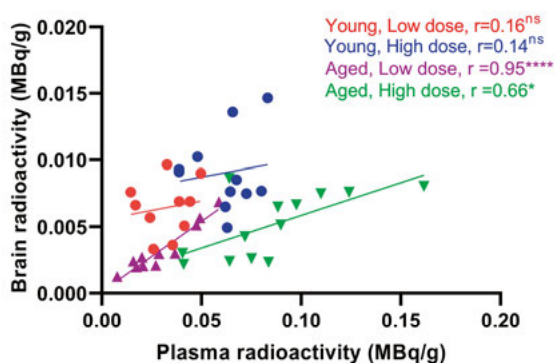


Figure 18: Brain concentration (MBq/g) over plasma concentrations (MBq/g) of [¹²⁵I]mAb3D6-scFv8D3, administered at 0.05 mg/kg and 1 mg/kg, in young (3-5 month) and old (17-20 month) WT mice. Pearson's correlation coefficient (r, significant p-value is defined as $p < 0.05$, *: $p < 0.05$, **: $p < 0.01$, ***: $p < 0.001$ and ****: $p < 0.0001$)

The other factor that can explain the differences in brain delivery between young and aged mice is the availability of TfR1 at the BBB. We found that young mice had more concentrated [¹²⁵I]mAb3D6-scFv8D3 in capillaries and more TfR protein in capillary-enriched brain samples. Additionally, the control antibody, mAb3D6, which lacks TfR binding, did not display age-related differences in overall brain uptake. Our results are in line with studies by Yang *et al.*, that proposed an altered transport mechanism over the BBB in aging, from specific receptor-mediated transcytosis to more unspecific calveolar transcytosis at old age, and that expression of TfR is decreased in aged mice²⁴⁵. Others have also observed decreased TfR levels or TfR-antibody uptake in aged WT mice^{246,247}. However, other studies show that TfR-antibody transport is not age-dependent^{248,249}. The different age ranges and measurement time points could explain the discrepancies; however, more systematic studies are needed to elucidate which antibodies, animal models, or ages have impaired TfR transport. Taken together, this suggests that young mice with more TfR1 available at the BBB had a more efficient TfR-mediated brain uptake of

mAb3D6-scFv8D3 than aged mice. However, it is also not clear yet how these results translate to humans.

Aging has been associated with physiological changes at the BBB²⁵⁰ and has been shown to increase the BBB permeability of IgG antibodies^{245,251–253}. However, there is also evidence against age-related “leakage” into the BBB of antibodies^{249,254}. It is unclear to what extent these changes affect the brain delivery of TfR-transported antibodies. Our studies mainly support the lack of a widespread influx of conventional antibodies in old age. Local disruptions, especially at vascular A β pathology, could be present. Despite this, it appears that these do not contribute significantly to an overall increase in TfR-mediated antibody delivery^{254,255}. TfR-antibodies are transported over the BBB at capillaries on a whole brain level, in contrast to IgGs, which display as local hotspots in the brain⁸⁹. Although there could be increased BBB permeability in aging mice, the large surface of interaction between the TfR-antibody and capillary bed likely has a more significant impact on total brain concentrations than local breaches of the BBB.

A β pathology

In **paper III**, we did not observe significantly higher brain concentrations of either bispecific antibody or the conventional mAb3D6 in tg-ArcSwe mice compared with WT mice. This suggests that A β pathology did not influence the brain delivery of either antibody, at least not at 2 h after injection. However, at later time points, we have shown that antibodies can be retained at A β pathology up to 28 days after injection²⁴³. Others have also concluded that WT and APP-transgenic mice have similar brain uptake of TfR-antibodies^{248,249}. However, the control antibody mAb3D6 did have higher distribution to capillary-enriched brain homogenates in aged tg-ArcSwe and visually accumulated at A β -stained capillaries. The antibody may encounter A β when transported in the PVS and then reaches the brain beyond the locally compromised BBB.

Dose

In PET applications, tracer doses are frequently used, with the aim of non-saturable binding to a target molecule while not directly changing the physiology or pathology. Thus, antibody-based PET experiments use lower doses, <1 mg/kg of bispecific antibody, while therapeutic studies are based on higher doses of 1-50 mg/kg.

Papers I-II and **IV** used tracer doses, while we also explored therapeutic doses in **paper III**. Three different doses were compared; a tracer dose, a low therapeutic dose, and a high therapeutic dose.

At tracer doses, a large portion of the injected [¹²⁵I]mAb3D6-scFv8D3 was bound to blood cell TfR. As previously stated, this could influence the amount of antibody available in the plasma; hence, we believe the amount available

for binding at the BBB. However, tracer doses may also result in higher brain transcytosis of high affinity/avidity bispecific antibodies, as indicated in **paper III**, where a low dose resulted in higher relative parenchymal distribution of [¹²⁵I]mAb3D6-scFv8D3, regardless of age or genotype.

The therapeutic dose for [¹²⁵I]mAb3D6-scFv8D3 in our studies (1 mg/kg) is low compared with other TfR-shuttles dosed at 10-50 mg/kg^{25,145,188,201}. As demonstrated in **paper III**, a 10 mg/kg dose resulted in saturation at the BBB and significantly lowered brain concentrations. It can be concluded that there is a bell-shaped relationship between dose and total brain delivery and that different TfR-shuttles have different optimal dosing windows. For mAb3D6-scFv8D3, the dose of 1 mg/kg might be ideal, as it results in saturation of blood cell TfR, leading to a high relative plasma distribution and high brain concentrations.

Doses are also chosen based on the application of the antibody. For therapeutic purposes, it is necessary to maximize the antibody brain delivery and to avoid down-regulation of TfR1 or toxicity; therefore, low affinity and high doses are used^{25,193,198}. PET applications rely more upon fast delivery to the target and rapid elimination of unbound radioligand to reduce background and generally do not require high amounts of antibody at the target site during extended periods. Thus, we believe it is crucial to adjust doses carefully for ideal brain delivery and desired application for each brain shuttle.

Conclusions and future perspectives

In this thesis, we have evaluated factors important for antibody-based protein delivery to the brain via TfR-mediated transcytosis for future PET imaging of brain A β .

One of the main challenges for developing antibody-based PET radioligands is that the biological half-life associated with antibody-based constructs is too long relative to the short-lived PET-compatible radionuclides used in clinics. This thesis has focused on creating TfR-binding bispecific antibodies of smaller size for use as future A β -PET radioligands, together with clinically preferred radionuclides, e.g., ^{18}F . A smaller protein size is associated with faster pharmacokinetics, which is desirable to increase the signal-to-noise ratio in PET. In **paper I**, we concluded that a small bispecific tandem protein of two scFvs had earlier elimination from blood and brain and, thus, was better suited for PET than an IgG-like antibody. However, previous studies showed that the required time between injection and PET scanning of the specific pathology-derived signal was still longer (14 h) than optimal for clinical use¹³⁷.

Therefore, in **paper II** and **paper IV**, we explored even smaller proteins with shorter half-lives. In **paper II**, affibody proteins were successfully delivered to the brain using TfR-mediated transcytosis, while the affibodies that did not have a TfR1-binder likely did not actively cross the BBB. Although the TfR-transported affibodies reached the brain parenchyma, they suffered from low A β -affinity, resulting in a low ability to be retained in the brain by A β . Future studies should focus on improving affibodies' binding capacity, with picomolar affinity to A β and potentially creating cross-reactive binders to mTfR1/hTfR1. This would enable the creation of a translatable, small-sized bispecific protein that can be transported across the BBB and bind A β to be used for PET imaging.

In **paper IV**, we used novel TfR1-binders based on camelid small heavy-chain only antibodies. Combining a small cross-reactive mTfR1/hTfR1 binder with an A β -binding domain based on 3D6, we could differentiate WT from AD-mice models already 6 h after injection in *ex vivo* studies. The difference was even greater 24 h after injection. We also observed that a lower affinity for mTfR was associated with faster pharmacokinetics and higher relative parenchymal delivery. We hope the construct also will be able to discriminate WT and AD in *in vivo* PET, in a clinically relevant time frame.

However, some challenges still remain in optimizing kinetics for antibody-based PET radioligands. The strategy used within this thesis was to reduce the size of the antibodies. However, there may be a limit to when this will be effective, as brain shuttles may be necessary to yield high enough brain concentrations, and circulation time also can determine the extent of brain delivery. An alternative strategy would be to use clearing agents that rapidly target the circulating antibody for degradation in the liver, thus reducing the half-life in blood²⁵⁶. Another promising strategy is pretargeting, a concept based on an *in vivo* click reaction between, e.g., a radiolabeled tetrazine and a TCO-modified antibody²⁵⁷. The antibody is injected hours or days before the radiolabeled molecule, which is administered shortly before scanning, thus minimizing the radiation exposure for the patient.

Antibody-based PET radioligands must have enhanced brain delivery to reach the brain parenchyma to image pathology in CNS diseases. Throughout this thesis's papers (**I-IV**), we have shown that TfR-mediated brain delivery is a robust method to improve brain concentrations of antibody-based proteins. We have also demonstrated that the delivery of TfR-transported antibodies could be age-dependent (**paper III**), likely related to the lower availability of TfR transcytosis at the BBB or the increased blood cell binding in aged mice. This is important to highlight since new constructs are often tested first in young individuals and could result in an overestimation of brain delivery. Furthermore, we evaluated a novel cross-reactive brain shuttle that binds both mTfR/hTfR in **paper IV**. Cross-reactivity facilitates translation to clinical use, and it may be used as a brain shuttle for other targets in the future. Hopefully, we have moved further toward clinical imaging of A β with antibody-based PET.

Bispecific antibody-based proteins optimized for PET imaging could be applied to targets other than A β within the brain, for example, to image neuroinflammation markers and other proteins that are increased in AD pathology or other CNS diseases. It should, however, be kept in mind that antibody-based ligands to date are limited to imaging of extracellular targets since the antibodies usually are degraded or recycled after cell internalization.

In conclusion, antibody-based PET has advantages like high selectivity and the ability to bind other types of targets compared with current PET radioligands. For intrabrain targets, efficient brain delivery is essential and can be facilitated by TfR-targeting. A smaller molecular size can improve the pharmacokinetics of the antibodies, but it is also crucial to optimize the constructs' affinity, avidity, and dose.

Popular Science Summary

Alzheimer's disease (AD) is the most common dementia. Symptoms include difficulties with memory, language, disorientation to time and place, and performing everyday tasks. AD is a heavy burden for patients but also families, caregivers, and society as a whole. The main risk factor for AD is old age. As the population of elderly increases, the number of AD cases in the world is expected to increase three-fold by 2050, from around 50 million to 150 million.

In the AD brain, senile plaques and neurofibrillary tangles are signs of disease processes. Senile plaques are produced by aggregation of toxic amyloid- β ($A\beta$) protein. This thesis focuses on how we can measure and visualize $A\beta$ in the brain.

Positron emission tomography (PET) is a brain scanning method and a crucial tool to help doctors diagnose AD and for researchers to evaluate new treatments. The PET-imaging agents (radioligands) used today target insoluble $A\beta$ -plaques. Before the $A\beta$ -plaques are formed in the brain, smaller soluble aggregates of $A\beta$ are built up over 15-20 years before clinical symptoms appear. Evidence points to these soluble pre-stages of $A\beta$ plaques as the disease-causing forms. They are believed to be toxic to neurons and worsen other disease processes in the brain. Today, we cannot image these pre-stages of $A\beta$ plaques with PET, although they have become the main target for new antibody-based AD treatments. For example, *lecanemab*, an antibody first developed at Uppsala University, targets these pre-stages of $A\beta$ -plaques. *Lecanemab* was recently approved as a drug for AD in the USA.

Our group is developing new radioligands, based on antibodies, that can bind these small soluble aggregates of $A\beta$. Antibodies are 1000 times larger than a "typical" drug molecule, like aspirin. The higher complexity of molecules like antibodies makes them interact more specifically and stronger with their target, which is an advantage. They can also be genetically designed in a laboratory to suit different purposes. For example, they can be made to bind strongly to two different targets. In this thesis, we produced such antibodies, called bispecific antibodies.

The drawback of antibodies' large size is that they are not able to cross the cells between the blood and the brain, the blood-brain barrier (BBB). The brain is a highly protected organ, where mainly small fat-soluble molecules can freely enter, or selected nutrients that are needed by the brain, that enter

via carriers or receptors. One of these essential molecules is iron, which is transported by a specific receptor called the transferrin receptor (TfR).

By engineering antibodies to bind both the TfR and a target within the brain, like A β , we can increase the amount of antibody that can reach the brain. When inside the brain, the antibody can bind to A β ; if it is radiolabelled, it can give us a signal in PET. Increasing brain delivery this way is also known as the “Trojan Horse” strategy. Just like the greeks hid in a wooden horse to get into Troy, we are persuading the BBB to let our antibodies enter the brain.

In this thesis, I have evaluated important properties of these bispecific antibodies for their use as radioligands in PET brain imaging. One desirable property is fast elimination from the blood. This will reduce the background signal that comes from the blood in the brain. In the first paper, we compared two antibodies of different size and ability to bind TfR. We concluded that the smaller format was eliminated earlier from both the blood and the brain. This means it produced less background signal, since unbound antibody disappeared faster. Therefore, we continued developing small-format bispecific antibodies.

In paper II, even smaller antibody-like proteins (affibodies) were evaluated, which had an even faster elimination in the blood. Bispecific affibodies bound TfR and entered the brain; however, the binding to A β was not strong enough, while TfR binding was too strong, and we concluded there was an imbalance between A β and TfR binding.

In Paper III, we compared the large bispecific antibody from paper I, with its conventional antibody version that lacked TfR binding. The brain concentrations of bispecific antibody were higher in young mice than in old mice. The old mice had less dense signal from the bispecific antibody and lower levels of TfR protein in their brain capillaries. This points to old mice having less available TfR to shuttle antibodies into the brain than young mice. There were no differences for the control antibody, which strengthens the hypothesis that the age difference was related to TfR. There was also a higher tendency of the antibody to bind to blood cells in old mice compared with young mice. This led us to believe that old mice had lower availability in the plasma of the antibody. Overall, these age differences are important because new drugs or antibodies are often first tested in young individuals, but at the same time, we usually want to treat an older population with AD. We also don't know yet if humans have similar age differences.

In paper IV, we returned to small format antibodies, but this time they were based on antibodies originally found in llamas. The part of the antibody that bind the target, the variable domain, is half the size in llamas compared with normal antibodies, but can still bind strongly. The llama antibodies we used could target both mouse and human TfR, which helps when we want to move from animal experiments to human clinical trials. One of the llama antibodies was promising; it had a high distribution to the brain and was not stuck in the

blood vessels to the same extent as the other tested antibodies. Most interestingly, it had a fast blood and brain elimination that made it possible to see differences between wild-type and AD mice only 6 h after injection of the antibody. Previously, we could only do PET scans 1-3 days after injecting the antibodies, which is not ideal when PET is used in humans as patients need to be hospitalized between the time of injection and the scanning. We think that this llama antibody could be developed into a clinical PET radioligand in the future.

All in all, in this thesis, we have explored different properties that are important for TfR-mediated brain delivery of antibodies, and moved closer to developing an antibody-based PET radioligand for use in AD.

Populärvetenskaplig sammanfattning

Alzheimers sjukdom (AD) är den vanligaste typen av demenssjukdom. Symtomen inkluderar svårigheter med minne, språk, att hitta, att hålla reda på tider och datum, och andra vardagliga sysslor. AD är en tung börda för patienter men också för familjer, vårdgivare och samhället som helhet. Den främsta riskfaktorn för AD är hög ålder. Antalet äldre blir allt högre, och det förväntas resultera i en trefaldig ökning av antalet fall av AD, från cirka 50 miljoner idag till 150 miljoner år 2050.

I AD-hjärnan är senila plack och neurofibrillära nystan tecken på sjukdomsprocesser. Senila plack bildas genom ansamling av toxiskt amyloid- β ($A\beta$) protein. Denna avhandling fokuserar på hur vi kan mäta och visualisera $A\beta$ i hjärnan.

Avbildning av den levande hjärnan med hjälp av positronemissionstomografi (PET), en hjärnskanningsmetod, är ett viktigt verktyg som hjälper läkare att diagnostisera AD och forskare att utvärdera nya läkemedel. PET-radioligander kan idag avbilda de olösliga $A\beta$ -placken i hjärnan. Små lösliga ansamlingar av $A\beta$ byggs dock upp i hjärnan under 15-20 år innan symtomen på AD blir tydliga. Under de senaste åren har fler bevis pekats mot att dessa lösliga förstadier av $A\beta$ -plack är de formerna som orsakar sjukdomen. De tros vara skadliga för neuroner och förvärra andra sjukdomsprocesser i hjärnan. Idag kan vi inte avbilda dessa förstadier av $A\beta$ -plack med PET, trots att de har blivit det huvudsakliga målet för nya antikroppsbaseerade AD-behandlingar. Till exempel riktar sig *lecanemab*, en antikropp som först utvecklades vid Uppsala universitet, mot dessa förstadier av $A\beta$ -plack. *Lecanemab* blev nyligen godkänt som läkemedel mot AD i USA.

Vår grupp utvecklar nya PET-radioligander, baserade på antikroppar, som kan binda dessa små lösliga aggregat av $A\beta$. Antikroppar är 1000 gånger större än en Alvedon-molekyl. Den högre komplexiteten hos antikroppar jämfört med traditionella läkemedelsmolekyler gör att de kan binda mera specifikt och starkare med sitt mål, vilket är deras främsta fördel. De kan också designas och produceras i ett laboratorium för att passa olika ändamål. Antikroppar kan t.ex. modifieras så att de kan binda starkt till två olika mål. I denna avhandling producerade vi sådana antikroppar, så kallade bispecifika antikroppar.

Nackdelen med antikropparnas stora storlek är att de inte kan passera cellerna mellan blodet och hjärnan, blod-hjärnbarriären. Hjärnan är ett mycket

skyddat organ, som främst släpper igenom små fettlösliga molekyler, eller utvalda näringsämnen som hjärnan behöver. Dessa kommer in via bärarmolekyler eller receptorer. En av dessa väsentliga molekyler är järn, som transporteras av en specifik receptor som kallas transferrin-receptorn (TfR).

Genom att konstruera antikroppar som binder både TfR och ett mål i hjärnan, som A β , kan vi öka mängden antikropp som kan nå hjärnan. Väl inne i hjärnan kan antikroppen binda till A β . Om den också är märkt med en radioaktiv markör kan den ge oss en signal i PET. Denna strategi för att öka antikropps-upptaget till hjärnan är också känd som den "trojanska hästen". Precis som grekerna gömde sig i en trähäst för att komma in i Troja, lurar vi hjärnan att släppa igenom våra antikroppar.

I denna avhandling har jag utvärderat viktiga egenskaper hos dessa bispecifika antikroppar för användning som radioligander vid hjärnabbildning med PET. En önskvärd egenskap är att den snabbt försvinner (elimineras) från blodet, vilket i sin tur minskar bakgrundssignalen från blod i målorganet, dvs hjärnan. I den första artikeln jämförde jag två antikroppar av olika storlekar och förmåga att binda till TfR. Vi drog slutsatsen att antikroppen med det mindre formatet försvann tidigare från både blodet och hjärnan. Detta innebär en lägre bakgrundssignal i PET, eftersom obunden antikropp försvann snabbare. Eftersom det lilla formatet var bättre, så fortsatte vi att utveckla små bispecifika antikroppar.

I artikel II utvärderades ännu mindre antikroppsliknande proteiner (affibodies), som hade en ännu snabbare eliminering i blodet. Affibodies som inte band till TfR kunde inte komma in i hjärnan särskilt väl och binda A β . Bispecifika affibodies kunde binda TfR och komma in i hjärnan; bindningen till A β var dock inte tillräckligt stark, medan TfR-bindningen var för hög. Vi drog slutsatsen att det fanns en obalans mellan A β - och TfR-bindning.

I artikel III jämförde jag den stora bispecifika antikroppen från artikel I, med en vanlig antikropp utan TfR-bindning. De gamla mössen hade mindre av den bispecifika antikroppen i sina hjärnor än unga, och lägre nivåer av TfR-protein i hjärnans blodkärl. Detta pekar på att gamla möss har mindre mängd tillgängligt TfR som kan transportera den bispecifika antikroppen än unga möss. Det fanns inga skillnader för kontrollantikroppen som inte binder TfR, mellan gamla och unga möss, vilket stärker hypotesen att ålderskillnaden var relaterad till TfR. Det fanns också en högre tendens hos antikroppen att binda till blodkroppar hos gamla möss jämfört med unga möss. Eventuellt kan detta betyda att det finns färre bispecifika antikroppar tillgängliga för transport till hjärnan i gamla möss. Sammantaget är dessa ålderskillnader viktiga eftersom nya läkemedel eller antikroppar ofta först testas i unga individer, medan vi samtidigt vill behandla en äldre population med AD. Vi vet inte heller än om det finns samma ålderskillnader hos människor.

I artikel IV återgick vi till antikroppar i smått format, men den här gången var de baserade på antikroppar som ursprungligen finns i lamadjur. Den del av antikroppen som binder målet, den "variabla domänen", är hälften så stor i

lamadjurs antikroppar jämfört med en normal antikropp, men kan fortfarande binda starkt. Lamaantikropparna vi använde kunde binda både mus och human TfR, vilket hjälper när vi vill gå från djurexperiment till kliniska prövningar i människa. En av lamaantikropparna var lovande; den hade en hög distribution till hjärnan och satt inte fast i blodkärlen i samma utsträckning som de andra antikropparna som testades. Mest intressant var dock att den hade en snabb eliminering i blodet och hjärnan som gjorde det möjligt att se skillnader mellan vildtyps- och AD-möss efter bara 6 timmar. Tidigare kunde vi bara göra PET-skanningar 1-3 dagar efter injicering av antikropparna. Det är inte idealiskt för PET i människa som behöver läggas in på sjukhus mellan tidpunkten för injektionen och skanningen. Vi tror att denna lamaantikropp skulle kunna utvecklas till en klinisk PET-radioligand i framtiden.

Sammantaget har vi i denna avhandling undersökt olika egenskaper som är viktiga för upptag av antikroppar i hjärnan med hjälp av TfR, och kommit närmare utvecklingen av en antikroppsbasead PET-radioligand för användning i AD.

Funding

The work in this thesis was performed at the Department of Public Health and Caring Sciences between 2018 and 2023, in the Molecular Geriatrics group, Rudbeck Laboratory, Uppsala University, Sweden. I would like to thank the funding bodies for financial support and travel grants over the years, including the Swedish Research Council, the Swedish Innovation Agency, Alzheimersfonden, Hjärnfonden, Torsten Söderbergs stiftelse, Åhlénstiftelsen, Magnus Bergwalls stiftelse, Stiftelsen för gamla tjänarinnor, Stohnes stiftelse, Apotekarsociteten, Konung Gustaf V:s och Drottning Victorias frimuaresstiftelse and Hans-Gabriel och Alice Trolle-Wachtmeisters stiftelse för medicinsk forskning.

Schematic illustrations were created by the author using Biorender.com

Acknowledgments

To my supervisors, **Stina** and **Dag**. I never got a third supervisor, but fortunately, you two have complementary areas of expertise (and personality) and I think we have worked well together. Thank you both for being available (almost) 24/7 and supporting me throughout my five years in MolGer! **Stina**, my main supervisor, I admire your leadership skills, especially since taking over the role after Martin. I also like that you are very efficient and practical, whether in the writing process or animal experiments. I remember clearly the day (I think it was a Tuesday in February, and I think it was snowy outside, but I cannot be sure) at PPP when you asked if I wanted to do a PhD. This was something that had been a goal of mine for a while, so I was very happy when you (and Dag) selected me for the position. I feel like you have always believed in me, which I am very grateful for. You are a young, strong, inspiring female professor with a soft heart. So, thank you, Stina, for taking me on, seeing the value in different personalities, and supporting me through the ups and downs of my Ph.D. **Dag**, the almost Norwegian, highly skilled scientist and baker. I admire your deep knowledge of the field, skills in ELISA and scientific way of thinking; sometimes, experiment ideas would just flow out of you and I had to keep good notes at our meetings. You are always curious about anything science related and an optimist, which I think are excellent qualities when working as a researcher. Thank you for teaching me how to keep the hope for my projects afloat in rough seas. I also really like that you have a taste for the good stuff in life, like coffee, cake, cheese and wine! I wish I could have been there for your famous croissant-semlas thought.

Thank you to my co-authors and collaborators for making the work in this thesis possible. Thank you to the affibody team at KTH, **John**, **Staffan** and **Hanna**, for supplying proteins and for great discussions. Thanks to the people in Copenhagen (DTU) and especially **Kasper Bendix Johnsen** for showing an interest in my work, answering my many questions on capillary depletion and initiating collaboration. Thank you **Jonas Eriksson**, who has been working behind the scenes delivering radiochemistry of high class. Thank you to our latest collaborators at Key2Brain AB, **Magnus Berglund**, and **Elisabet Ohlin Sjöström**. **Elisabet**, how you initiate and manage different exciting projects is very inspiring. Thank you for all your help regarding experiment protocols and to you both for input on the last manuscript!

Thank you **Tsong** for taking me on as a student, and for your valuable input on the writing of manuscripts and abstracts. To other now “old school” MolGer members, **Leire, Gustaf, Bodil, Elisabeth, Silvio** and **María**; thank you for welcoming me to the MolGer lab and contributing to me wanting to stay 😊

Jinar, Chiara, Emma thank you for the knitting club and for being there for venting over the years. **Jinar**, you are such a strong independent woman and one of my role models, thank you for being there as a friend and colleague. **Chiara**, you are cool and funny, and I admire your PhDing’ with two kids. I think we have quite similar personalities, so thumbs up for going to sleep early! **Emma**, you must be one of the most kind and generous persons I know. I am very glad it was you whom I shared office with in our stressful and intense pre-dissertation times. You did a fantastic job on your day, and I wish you good luck for the future! Thank you to **Toby G** for always being kind and helpful in the lab whenever I needed. I have always considered you my “older brother” in the lab, paving the way. Thanks, **Anish**, for game nights, helping us move, and always knowing the latest and best shows to watch on Netflix. You are smart and funny, and I like talking to you. Thank you to the triplets, **Gillian** for your hard work and our scientific collaborations, as well as being a supportive friend! Thanks, **Mengfei**, for being great company on travels, a great journal club partner even though we pick complicated papers... and letting me help you with your Swedish course. Thank you **Eva**, for your curiosity and openness. I find it cool that you can talk to everyone and anyone (and still consider yourself shy!). We should take up our music sessions again once we’re both finished! Soon it will be your turn to finish your PhDs and leave MolGer, which feels a bit odd to me as I still feel like you just started! Good luck, I am convinced you will excel at your dissertations! **Evangelos**, congratulations on the new little family member 😊 and σ’ ευχαριστώ for always being friendly. I think I have never not seen you smile when we meet in the corridors (even during Covid I could tell you were smiling!). **Tobias M**, thank you for being the party animal of the lab, sharing food inspiration, and keep up making tasty beer! Newcomers **Abdul, Amelia**, and **Elin**, please take good care of the MolGer group now that the old gang are all dropping off one by one! The best of luck with your work/PhDs. Thank you to my former student **Emma C** for your contribution to my project. I wish you good luck and as much Greek food as you can eat!

Thank you **Anna** for knowing how to tell a good story at lunch, and for our conversations about our next creative endeavors – I hope to see your photos in a gallery someday! ;) Thanks to **Johanna Rokka** for always encouraging me, and **Ulrika Julku** for diving inspiration, I hope you both are happy back in Finland, where apartments have saunas. Thank you **Sahar** for enriching the lab with your humor in all situations; good luck with your new big “little”

family, let's keep in touch at @officialsahar! Thank you, **Ximena**, for all the help and your care for each of us PhDs, especially as we arrive as newcomers in the lab. Thanks to **Agnieszka** for being supportive and friendly. You are going to knit so many awesome sweaters, I know it ☺

A huge thank you to past and present members of the MolGer group: **Lars, Martin, Joakim, Vilmantas, Linn, Sara, and Agata**.

I would also like to thank **Greta** and her group, the ProDDe team. **Nicole**, you are always so nice to me when we meet, thank you for your support with animal work! Thank you **Fadi** for your encouraging words, and thank you **Inga** for helping to purify my protein. **Andrés**, I would like to thank you for scientific collaboration, interesting lunch conversations and teaching me about philosophy. I am glad to have found a new friend in you ☺

I am so lucky to have so many wonderful friends outside of work that support me. You know who you are and you are so important to me. It means a lot that you are my personal “hejarklack” on this journey. I would also like to thank my in-law family, or “Superfamiljen”, for hospitality and welcoming me in the family. I know that you all support me as well.

A special thank you to my parents **Tomas** and **Áshild** for introducing me to the academic world, and inspiring me to explore and be curious about science. The scientific approach and your support have been very valuable to me during my years of education and work. Thank you also for letting me come with you to various conferences around the world ☺ and gaining many international family friends to visit from Iceland, to Greece and Australia.

To my husband **Joel**, it is hard for me to put into words how much you mean to me, but *thank you* for cooking so much food and supporting me. Thank you for always believing in me and loving me through it all. I am excited about the next step in our journey together; I look forward to our future adventures!

References

1. Makurvet, F. D. Biologics vs. small molecules: Drug costs and patient access. *Medicine in Drug Discovery* **9**, 100075 (2021).
2. Zhang, G., Zhang, J., Gao, Y., Li, Y. & Li, Y. Strategies for targeting undruggable targets. *Expert Opinion on Drug Discovery* **17**, 55–69 (2022).
3. Lu, R.-M. *et al.* Development of therapeutic antibodies for the treatment of diseases. *Journal of Biomedical Science* **27**, 1 (2020).
4. Kinch, M. S. An overview of FDA-approved biologics medicines. *Drug Discovery Today* **20**, 393–398 (2015).
5. LeBien, T. W. & Tedder, T. F. B lymphocytes: how they develop and function. *Blood* **112**, 1570–1580 (2008).
6. Wang, W., Wang, E. & Balthasar, J. Monoclonal Antibody Pharmacokinetics and Pharmacodynamics. *Clinical Pharmacology & Therapeutics* **84**, 548–558 (2008).
7. Carter, P. J. Potent antibody therapeutics by design. *Nature Reviews Immunology* **6**, 343–357 (2006).
8. Wang, X., Mathieu, M. & Brezski, R. J. IgG Fc engineering to modulate antibody effector functions. *Protein Cell* **9**, 63–73 (2018).
9. Candelaria, P. V., Leoh, L. S., Penichet, M. L. & Daniels-Wells, T. R. Antibodies Targeting the Transferrin Receptor 1 (TfR1) as Direct Anti-cancer Agents. *Frontiers in Immunology* **12**, 583 (2021).
10. Kang, T. H. & Jung, S. T. Boosting therapeutic potency of antibodies by taming Fc domain functions. *Experimental & Molecular Medicine* **51**, 1–9 (2019).
11. Antczak, D. F. Monoclonal antibodies: technology and potential use. *J Am Vet Med Assoc* **181**, 1005–1010 (1982).
12. Rajewsky, K. The advent and rise of monoclonal antibodies. *Nature* **575**, 47–49 (2019).
13. Danese, S., Vuitton, L. & Peyrin-Biroulet, L. Biologic agents for IBD: practical insights. *Nature Reviews Gastroenterology & Hepatology* **12**, 537–545 (2015).
14. Jin, J., Chang, Y. & Wei, W. Clinical application and evaluation of anti-TNF-alpha agents for the treatment of rheumatoid arthritis. *Acta Pharmacologica Sinica* **31**, 1133–1140 (2010).
15. Kaushik, S. B. & Lebwohl, M. G. Review of safety and efficacy of approved systemic psoriasis therapies. *International Journal of Dermatology* **58**, 649–658 (2019).
16. Lorusso, M. *et al.* Radiolabelled Trastuzumab PET/CT imaging: a promising non-invasive tool for the in vivo assessment of HER2 status in breast cancer patients. *Clin Transl Imaging* **8**, 95–105 (2020).
17. Zahavi, D. & Weiner, L. Monoclonal Antibodies in Cancer Therapy. *Antibodies* **9**, 34 (2020).

18. Arbabi-Ghahroudi, M. Camelid Single-Domain Antibodies: Historical Perspective and Future Outlook. *Front Immunol* **8**, (2017).
19. Cheong, W. S., Leow, C. Y., Abdul Majeed, A. B. & Leow, C. H. Diagnostic and therapeutic potential of shark variable new antigen receptor (VNAR) single domain antibody. *Int J Biol Macromol* **147**, 369–375 (2020).
20. Hamers-Casterman, C. *et al.* Naturally occurring antibodies devoid of light chains. *Nature* **363**, 446–448 (1993).
21. Duggan, S. Caplacizumab: First Global Approval. *Drugs* **78**, 1639–1642 (2018).
22. Bao, G., Tang, M., Zhao, J. & Zhu, X. Nanobody: a promising toolkit for molecular imaging and disease therapy. *EJNMMI Research* **11**, 6 (2021).
23. Krah, S., Kolmar, H., Becker, S. & Zielonka, S. Engineering IgG-Like Bispecific Antibodies—An Overview. *Antibodies (Basel)* **7**, (2018).
24. Hultqvist, G., Syvänen, S., Fang, X. T., Lannfelt, L. & Sehlin, D. Bivalent Brain Shuttle Increases Antibody Uptake by Monovalent Binding to the Transferrin Receptor. *Theranostics* **7**, 308–318 (2017).
25. Yu, Y. J. *et al.* Boosting brain uptake of a therapeutic antibody by reducing its affinity for a transcytosis target. *Sci Transl Med* **3**, 84ra44 (2011).
26. Beshir, S. A. *et al.* Aducanumab Therapy to Treat Alzheimer’s Disease: A Narrative Review. *Int J Alzheimers Dis* **2022**, 9343514 (2022).
27. Bruno, R. *et al.* Population pharmacokinetics of trastuzumab in patients with HER2+ metastatic breast cancer. *Cancer Chemother Pharmacol* **56**, 361–369 (2005).
28. Li, Z., Krippendorff, B.-F. & Shah, D. K. Influence of molecular size on the clearance of antibody fragments. *Pharm Res* **34**, 2131–2141 (2017).
29. Löfblom, J. *et al.* Affibody molecules: Engineered proteins for therapeutic, diagnostic and biotechnological applications. *FEBS Letters* **584**, 2670–2680 (2010).
30. Nord, K. *et al.* Binding proteins selected from combinatorial libraries of an α -helical bacterial receptor domain. *Nature Biotechnology* **15**, 772–777 (1997).
31. Nilsson, B. *et al.* A synthetic IgG-binding domain based on staphylococcal protein A. *Protein Engineering, Design and Selection* **1**, 107–113 (1987).
32. Ståhl, S. *et al.* Affibody Molecules in Biotechnological and Medical Applications. *Trends in Biotechnology* **35**, 691–712 (2017).
33. Andersson, M., Rönmark, J., Areström, I., Nygren, P. A. & Ahlberg, N. Inclusion of a non-immunoglobulin binding protein in two-site ELISA for quantification of human serum proteins without interference by heterophilic serum antibodies. *J Immunol Methods* **283**, 225–234 (2003).
34. Lyakhov, I. *et al.* HER2-and EGFR-specific Affiprobe—Novel Recombinant Optical Probes for Cell Imaging. *Chembiochem* **11**, 345–350 (2010).
35. Nord, K., Gunneriusson, E., Uhlén, M. & Nygren, P. A. Ligands selected from combinatorial libraries of protein A for use in affinity capture of apolipoprotein A-1M and taq DNA polymerase. *J Biotechnol* **80**, 45–54 (2000).
36. Kumar, K. & Ghosh, A. 18F-AIF Labeled Peptide and Protein Conjugates as Positron Emission Tomography Imaging Pharmaceuticals. *Bioconjugate Chem.* **29**, 953–975 (2018).
37. Chen, W., Shen, B. & Sun, X. Analysis of Progress and Challenges of EGFR-Targeted Molecular Imaging in Cancer With a Focus on Affibody Molecules. *Mol Imaging* **18**, 1536012118823473 (2019).

38. Tolmachev, V. & Orlova, A. Affibody Molecules as Targeting Vectors for PET Imaging. *Cancers* **12**, 651 (2020).
39. Iveson, P. B. *et al.* FASTLab Radiosynthesis of the ¹⁸F-labelled HER2-binding Affibody molecule [¹⁸F]GE-226. *Journal of Labelled Compounds and Radiopharmaceuticals* **62**, 925–932 (2019).
40. Liu, Y., Sorensen, J. B., Brun, N. C., Frejd, F. Y. & Tolmachev, V. Theranostic pairing: ABY-025/251 targeting HER2 with ⁶⁸Ga and ¹⁸⁸Re—Minimized radioligands using Affibody peptide scaffold technology. *JCO* **40**, 3093–3093 (2022).
41. Meister, S. W. *et al.* An Affibody Molecule Is Actively Transported into the Cerebrospinal Fluid via Binding to the Transferrin Receptor. *Int J Mol Sci* **21**, (2020).
42. Association, A. 2018 Alzheimer’s disease facts and figures. *Alzheimer’s & Dementia* **14**, 367–429 (2018).
43. Wolters, F. J. & Ikram, M. Epidemiology of Dementia: The Burden on Society, the Challenges for Research. in *Biomarkers for Alzheimer’s Disease Drug Development* (ed. Perneczky, R.) 3–14 (Springer, 2018). doi:10.1007/978-1-4939-7704-8_1.
44. Rohan de Silva, H. A. *et al.* Cell-specific expression of β -amyloid precursor protein isoform mRNAs and proteins in neurons and astrocytes. *Molecular Brain Research* **47**, 147–156 (1997).
45. Hur, J.-Y. γ -Secretase in Alzheimer’s disease. *Exp Mol Med* **54**, 433–446 (2022).
46. Jarrett, J. T., Berger, E. P. & Lansbury, P. T. The C-terminus of the beta protein is critical in amyloidogenesis. *Ann. N. Y. Acad. Sci.* **695**, 144–148 (1993).
47. Bitan, G. *et al.* Amyloid β -protein (A β) assembly: A β 40 and A β 42 oligomerize through distinct pathways. *PNAS* **100**, 330–335 (2003).
48. Iwatsubo, T. *et al.* Visualization of A β 42(43) and A β 40 in senile plaques with end-specific A β monoclonals: Evidence that an initially deposited species is A β 42(43). *Neuron* **13**, 45–53 (1994).
49. Morley, J. E. & Farr, S. A. The role of amyloid-beta in the regulation of memory. *Biochemical Pharmacology* **88**, 479–485 (2014).
50. Soscia, S. J. *et al.* The Alzheimer’s disease-associated amyloid beta-protein is an antimicrobial peptide. *PLoS ONE* **5**, e9505 (2010).
51. Atwood, C. S., Bowen, R. L., Smith, M. A. & Perry, G. Cerebrovascular requirement for sealant, anti-coagulant and remodeling molecules that allow for the maintenance of vascular integrity and blood supply. *Brain Research Reviews* **43**, 164–178 (2003).
52. Stone, J. What initiates the formation of senile plaques? The origin of Alzheimer-like dementias in capillary haemorrhages. *Medical Hypotheses* **71**, 347–359 (2008).
53. Burgmans, S., van de Haar, H. J., Verhey, F. R. J. & Backes, W. H. Amyloid- β Interacts with Blood-Brain Barrier Function in Dementia: A Systematic Review. *Journal of Alzheimer’s Disease* **35**, 859–873 (2013).
54. Köpke, E. *et al.* Microtubule-associated protein tau. Abnormal phosphorylation of a non-paired helical filament pool in Alzheimer disease. *Journal of Biological Chemistry* **268**, 24374–24384 (1993).

55. Alavi Naini, S. M. & Soussi-Yanicostas, N. Tau Hyperphosphorylation and Oxidative Stress, a Critical Vicious Circle in Neurodegenerative Tauopathies? *Oxidative Medicine and Cellular Longevity* **2015**, e151979 (2015).
56. Devous Sr., M. D. *et al.* Relationships Between Cognition and Neuropathological Tau in Alzheimer's Disease Assessed by 18F Flortaucipir PET. *Journal of Alzheimer's Disease* **80**, 1091–1104 (2021).
57. Dani, M. *et al.* Tau Aggregation Correlates with Amyloid Deposition in Both Mild Cognitive Impairment and Alzheimer's Disease Subjects. *J Alzheimers Dis* **70**, 455–465 (2019).
58. Takashima, A. *et al.* Activation of tau protein kinase I/glycogen synthase kinase-3 β by amyloid β peptide (25–35) enhances phosphorylation of tau in hippocampal neurons. *Neuroscience Research* **31**, 317–323 (1998).
59. Rapoport, M., Dawson, H. N., Binder, L. I., Vitek, M. P. & Ferreira, A. Tau is essential to beta -amyloid-induced neurotoxicity. *Proc Natl Acad Sci U S A* **99**, 6364–6369 (2002).
60. Shin, W. S. *et al.* Amyloid β -protein oligomers promote the uptake of tau fibril seeds potentiating intracellular tau aggregation. *Alzheimers Res Ther* **11**, 86 (2019).
61. Hardy, J. A. & Higgins, G. A. Alzheimer's disease: the amyloid cascade hypothesis. *Science* **256**, 184–185 (1992).
62. Harper, J. D., Wong, S. S., Lieber, C. M. & Lansbury, P. T. Observation of metastable A β amyloid protofibrils by atomic force microscopy. *Chemistry & Biology* **4**, 119–125 (1997).
63. Antzutkin, O. N. *et al.* Multiple quantum solid-state NMR indicates a parallel, not antiparallel, organization of β -sheets in Alzheimer's β -amyloid fibrils. *Proceedings of the National Academy of Sciences* **97**, 13045–13050 (2000).
64. Röhr, D. *et al.* Label-free vibrational imaging of different A β plaque types in Alzheimer's disease reveals sequential events in plaque development. *Acta Neuropathologica Communications* **8**, 222 (2020).
65. Koffie, R. M. *et al.* Oligomeric amyloid beta associates with postsynaptic densities and correlates with excitatory synapse loss near senile plaques. *Proc Natl Acad Sci U S A* **106**, 4012–4017 (2009).
66. Kinney, J. W. *et al.* Inflammation as a central mechanism in Alzheimer's disease. *Alzheimer's & Dementia: Translational Research & Clinical Interventions* **4**, 575–590 (2018).
67. Terry, R. D. *et al.* Physical basis of cognitive alterations in Alzheimer's disease: synapse loss is the major correlate of cognitive impairment. *Ann. Neurol.* **30**, 572–580 (1991).
68. Chételat, G. *et al.* Amyloid imaging in cognitively normal individuals, at-risk populations and preclinical Alzheimer's disease. *NeuroImage: Clinical* **2**, 356–365 (2013).
69. Cleary, J. P. *et al.* Natural oligomers of the amyloid- β protein specifically disrupt cognitive function. *Nature Neuroscience* **8**, 79–84 (2005).
70. Dahlgren, K. N. *et al.* Oligomeric and fibrillar species of amyloid-beta peptides differentially affect neuronal viability. *J. Biol. Chem.* **277**, 32046–32053 (2002).
71. Kaye, R. *et al.* Common Structure of Soluble Amyloid Oligomers Implies Common Mechanism of Pathogenesis. *Science* **300**, 486–489 (2003).

72. Klyubin, I. *et al.* Amyloid β Protein Dimer-Containing Human CSF Disrupts Synaptic Plasticity: Prevention by Systemic Passive Immunization. *J. Neurosci.* **28**, 4231–4237 (2008).
73. Lambert, M. P. *et al.* Diffusible, nonfibrillar ligands derived from A β 1–42 are potent central nervous system neurotoxins. *Proceedings of the National Academy of Sciences* **95**, 6448–6453 (1998).
74. Shankar, G. M. *et al.* Amyloid- β protein dimers isolated directly from Alzheimer's brains impair synaptic plasticity and memory. *Nat Med* **14**, 837–842 (2008).
75. Townsend, M., Shankar, G. M., Mehta, T., Walsh, D. M. & Selkoe, D. J. Effects of secreted oligomers of amyloid β -protein on hippocampal synaptic plasticity: a potent role for trimers. *The Journal of Physiology* **572**, 477–492 (2006).
76. Poling, A. *et al.* Oligomers of the amyloid- β protein disrupt working memory: Confirmation with two behavioral procedures. *Behavioural Brain Research* **193**, 230–234 (2008).
77. Townsend, M. *et al.* Orally available compound prevents deficits in memory caused by the Alzheimer amyloid- β oligomers. *Annals of Neurology* **60**, 668–676 (2006).
78. Chávez-Gutiérrez, L. *et al.* The mechanism of γ -Secretase dysfunction in familial Alzheimer disease. *The EMBO Journal* **31**, 2261–2274 (2012).
79. Haass, C. *et al.* The Swedish mutation causes early-onset Alzheimer's disease by β -secretase cleavage within the secretory pathway. *Nat Med* **1**, 1291–1296 (1995).
80. Lord, A. *et al.* The Arctic Alzheimer mutation facilitates early intraneuronal Abeta aggregation and senile plaque formation in transgenic mice. *Neurobiol. Aging* **27**, 67–77 (2006).
81. Guerreiro, R. J. *et al.* Genetic screening of Alzheimer's disease genes in Iberian and African samples yields novel mutations in presenilins and APP. *Neurobiol. Aging* **31**, 725–731 (2010).
82. Belloy, M. E., Napolioni, V. & Greicius, M. D. A Quarter Century of APOE and Alzheimer's Disease: Progress to Date and the Path Forward. *Neuron* **101**, 820–838 (2019).
83. Castellano, J. M. *et al.* Human apoE Isoforms Differentially Regulate Brain Amyloid- β Peptide Clearance. *Science Translational Medicine* **3**, 89ra57–89ra57 (2011).
84. Fleisher, A. S. *et al.* Apolipoprotein E ϵ 4 and age effects on florbetapir positron emission tomography in healthy aging and Alzheimer disease. *Neurobiology of Aging* **34**, 1–12 (2013).
85. Mawuenyega, K. G. *et al.* Decreased Clearance of CNS β -Amyloid in Alzheimer's Disease. *Science* **330**, 1774–1774 (2010).
86. Jack, C. R. *et al.* Tracking pathophysiological processes in Alzheimer's disease: an updated hypothetical model of dynamic biomarkers. *Lancet Neurol* **12**, 207–216 (2013).
87. Palmqvist, S. *et al.* Cerebrospinal fluid and plasma biomarker trajectories with increasing amyloid deposition in Alzheimer's disease. *EMBO Molecular Medicine* **11**, e11170 (2019).
88. Fiandaca, M. S., Mapstone, M. E., Cheema, A. K. & Federoff, H. J. The critical need for defining preclinical biomarkers in Alzheimer's disease. *Alzheimer's & Dementia* **10**, S196–S212 (2014).

89. Sehlin, D., Syvänen, S., & MINC faculty. Engineered antibodies: new possibilities for brain PET? *Eur J Nucl Med Mol Imaging* **46**, 2848–2858 (2019).
90. Tolar, M., Abushakra, S., Hey, J. A., Porsteinsson, A. & Sabbagh, M. Aducanumab, gantenerumab, BAN2401, and ALZ-801—the first wave of amyloid-targeting drugs for Alzheimer’s disease with potential for near term approval. *Alzheimers Res Ther* **12**, 95 (2020).
91. Dhillon, S. Aducanumab: First Approval. *Drugs* **81**, 1437–1443 (2021).
92. Haerberlein, S. B. *et al.* Emerge and Engage topline results: Phase 3 studies of aducanumab in early Alzheimer’s disease. *Alzheimer’s & Dementia* **16**, e047259 (2020).
93. Commissioner, O. of the. FDA Grants Accelerated Approval for Alzheimer’s Disease Treatment. *FDA* <https://www.fda.gov/news-events/press-announcements/fda-grants-accelerated-approval-alzheimers-disease-treatment> (2023).
94. Englund, H. *et al.* Sensitive ELISA detection of amyloid-beta protofibrils in biological samples. *J. Neurochem.* **103**, 334–345 (2007).
95. Swanson, C. J. *et al.* A randomized, double-blind, phase 2b proof-of-concept clinical trial in early Alzheimer’s disease with lecanemab, an anti-A β protofibril antibody. *Alzheimers Res Ther* **13**, 80 (2021).
96. van Dyck, C. H. *et al.* Lecanemab in Early Alzheimer’s Disease. *N Engl J Med* (2022) doi:10.1056/NEJMoa2212948.
97. Reish, N. J. *et al.* Multiple Cerebral Hemorrhages in a Patient Receiving Lecanemab and Treated with t-PA for Stroke. *N Engl J Med* (2023) doi:10.1056/NEJMc2215148.
98. Whittington, M. D. *et al.* Cost-Effectiveness and Value-Based Pricing of Aducanumab for Patients With Early Alzheimer Disease. *Neurology* **98**, e968–e977 (2022).
99. Bohrmann, B. *et al.* Gantenerumab: A Novel Human Anti-A β Antibody Demonstrates Sustained Cerebral Amyloid- β Binding and Elicits Cell-Mediated Removal of Human Amyloid- β . *Journal of Alzheimer’s Disease* **28**, 49–69 (2012).
100. Crehan, H. *et al.* Effector function of anti-pyroglutamate-3 A β antibodies affects cognitive benefit, glial activation and amyloid clearance in Alzheimer’s-like mice. *Alzheimer’s Research & Therapy* **12**, 12 (2020).
101. Kaplow, J. M. *et al.* P4–281: Microglial involvement and amyloid reduction with BAN2401/mAb158, a monoclonal antibody with high selectivity for protofibrils: In vitro and ex vivo analyses. *Alzheimer’s & Dementia* **9**, P807–P808 (2013).
102. Sevigny, J. *et al.* The antibody aducanumab reduces A β plaques in Alzheimer’s disease. *Nature* **537**, 50–56 (2016).
103. Söderberg, L. *et al.* Lecanemab, Aducanumab, and Gantenerumab — Binding Profiles to Different Forms of Amyloid-Beta Might Explain Efficacy and Side Effects in Clinical Trials for Alzheimer’s Disease. *Neurotherapeutics* (2022) doi:10.1007/s13311-022-01308-6.
104. van Dyck, C. H. Anti-Amyloid- β Monoclonal Antibodies for Alzheimer’s Disease: Pitfalls and Promise. *Biological Psychiatry* **83**, 311–319 (2018).
105. Feinberg, H. *et al.* Crystal structure reveals conservation of amyloid- β conformation recognized by 3D6 following humanization to bapineuzumab. *Alzheimers Res Ther* **6**, 31 (2014).

106. Rinne, J. O. *et al.* 11C-PiB PET assessment of change in fibrillar amyloid-beta load in patients with Alzheimer's disease treated with bapineuzumab: a phase 2, double-blind, placebo-controlled, ascending-dose study. *Lancet Neurol* **9**, 363–372 (2010).
107. Salloway, S. *et al.* Two Phase 3 Trials of Bapineuzumab in Mild-to-Moderate Alzheimer's Disease. *N Engl J Med* **370**, 322–333 (2014).
108. Sperling, R. *et al.* Amyloid-related imaging abnormalities in patients with Alzheimer's disease treated with bapineuzumab: a retrospective analysis. *The Lancet Neurology* **11**, 241–249 (2012).
109. Klein, G. *et al.* Gantenerumab reduces amyloid- β plaques in patients with prodromal to moderate Alzheimer's disease: a PET substudy interim analysis. *Alzheimer's Research & Therapy* **11**, 101 (2019).
110. Foley, K. E. & Wilcock, D. M. Vascular Considerations for Amyloid Immunotherapy. *Curr Neurol Neurosci Rep* **22**, 709–719 (2022).
111. Abbott, N. J. Evidence for bulk flow of brain interstitial fluid: significance for physiology and pathology. *Neurochem Int* **45**, 545–552 (2004).
112. Iliff, J. J. *et al.* A paravascular pathway facilitates CSF flow through the brain parenchyma and the clearance of interstitial solutes, including amyloid β . *Sci Transl Med* **4**, 147ra111 (2012).
113. Olsson, B. *et al.* CSF and blood biomarkers for the diagnosis of Alzheimer's disease: a systematic review and meta-analysis. *Lancet Neurol* **15**, 673–684 (2016).
114. Hansson, O., Lehmann, S., Otto, M., Zetterberg, H. & Lewczuk, P. Advantages and disadvantages of the use of the CSF Amyloid β (A β) 42/40 ratio in the diagnosis of Alzheimer's Disease. *Alz Res Therapy* **11**, 34 (2019).
115. Hampel, H., Goernitz, A. & Buerger, K. Advances in the development of biomarkers for Alzheimer's disease: from CSF total tau and A β 1–42 proteins to phosphorylated tau protein. *Brain Research Bulletin* **61**, 243–253 (2003).
116. Neselius, S. *et al.* CSF-Biomarkers in Olympic Boxing: Diagnosis and Effects of Repetitive Head Trauma. *PLOS ONE* **7**, e33606 (2012).
117. Tapiola, T. *et al.* Cerebrospinal Fluid β -Amyloid 42 and Tau Proteins as Biomarkers of Alzheimer-Type Pathologic Changes in the Brain. *Arch Neurol* **66**, 382–389 (2009).
118. Pereira, J. B. *et al.* Untangling the association of amyloid- β and tau with synaptic and axonal loss in Alzheimer's disease. *Brain* **144**, 310–324 (2021).
119. Wellington, H. *et al.* Increased CSF neurogranin concentration is specific to Alzheimer disease. *Neurology* **86**, 829–835 (2016).
120. Bellaver, B. *et al.* Astrocyte Biomarkers in Alzheimer Disease: A Systematic Review and Meta-analysis. *Neurology* **96**, e2944–e2955 (2021).
121. Heslegrave, A. *et al.* Increased cerebrospinal fluid soluble TREM2 concentration in Alzheimer's disease. *Molecular Neurodegeneration* **11**, 3 (2016).
122. Palmqvist, S. *et al.* Discriminative Accuracy of Plasma Phospho-tau217 for Alzheimer Disease vs Other Neurodegenerative Disorders. *JAMA* **324**, 772–781 (2020).
123. Ashton, N. J. *et al.* Differential roles of A β 42/40, p-tau231 and p-tau217 for Alzheimer's trial selection and disease monitoring. *Nat Med* **28**, 2555–2562 (2022).

124. Shea, D. *et al.* SOBA: Development and testing of a soluble oligomer binding assay for detection of amyloidogenic toxic oligomers. *Proceedings of the National Academy of Sciences* **119**, e2213157119 (2022).
125. Klunk, W. E. *et al.* Imaging brain amyloid in Alzheimer's disease with Pittsburgh Compound-B. *Ann. Neurol.* **55**, 306–319 (2004).
126. Leinonen, V. *et al.* Assessment of beta-amyloid in a frontal cortical brain biopsy specimen and by positron emission tomography with carbon 11-labeled Pittsburgh Compound B. *Arch. Neurol.* **65**, 1304–1309 (2008).
127. Schöll, M. *et al.* Low PiB PET retention in presence of pathologic CSF biomarkers in Arctic APP mutation carriers. *Neurology* **79**, 229–236 (2012).
128. Jack, C. R., Barrio, J. R. & Kepe, V. Cerebral amyloid PET imaging in Alzheimer's disease. *Acta Neuropathol* **126**, 643–657 (2013).
129. Le Loirec, C. & Champion, C. Track structure simulation for positron emitters of medical interest. Part I: The case of the allowed decay isotopes. *Nuclear Instruments and Methods in Physics Research Section A: Accelerators, Spectrometers, Detectors and Associated Equipment* **582**, 644–653 (2007).
130. Chételat, G. *et al.* Amyloid-PET and 18F-FDG-PET in the diagnostic investigation of Alzheimer's disease and other dementias. *The Lancet Neurology* **19**, 951–962 (2020).
131. Palmqvist, S. *et al.* Earliest accumulation of β -amyloid occurs within the default-mode network and concurrently affects brain connectivity. *Nat Commun* **8**, 1214 (2017).
132. Pagnon de la Vega, M. *et al.* The Uppsala APP deletion causes early onset autosomal dominant Alzheimer's disease by altering APP processing and increasing amyloid β fibril formation. *Science Translational Medicine* **13**, eabc6184 (2021).
133. Ossenkoppele, R. *et al.* Tau PET correlates with different Alzheimer's disease-related features compared to CSF and plasma p-tau biomarkers. *EMBO Molecular Medicine* **13**, e14398 (2021).
134. Dewulf, J., Adhikari, K., Vangestel, C., Wyngaert, T. V. D. & Elvas, F. Development of Antibody Immuno-PET/SPECT Radiopharmaceuticals for Imaging of Oncological Disorders—An Update. *Cancers* **12**, 1868 (2020).
135. Sehlin, D. *et al.* Antibody-based PET imaging of amyloid beta in mouse models of Alzheimer's disease. *Nat Commun* **7**, 10759 (2016).
136. Syvänen, S. *et al.* Fluorine-18-Labeled Antibody Ligands for PET Imaging of Amyloid- β in Brain. *ACS Chem. Neurosci.* (2020) doi:10.1021/acschemneuro.0c00652.
137. Fang, X. T. *et al.* High detection sensitivity with antibody-based PET radioligand for amyloid beta in brain. *Neuroimage* **184**, 881–888 (2019).
138. Bonvicini, G. *et al.* ImmunoPET imaging of amyloid-beta in a rat model of Alzheimer's disease with a bispecific, brain-penetrating fusion protein. *Translational Neurodegeneration* **11**, 55 (2022).
139. Habashi, M. *et al.* Early diagnosis and treatment of Alzheimer's disease by targeting toxic soluble A β oligomers. *Proceedings of the National Academy of Sciences* **119**, e2210766119 (2022).
140. Meier, S. R. *et al.* Antibody-Based In Vivo PET Imaging Detects Amyloid- β Reduction in Alzheimer Transgenic Mice After BACE-1 Inhibition. *J Nucl Med* **59**, 1885–1891 (2018).

141. Meier, S. R. *et al.* 11C-PiB and 124I-Antibody PET Provide Differing Estimates of Brain Amyloid- β After Therapeutic Intervention. *Journal of Nuclear Medicine* **63**, 302–309 (2022).
142. Bard, F. *et al.* Peripherally administered antibodies against amyloid beta-peptide enter the central nervous system and reduce pathology in a mouse model of Alzheimer disease. *Nat. Med.* **6**, 916–919 (2000).
143. Wang, Q. *et al.* Monoclonal antibody exposure in rat and cynomolgus monkey cerebrospinal fluid following systemic administration. *Fluids Barriers CNS* **15**, (2018).
144. Abbott, N. J., Pizzo, M. E., Preston, J. E., Janigro, D. & Thorne, R. G. The role of brain barriers in fluid movement in the CNS: is there a ‘glymphatic’ system? *Acta Neuropathol.* **135**, 387–407 (2018).
145. Kariolis, M. S. *et al.* Brain delivery of therapeutic proteins using an Fc fragment blood-brain barrier transport vehicle in mice and monkeys. *Science Translational Medicine* **12**, (2020).
146. Pardridge, W. M. CSF, blood-brain barrier, and brain drug delivery. *Expert Opinion on Drug Delivery* **13**, 963–975 (2016).
147. St-Amour, I. *et al.* Brain bioavailability of human intravenous immunoglobulin and its transport through the murine blood–brain barrier. *J Cereb Blood Flow Metab* **33**, 1983–1992 (2013).
148. Roshanbin, S. *et al.* Reduction of α SYN Pathology in a Mouse Model of PD Using a Brain-Penetrating Bispecific Antibody. *Pharmaceutics* **14**, 1412 (2022).
149. Sehlin, D. *et al.* Brain delivery of biologics using a cross-species reactive transferrin receptor 1 VNAR shuttle. *The FASEB Journal* **34**, 13272–13283 (2020).
150. Syvänen, S. *et al.* Efficient clearance of A β protofibrils in A β PP-transgenic mice treated with a brain-penetrating bifunctional antibody. *Alzheimers Res Ther* **10**, 49 (2018).
151. Magnusson, K. *et al.* Specific uptake of an amyloid- β protofibril-binding antibody-tracer in A β PP transgenic mouse brain. *J. Alzheimers Dis.* **37**, 29–40 (2013).
152. Abbott, N. J., Patabendige, A. A. K., Dolman, D. E. M., Yusof, S. R. & Begley, D. J. Structure and function of the blood–brain barrier. *Neurobiology of Disease* **37**, 13–25 (2010).
153. Stanimirovic, D. B. & Friedman, A. Pathophysiology of the Neurovascular Unit: Disease Cause or Consequence? *J Cereb Blood Flow Metab* **32**, 1207–1221 (2012).
154. Abbott, N. J., Rönnebeck, L. & Hansson, E. Astrocyte–endothelial interactions at the blood–brain barrier. *Nature Reviews Neuroscience* **7**, 41–53 (2006).
155. Banks, W. A. From blood–brain barrier to blood–brain interface: new opportunities for CNS drug delivery. *Nature Reviews Drug Discovery* **15**, 275–292 (2016).
156. Yokel, R. A. Nanoparticle brain delivery: a guide to verification methods. *Nanomedicine* **15**, 409–432 (2020).
157. Redzic, Z. B. & Segal, M. B. The structure of the choroid plexus and the physiology of the choroid plexus epithelium. *Advanced Drug Delivery Reviews* **56**, 1695–1716 (2004).

158. Pizzo, M. E. *et al.* Intrathecal antibody distribution in the rat brain: surface diffusion, perivascular transport and osmotic enhancement of delivery. *J Physiol* **596**, 445–475 (2018).
159. Fu, B. M. Transport Across the Blood-Brain Barrier. in *Molecular, Cellular, and Tissue Engineering of the Vascular System* (eds. Fu, B. M. & Wright, N. T.) 235–259 (Springer International Publishing, 2018). doi:10.1007/978-3-319-96445-4_13.
160. Abbott, N. J. Blood–brain barrier structure and function and the challenges for CNS drug delivery. *J Inherit Metab Dis* **36**, 437–449 (2013).
161. Kumagai, A. K., Eisenberg, J. B. & Pardridge, W. M. Absorptive-mediated endocytosis of cationized albumin and a beta-endorphin-cationized albumin chimeric peptide by isolated brain capillaries. Model system of blood-brain barrier transport. *Journal of Biological Chemistry* **262**, 15214–15219 (1987).
162. Johnsen, K. B., Burkhart, A., Thomsen, L. B., Andresen, T. L. & Moos, T. Targeting the transferrin receptor for brain drug delivery. *Prog. Neurobiol.* **181**, 101665 (2019).
163. Cooper, P. R. *et al.* Efflux of monoclonal antibodies from rat brain by neonatal Fc receptor, FcRn. *Brain Res.* **1534**, 13–21 (2013).
164. Schlachetzki, F., Zhu, C. & Pardridge, W. M. Expression of the neonatal Fc receptor (FcRn) at the blood–brain barrier. *Journal of Neurochemistry* **81**, 203–206 (2002).
165. Garg, A. & Balthasar, J. P. Investigation of the influence of FcRn on the distribution of IgG to the brain. *AAPS J* **11**, 553–557 (2009).
166. Kroll, R. A. & Newwelt, E. A. Outwitting the blood-brain barrier for therapeutic purposes: osmotic opening and other means. *Neurosurgery* **42**, 1083–1099; discussion 1099-1100 (1998).
167. Shin, J. *et al.* Focused ultrasound–mediated noninvasive blood-brain barrier modulation: preclinical examination of efficacy and safety in various sonication parameters. *Neurosurgical Focus* **44**, E15 (2018).
168. Gabathuler, R. Approaches to transport therapeutic drugs across the blood–brain barrier to treat brain diseases. *Neurobiology of Disease* **37**, 48–57 (2010).
169. Kumar, N. N. *et al.* Delivery of immunoglobulin G antibodies to the rat nervous system following intranasal administration: Distribution, dose-response, and mechanisms of delivery. *Journal of Controlled Release* **286**, 467–484 (2018).
170. Boado, R. J., Lu, J. Z., Hui, E. K.-W. & Pardridge, W. M. IgG-single chain Fv fusion protein therapeutic for Alzheimer’s disease: Expression in CHO cells and pharmacokinetics and brain delivery in the rhesus monkey. *Biotechnol Bioeng* **105**, 627–635 (2010).
171. Alata, W. *et al.* Targeting insulin-like growth factor-1 receptor (IGF1R) for brain delivery of biologics. *The FASEB Journal* **36**, e22208 (2022).
172. Molino, Y. *et al.* Use of LDL receptor—targeting peptide vectors for in vitro and in vivo cargo transport across the blood-brain barrier. *The FASEB Journal* **31**, 1807–1827 (2017).
173. Zuchero, Y. J. Y. *et al.* Discovery of Novel Blood-Brain Barrier Targets to Enhance Brain Uptake of Therapeutic Antibodies. *Neuron* **89**, 70–82 (2016).
174. Farrington, G. K. *et al.* A novel platform for engineering blood-brain barrier-crossing bispecific biologics. *The FASEB Journal* **28**, 4764–4778 (2014).

175. Lessard, E. *et al.* Pharmacokinetics and Pharmacodynamic Effect of a Blood-Brain Barrier-Crossing Fusion Protein Therapeutic for Alzheimer's Disease in Rat and Dog. *Pharm Res* (2022) doi:10.1007/s11095-022-03285-z.
176. Peng, Y., Chang, X. & Lang, M. Iron Homeostasis Disorder and Alzheimer's Disease. *International Journal of Molecular Sciences* **22**, 12442 (2021).
177. Cairo, G., Bernuzzi, F. & Recalcati, S. A precious metal: Iron, an essential nutrient for all cells. *Genes Nutr* **1**, 25–39 (2006).
178. Gatter, K. C., Brown, G., Trowbridge, I. S., Woolston, R. E. & Mason, D. Y. Transferrin receptors in human tissues: their distribution and possible clinical relevance. *Journal of Clinical Pathology* **36**, 539–545 (1983).
179. Kawabata, H. *et al.* Molecular Cloning of Transferrin Receptor 2: A NEW MEMBER OF THE TRANSFERRIN RECEPTOR-LIKE FAMILY *. *Journal of Biological Chemistry* **274**, 20826–20832 (1999).
180. Kawabata, H. *et al.* Transferrin Receptor 2- α Supports Cell Growth Both in Iron-chelated Cultured Cells and in Vivo *. *Journal of Biological Chemistry* **275**, 16618–16625 (2000).
181. Kleven, M. D., Jue, S. & Enns, C. A. The Transferrin Receptors, TfR1 and TfR2 Bind Transferrin through Differing Mechanisms. *Biochemistry* **57**, 1552–1559 (2018).
182. Hamdi, A., Garcia dos Santos, D., Lok, C.-N., Schranzhofer, M. & Ponka, P. Role of Heme in the Regulation of Transferrin Receptor Expression in Erythroid Cells. *Blood* **130**, 3495–3495 (2017).
183. Jefferies, W. A. *et al.* Transferrin receptor on endothelium of brain capillaries. *Nature* **312**, 162–163 (1984).
184. Fishman, J. B., Rubin, J. B., Handrahan, J. V., Connor, J. R. & Fine, R. E. Receptor-mediated transcytosis of transferrin across the blood-brain barrier. *J. Neurosci. Res.* **18**, 299–304 (1987).
185. Boado, R. J., Zhang, Y., Wang, Y. & Pardridge, W. M. Engineering and expression of a chimeric transferrin receptor monoclonal antibody for blood-brain barrier delivery in the mouse. *Biotechnol Bioeng* **102**, 1251–1258 (2009).
186. Friden, P. M. *et al.* Anti-transferrin receptor antibody and antibody-drug conjugates cross the blood-brain barrier. *PNAS* **88**, 4771–4775 (1991).
187. Johnsen, K. B. *et al.* Targeting transferrin receptors at the blood-brain barrier improves the uptake of immunoliposomes and subsequent cargo transport into the brain parenchyma. *Sci Rep* **7**, 10396 (2017).
188. Niewoehner, J. *et al.* Increased brain penetration and potency of a therapeutic antibody using a monovalent molecular shuttle. *Neuron* **81**, 49–60 (2014).
189. Rofo, F. *et al.* Enhanced neprilysin-mediated degradation of hippocampal A β 42 with a somatostatin peptide that enters the brain. *Theranostics* **11**, 789–804 (2021).
190. van Lengerich, B. *et al.* A TREM2-activating antibody with a blood–brain barrier transport vehicle enhances microglial metabolism in Alzheimer's disease models. *Nat Neurosci* 1–14 (2023) doi:10.1038/s41593-022-01240-0.
191. Haqqani, A. S. *et al.* Intracellular sorting and transcytosis of the rat transferrin receptor antibody OX26 across the blood-brain barrier in vitro is dependent on its binding affinity. *J. Neurochem.* **146**, 735–752 (2018).
192. Villaseñor, R., Schilling, M., Sundaresan, J., Lutz, Y. & Collin, L. Sorting Tubules Regulate Blood-Brain Barrier Transcytosis. *Cell Reports* **21**, 3256–3270 (2017).

193. Bien-Ly, N. *et al.* Transferrin receptor (TfR) trafficking determines brain uptake of TfR antibody affinity variants. *J Exp Med* **211**, 233–244 (2014).
194. Nielsen, S. S. E. *et al.* Apicobasal transferrin receptor localization and trafficking in brain capillary endothelial cells. *Fluids and Barriers of the CNS* **20**, 2 (2023).
195. Yu, Y. J. *et al.* Therapeutic bispecific antibodies cross the blood-brain barrier in nonhuman primates. *Sci Transl Med* **6**, 261ra154 (2014).
196. Zhao, P. *et al.* Enhanced anti-angiogenic effect of transferrin receptor-mediated delivery of VEGF-trap in a glioblastoma mouse model. *mAbs* **14**, 2057269 (2022).
197. Edavettal, S. *et al.* Enhanced delivery of antibodies across the blood-brain barrier via TEMs with inherent receptor-mediated phagocytosis. *Med* (2022) doi:10.1016/j.medj.2022.09.007.
198. Couch, J. A. *et al.* Addressing safety liabilities of TfR bispecific antibodies that cross the blood-brain barrier. *Sci Transl Med* **5**, 183ra57, 1–12 (2013).
199. Sade, H. *et al.* A Human Blood-Brain Barrier Transcytosis Assay Reveals Antibody Transcytosis Influenced by pH-Dependent Receptor Binding. *PLoS One* **9**, (2014).
200. Johnsen, K. B. *et al.* Antibody affinity and valency impact brain uptake of transferrin receptor-targeted gold nanoparticles. *Theranostics* **8**, 3416–3436 (2018).
201. Arguello, A. *et al.* Molecular architecture determines brain delivery of a transferrin receptor-targeted lysosomal enzyme. *J Exp Med* **219**, e20211057 (2022).
202. Kissel, K. *et al.* Immunohistochemical localization of the murine transferrin receptor (TfR) on blood-tissue barriers using a novel anti-TfR monoclonal antibody. *Histochem. Cell Biol.* **110**, 63–72 (1998).
203. Roshanbin, S. *et al.* In vivo imaging of alpha-synuclein with antibody-based PET. *Neuropharmacology* **208**, 108985 (2022).
204. Syvänen, S. *et al.* A bispecific Tribody PET radioligand for visualization of amyloid-beta protofibrils - a new concept for neuroimaging. *Neuroimage* **148**, 55–63 (2017).
205. Sonoda, H. *et al.* A Blood-Brain-Barrier-Penetrating Anti-human Transferrin Receptor Antibody Fusion Protein for Neuronopathic Mucopolysaccharidosis II. *Molecular Therapy* **26**, 1366–1374 (2018).
206. Clarke, E. *et al.* A Single Domain Shark Antibody Targeting the Transferrin Receptor 1 Delivers a TrkB Agonist Antibody to the Brain and Provides Full Neuroprotection in a Mouse Model of Parkinson’s Disease. *Pharmaceutics* **14**, 1335 (2022).
207. Cohen, R., David, M. & Khrestchatsky, M. Transferrin receptor-binding molecules, conjugates thereof and their uses. (2022).
208. Stocki, P. *et al.* High efficiency blood-brain barrier transport using a VNAR targeting the Transferrin Receptor 1 (TfR1). <http://biorxiv.org/lookup/doi/10.1101/816900> (2019) doi:10.1101/816900.
209. Okuyama, T. *et al.* A Phase 2/3 Trial of Pabinafusp Alfa, IDS Fused with Anti-Human Transferrin Receptor Antibody, Targeting Neurodegeneration in MPS-II. *Molecular Therapy* **29**, 671–679 (2021).

210. Okuyama, T. *et al.* A Phase 2/3 Trial of Pabinafusp Alfa, IDS Fused with Anti-Human Transferrin Receptor Antibody, Targeting Neurodegeneration in MPS-II. *Mol Ther* (2020) doi:10.1016/j.ymthe.2020.09.039.
211. Ullman, J. C. *et al.* Brain delivery and activity of a lysosomal enzyme using a blood-brain barrier transport vehicle in mice. *Science Translational Medicine* **12**, (2020).
212. Pipeline. *Denali* <https://www.denalitherapeutics.com/pipeline>.
213. Trontinemab | ALZFORUM. <https://www.alzforum.org/therapeutics/trontinemab>.
214. Keizer, R. J., Huitema, A. D. R., Schellens, J. H. M. & Beijnen, J. H. Clinical Pharmacokinetics of Therapeutic Monoclonal Antibodies. *Clin Pharmacokinet* **49**, 493–507 (2010).
215. Tabrizi, M., Bornstein, G. G. & Suria, H. Biodistribution mechanisms of therapeutic monoclonal antibodies in health and disease. *AAPS J* **12**, 33–43 (2010).
216. Kraft, T. E. *et al.* Heparin chromatography as an in vitro predictor for antibody clearance rate through pinocytosis. *mAbs* **12**, 1683432 (2020).
217. Ryman, J. T. & Meibohm, B. Pharmacokinetics of Monoclonal Antibodies. *CPT Pharmacometrics Syst Pharmacol* **6**, 576–588 (2017).
218. Chen, Y. & Xu, Y. Pharmacokinetics of Bispecific Antibody. *Curr Pharmacol Rep* **3**, 126–137 (2017).
219. Kanodia, J. *et al.* Prospective Design of Anti-Transferrin Receptor Bispecific Antibodies for Optimal Delivery into the Human Brain. *CPT Pharmacometrics Syst Pharmacol* **5**, 283–291 (2016).
220. Fang, X. T., Sehlin, D., Lannfelt, L., Syvänen, S. & Hultqvist, G. Efficient and inexpensive transient expression of multispecific multivalent antibodies in Expi293 cells. *Biol Proced Online* **19**, 11 (2017).
221. Philipson, O. *et al.* A highly insoluble state of A β similar to that of Alzheimer's disease brain is found in Arctic APP transgenic mice. *Neurobiology of Aging* **30**, 1393–1405 (2009).
222. Sehlin, D., Fang, X. T., Meier, S. R., Jansson, M. & Syvänen, S. Pharmacokinetics, biodistribution and brain retention of a bispecific antibody-based PET radioligand for imaging of amyloid- β . *Sci Rep* **7**, 17254 (2017).
223. Saito, T. *et al.* Single App knock-in mouse models of Alzheimer's disease. *Nat Neurosci* **17**, 661–663 (2014).
224. Sacher, C. *et al.* Longitudinal PET Monitoring of Amyloidosis and Microglial Activation in a Second-Generation Amyloid- β Mouse Model. *Journal of Nuclear Medicine* **60**, 1787–1793 (2019).
225. Greenwood, F. C., Hunter, W. M. & Glover, J. S. The preparation of ¹³¹I-labelled human growth hormone of high specific radioactivity. *Biochem J* **89**, 114–123 (1963).
226. Bertozzi, C. A Special Virtual Issue Celebrating the 2022 Nobel Prize in Chemistry for the Development of Click Chemistry and Bioorthogonal Chemistry. *ACS Cent. Sci.* (2022) doi:10.1021/acscentsci.2c01430.
227. Björke, H. & Andersson, K. Automated, high-resolution cellular retention and uptake studies in vitro. *Applied Radiation and Isotopes* **64**, 901–905 (2006).
228. Liu, H., Gaza-Bulsecu, G., Chumsae, C. & Newby-Kew, A. Characterization of lower molecular weight artifact bands of recombinant monoclonal IgG1

- antibodies on non-reducing SDS-PAGE. *Biotechnol Lett* **29**, 1611–1622 (2007).
229. Solon, E. G. Autoradiography techniques and quantification of drug distribution. *Cell Tissue Res* **360**, 87–107 (2015).
230. Triguero, D., Buciak, J. & Pardridge, W. M. Capillary depletion method for quantification of blood-brain barrier transport of circulating peptides and plasma proteins. *J. Neurochem.* **54**, 1882–1888 (1990).
231. Gutierrez, E. G., Banks, W. A. & Kastin, A. J. Blood-borne interleukin-1 receptor antagonist crosses the blood-brain barrier. *Journal of Neuroimmunology* **55**, 153–160 (1994).
232. Kafa, H. *et al.* The interaction of carbon nanotubes with an in vitro blood-brain barrier model and mouse brain in vivo. *Biomaterials* **53**, 437–452 (2015).
233. Moos, T. & Morgan, E. H. Restricted transport of anti-transferrin receptor antibody (OX26) through the blood–brain barrier in the rat. *Journal of Neurochemistry* **79**, 119–129 (2001).
234. Rhea, E. M., Rask-Madsen, C. & Banks, W. A. Insulin transport across the blood–brain barrier can occur independently of the insulin receptor. *The Journal of Physiology* **596**, 4753–4765 (2018).
235. Wynendaele, E. *et al.* Quorum Sensing Peptides Selectively Penetrate the Blood-Brain Barrier. *PLoS One* **10**, (2015).
236. Zlokovic, B. V. *et al.* Transport, uptake, and metabolism of blood-borne vasopressin by the blood-brain barrier. *Brain Res* **590**, 213–218 (1992).
237. Chang, H.-Y. *et al.* Effect of the Size of Protein Therapeutics on Brain Pharmacokinetics Following Systematic Administration. *AAPS J* **24**, 62 (2022).
238. Thorne, R. G. & Nicholson, C. In vivo diffusion analysis with quantum dots and dextrans predicts the width of brain extracellular space. *Proceedings of the National Academy of Sciences* **103**, 5567–5572 (2006).
239. Boutajangout, A. *et al.* Affibody-Mediated Sequestration of Amyloid β Demonstrates Preventive Efficacy in a Transgenic Alzheimer’s Disease Mouse Model. *Front. Aging Neurosci.* **11**, (2019).
240. Syvänen, S., Edén, D. & Sehlin, D. Cationization increases brain distribution of an amyloid-beta protofibril selective F(ab’)₂ fragment. *Biochem Biophys Res Commun* **493**, 120–125 (2017).
241. Gadkar, K. *et al.* Mathematical PKPD and safety model of bispecific TfR/BACE1 antibodies for the optimization of antibody uptake in brain. *Eur J Pharm Biopharm* **101**, 53–61 (2016).
242. Webster, C. I. *et al.* Brain penetration, target engagement, and disposition of the blood-brain barrier-crossing bispecific antibody antagonist of metabotropic glutamate receptor type 1. *The FASEB Journal* **30**, 1927–1940 (2016).
243. Gustavsson, T., Syvänen, S., O’Callaghan, P. & Sehlin, D. SPECT imaging of distribution and retention of a brain-penetrating bispecific amyloid- β antibody in a mouse model of Alzheimer’s disease. *Transl Neurodegener* **9**, 37 (2020).
244. Magnani, M. *et al.* Effect of age on some properties of mice erythrocytes. *Mechanisms of Ageing and Development* **42**, 37–47 (1988).
245. Yang, A. C. *et al.* Physiological blood-brain transport is impaired with age by a shift in transcytosis. *Nature* **583**, 425–430 (2020).
246. Belaidi, A. A. *et al.* Marked Age-Related Changes in Brain Iron Homeostasis in Amyloid Protein Precursor Knockout Mice. *Neurotherapeutics* **15**, 1055–1062 (2018).

247. Stergiou, N. *et al.* Application of ^{89}Zr -DFO*-immuno-PET to assess improved target engagement of a bispecific anti-amyloid- β monoclonal antibody. *Eur J Nucl Med Mol Imaging* (2023) doi:10.1007/s00259-023-06109-3.
248. Bourassa, P., Alata, W., Tremblay, C., Paris-Robidas, S. & Calon, F. Transferrin Receptor-Mediated Uptake at the Blood–Brain Barrier Is Not Impaired by Alzheimer’s Disease Neuropathology. *Mol. Pharmaceutics* **16**, 583–594 (2019).
249. Bien-Ly, N. *et al.* Lack of Widespread BBB Disruption in Alzheimer’s Disease Models: Focus on Therapeutic Antibodies. *Neuron* **88**, 289–297 (2015).
250. Banks, W. A., Reed, M. J., Logsdon, A. F., Rhea, E. M. & Erickson, M. A. Healthy aging and the blood-brain barrier. *Nat Aging* **1**, 243–254 (2021).
251. Elahy, M. *et al.* Blood–brain barrier dysfunction developed during normal aging is associated with inflammation and loss of tight junctions but not with leukocyte recruitment. *Immun Ageing* **12**, 2 (2015).
252. Nyúl-Tóth, Á. *et al.* Demonstration of age-related blood-brain barrier disruption and cerebromicrovascular rarefaction in mice by longitudinal intravital two-photon microscopy and optical coherence tomography. *Am J Physiol Heart Circ Physiol* **320**, H1370–H1392 (2021).
253. Pelegrí, C. *et al.* Increased permeability of blood–brain barrier on the hippocampus of a murine model of senescence. *Mechanisms of Ageing and Development* **128**, 522–528 (2007).
254. Gustafsson, S. *et al.* Blood-brain barrier integrity in a mouse model of Alzheimer’s disease with or without acute 3D6 immunotherapy. *Neuropharmacology* **143**, 1–9 (2018).
255. Julku, U. *et al.* Brain pharmacokinetics of mono- and bispecific amyloid- β antibodies in wild-type and Alzheimer’s disease mice measured by high cut-off microdialysis. *Fluids and Barriers of the CNS* **19**, 99 (2022).
256. Schlein, E. *et al.* Functionalization of Radiolabeled Antibodies to Enhance Peripheral Clearance for High Contrast Brain Imaging. *Mol. Pharmaceutics* **19**, 4111–4122 (2022).
257. Lopes van den Broek, S. *et al.* Pretargeted Imaging beyond the Blood–Brain Barrier—Utopia or Feasible? *Pharmaceutics* **15**, 1191 (2022).

Acta Universitatis Upsaliensis

*Digital Comprehensive Summaries of Uppsala Dissertations
from the Faculty of Medicine 1893*

Editor: The Dean of the Faculty of Medicine

A doctoral dissertation from the Faculty of Medicine, Uppsala University, is usually a summary of a number of papers. A few copies of the complete dissertation are kept at major Swedish research libraries, while the summary alone is distributed internationally through the series Digital Comprehensive Summaries of Uppsala Dissertations from the Faculty of Medicine. (Prior to January, 2005, the series was published under the title “Comprehensive Summaries of Uppsala Dissertations from the Faculty of Medicine”.)

Distribution: publications.uu.se
urn:nbn:se:uu:diva-494103



ACTA
UNIVERSITATIS
UPSALIENSIS
UPPSALA
2023